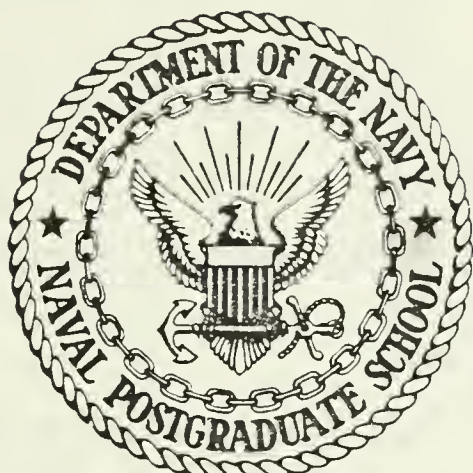




DUDLEY KNOX LIBRARY
NAVAL POSTGRADUATE SCHOOL
MONTEREY, CALIFORNIA 93943

NAVAL POSTGRADUATE SCHOOL

Monterey, California



THESIS

OBSERVATIONS OF THE
CALIFORNIA COUNTERCURRENT

by

Robert L. Harrod

June 1984

Thesis Advisors:

J. B. Wickham
S. P. Tucker

Approved for public release; distribution unlimited.

T222093

UNCLASSIFIED

SECURITY CLASSIFICATION OF THIS PAGE (When Data Entered)

REPORT DOCUMENTATION PAGE		READ INSTRUCTIONS BEFORE COMPLETING FORM
1. REPORT NUMBER	2. GOVT ACCESSION NO	3. REC'D ENT'D CATALOG NUMBER
4. TITLE (and Subtitle) Observations of the California Countercurrent		5. TYPE OF REPORT & PERIOD COVERED Master's Thesis June 1984
7. AUTHOR(s) Robert L. Harrod		6. PERFORMING ORG. REPORT NUMBER
9. PERFORMING ORGANIZATION NAME AND ADDRESS Naval Postgraduate School Monterey, California 93943		10. PROGRAM ELEMENT PROJECT TASK AREA & WORK UNIT NUMBERS
11. CONTROLLING OFFICE NAME AND ADDRESS Naval Postgraduate School Monterey, California 93943		12. REPORT DATE June 1984
14. MONITORING AGENCY NAME & ADDRESS (if different from Controlling Office)		13. NUMBER OF PAGES 147
		15. SECURITY CLASS. (of this report) UNCLASSIFIED
		15a. DECLASSIFICATION/DOWNGRADING SCHEDULE
16. DISTRIBUTION STATEMENT (of this Report) Approved for public release; distribution unlimited.		
17. DISTRIBUTION STATEMENT (of the abstract entered in Block 20, if different from Report)		
18. SUPPLEMENTARY NOTES		
19. KEY WORDS (Continue on reverse side if necessary and identify by block number) California Countercurrent, California Undercurrent, Davidson Current, California Current, Eastern boundary currents, metered currents.		
20. ABSTRACT (Continue on reverse side if necessary and identify by block number) Results from moored current meters, 150-350 m, are described for a region over the continental slope off Cape San Martin from January 1979 to April 1980. Current vector time series were constructed from the data and compared to the local coastal upwelling index. Progressive vector diagrams were also constructed, and spectrum analysis was performed for alongshore		

and cross-slope currents.

The California Countercurrent was found to be present in the study area during the entire period. Seasonally, the countercurrent was substantially stronger during the spring. Frequent current reversals and oscillations occurred between equatorward and poleward flow, less often at the nearshore station. Preferred low frequency energy peaks were found at periods of about 10 days. The intensity of the countercurrent increased with increasing coastal upwelling index, and the cross-slope flow also appeared to be related to the local coastal upwelling index.

Approved for public release; distribution unlimited.

Observations of the
California Countercurrent

by

Robert L. Harrod
Lieutenant Commander, United States Navy
B.S., Oregon State University, 1975

Submitted in partial fulfillment of the
requirements for the degress of

MASTER OF SCIENCE IN METEOROLOGY AND OCEANOGRAPHY

from the

NAVAL POSTGRADUATE SCHOOL
June 1984

Results from moored current meters, 150 - 350 m, are discussed for a region over the continental slope off Cape San Martin, California from January 1979 to April 1980.

Current vector time series were constructed from the data and compared to a local upwelling index. Progressive vector diagrams of the data were also constructed, and spectrum analysis was performed for alongshore and cross-slope currents.

The California Countercurrent was found to be present in the study area during the entire period. Seasonally, the countercurrent was substantially stronger during the spring. Frequent current reversals and oscillations occurred between equatorward and poleward flow, less often at the nearshore station. Preferred low frequency energy peaks were found at periods of about 10 days. The intensity of the countercurrent increased with increasing coastal upwelling index, and the cross-slope flow also appeared to be related to the local coastal upwelling index.

TABLE OF CONTENTS

DUDLEY KNOX LIBRARY
NAVAL POSTGRADUATE SCHOOL
MONTEREY, CALIFORNIA 93943

I.	INTRODUCTION AND BACKGROUND -----	12
II.	DIRECT CURRENT OBSERVATIONS -----	20
	A. DATA COLLECTION -----	20
	B. DATA PROCESSING -----	21
III.	STUDY OBJECTIVES -----	24
IV.	DESCRIPTION AND ORGANIZATION OF GRAPHICS -----	25
V.	ANALYSIS -----	28
	A. RELATION BETWEEN CURRENT AND LOCAL WIND FORCING -----	28
	1. Analysis at Station 2 -----	29
	2. Analysis at Station 7 -----	31
	3. Comparison of Stations 2 and 7 -----	32
	B. SPECTRUM ANALYSIS -----	34
	C. INFERENCES FROM PROGRESSIVE VECTOR DIAGRAMS -----	36
	D. CROSS-SLOPE CURRENT -----	41
	E. TIME SERIES -----	41
VI.	CONCLUSIONS -----	43
APPENDIX A:	TIME SERIES PLOTS -----	52
APPENDIX B:	SPECTRUM ANALYSES OF ALONGSHORE FLOW AND ON/OFFSHORE FLOW -----	75
APPENDIX C:	PROGRESSIVE VECTOR DIAGRAMS -----	91
APPENDIX D:	COMPUTER PROGRAM LISTINGS -----	107
LIST OF REFERENCES -----		143
INITIAL DISTRIBUTION LIST -----		146

LIST OF TABLES

TABLES	PAGE
I. Comparison of high energy peaks-----	37
II. Comparison of mean current and temperature-----	38

LIST OF FIGURES

FIGURES	PAGE
1. The study area-----	45
2. Chronology of current meter deployment-----	46
3. Vertical section showing representative locations of current meters off Cape San Martin, California-----	47
4. Current meter array-----	48
5. Mean onshore currents-----	49
6. Mean temperatures at Station 2-----	50
7. Mean temperatures at Station 7-----	51
8. Point Sur Upwelling Index and stickplots of hourly current vectors for the current meters at Station 7 deployed on 5 January 1979-----	52
9. U component, V component, and temperature plots versus time for the current meter at 152 m depth at Station 7 deployed on 5 January 1979-----	53
10. U component, V component, and temperature plots versus time for the current meter at 223 m depth at Station 7 deployed on 5 January 1979-----	54
11. Point Sur Upwelling Index and stickplots of hourly current vectors for the current meters at Station 2 deployed on 23 April 1979-----	55
12. U component, V component, and temperature plots versus time for the current meter at 169 m depth at Station 2 deployed on 23 April 1979-----	56
13. U component, V component, and temperature plots versus time for the current meter at 241 m depth at Station 2 deployed on 23 April 1979-----	57
14. Point Sur Upwelling Index and stickplots of hourly current vectors for the current meters at Station 7 deployed on 7 July 1979-----	58
15. U component, V component, and temperature plots versus time for the current meter at 158 m depth at Station 7 deployed on 7 July 1979-----	59

16.	U component, V component, and temperature plots versus time for the current meter at 231 m depth at Station 7 deployed on 7 July 1979-----	60
17.	U component, V component, and temperature plots versus time for the current meter at 356 m depth at Station 7 deployed on 7 July 1979-----	61
18.	Point Sur Upwelling Index and stickplots of hourly current vectors for the current meters at Station 2 deployed on 21 July 1979-----	62
19.	U component, V component, and temperature plots versus time for the current meter at 165 m depth at Station 2 deployed on 21 July 1979-----	63
20.	U component, V component, and temperature plots versus time for the current meter at 237 m depth at Station 2 deployed on 21 July 1979-----	64
21.	Point Sur Upwelling Index and stickplots of hourly current vectors for the current meters at Station 7 deployed on 7 October 1979-----	65
22.	U component, V component, and temperature plots versus time for the current meter at 127 m depth at Station 7 deployed on 7 October 1979-----	66
23.	U component, V component, and temperature plots versus time for the current meter at 200 m depth at Station 7 deployed on 7 October 1979-----	67
24.	Point Sur Upwelling Index and stickplots of hourly current vectors for the current meters at Station 2 deployed on 24 November 1979-----	68
25.	U component, V component, and temperature plots versus time for the current meter at 194 m depth at Station 2 deployed on 24 November 1979---	69
26.	U component, V component, and temperature plots versus time for the current meter at 266 m depth at Station 2 deployed on 24 November 1979-----	70
27.	Point Sur Upwelling Index and stickplots of hourly current vectors for the current meters at Station 7 deployed on 3 March 1980-----	71
28.	U component, V component, and temperature plots versus time for the current meter at 113 m depth at Station 7 deployed on 3 March 1980-----	72

29.	U component, V component, and temperature plots versus time for the current meters at 186 m depth at Station 7 deployed on 3 March 1980-----	73
30.	U component, V component, and temperature plots versus time for the current meter at 311 m depth at Station 7 deployed on 3 March 1980-----	74
31.	Energy density spectrum of current meter at 152 m depth at Station 7 deployed on 5 January 1979-----	75
32.	Energy density spectrum of current meter at 223 m depth at Station 7 deployed on 5 January 1979-----	76
33.	Energy density spectrum of current meter at 169 m depth at Station 2 deployed on 23 April 1979-----	77
34.	Energy density spectrum of current meter at 241 m depth at Station 2 deployed on 23 April 1979-----	78
35.	Energy density spectrum of current meter at 158 m depth at Station 7 deployed on 7 July 1979-----	79
36.	Energy density spectrum of current meter at 231 m depth at Station 7 deployed on 7 July 1979-----	80
37.	Energy density spectrum of current meter at 356 m depth at Station 7 deployed on 7 July 1979-----	81
38.	Energy density spectrum of current meter at 165 m depth at Station 2 deployed on 21 July 1979-----	82
39.	Energy density spectrum of current meter at 237 m depth at Station 2 deployed on 21 July 1979-----	83
40.	Energy density spectrum of current meter at 127 m depth at Station 7 deployed on 7 October 1979-----	84
41.	Energy density spectrum of current meter at 200 m depth at Station 7 deployed on 7 October 1979-----	85
42.	Energy density spectrum of current meter at 194 m depth at Station 2 deployed on 24 November 1979---	86
43.	Energy density spectrum of current meter at 266 m depth at Station 2 deployed on 24 November 1979---	87
44.	Energy density spectrum of current meter at 113 m depth at Station 7 deployed on 3 March 1980-----	88

45.	Energy density spectrum of current meter at 136 m depth at Station 7 deployed on 3 March 1980-----	89
46.	Energy density spectrum of current meter at 311 m depth at Station 7 deployed on 3 March 1980-----	90
47.	Progressive vector diagram for the current meter at 127 m depth at Station 7 from 9 January to 28 February 1979-----	91
48.	Progressive vector diagram for the current meter at 223 m depth at Station 7 from 9 January to 26 February 1979-----	92
49.	Progressive vector diagram for the current meter at 169 m depth at Station 2 from 24 April to 13 June 1979-----	93
50.	Progressive vector diagram for the current meter at 241 m depth at Station 2 from 24 April to 12 June 1979-----	94
51.	Progressive vector diagram for the current meter at 158 m depth at Station 7 from 9 July to 30 August 1979-----	95
52.	Progressive vector diagram for the current meter at 231 m depth at Station 7 from 9 July to 29 August 1979-----	96
53.	Progressive vector diagram for the current meter at 356 m depth at Station 7 from 9 July to 30 August 1979-----	97
54.	Progressive vector diagram for the current meter at 165 m depth at Station 2 from 23 July to 11 September 1979-----	98
55.	Progressive vector diagram for the current meter at 237 m depth at Station 2 from 23 July to 13 September 1979-----	99
56.	Progressive vector diagram for the current meter at 127 m depth at Station 7 from 9 October to 29 November 1979-----	100
57.	Progressive vector diagram for the current meter at 200 m depth at Station 7 from 9 October to 29 November 1979-----	101

58. Progressive vector diagram for the current meter
at 169 m depth at Station 2 from 27 November 1979
to 16 January 1980----- 102
59. Progressive vector diagram for the current meter
at 266 m depth at Station 2 from 27 November 1979
to 18 January 1980----- 103
60. Progressive vector diagram for the current meter
at 311 m depth at Station 7 from 4 March to
15 April 1980----- 104
61. Progressive vector diagram for the current meter
at 186 m depth at Station 7 from 4 March to
12 April 1980----- 105
62. Progressive vector diagram for the current meter
at 311 m depth at Station 7 from 4 March to
10 April 1980----- 106

I. INTRODUCTION AND BACKGROUND

Eastern boundary currents are the subject of scientific investigation for a variety of reasons, particularly the impact of these currents on the fishing industry. Ryther (1969) concluded certain fishing grounds such as those off Peru, California, northwest and southwest Africa, Somalia, and the Arabian coast are so fertile, that they supply over half of the world's fish harvest, yet constitute less than one percent of the oceans. These fishing grounds are invariably located close to shore, and their great fertility is due to frequent replenishment of near-surface nutrients from a few hundred meters deep in the open ocean offshore. The primary process for this is coastal upwelling, which in the Western Hemisphere is associated most markedly with the eastern boundary currents off North and South America. The economic need to understand these currents is made evident by the devastation of the coastal regions of Ecuador and Peru in 1982-1983 by the sudden influx of warm water termed El Niño. The socioeconomic effects included; flooding, landslides, destruction of transportation facilities, huge agricultural losses, disturbance of coastal fisheries, and loss of life (Halpern et al., 1983). This warm water influx takes place from

time-to-time, and recovery from a severe occurrence may take several years (Smith 1983).

Off the North American west coast, the eastern boundary flow regime is known as the California Current System. A comprehensive summary of the present knowledge of this system is given by Hickey (1978). The California Current System includes the southward flowing California Current, and a number of manifestations of a counter-flow: the California Undercurrent, the Davidson Current, and the Southern California Countercurrent. This system is part of the general circulation of the North Pacific Ocean which is dominated by an oceanwide, clockwise circulation known as the North Pacific Gyre. The eastern limb of the gyre is the California Current System, which extends along the North American continent from southern Canada to Mexico. The system includes both poleward and equatorward flows which vary on many time-scales. There are, for example, inter-annual variations such as El Niño, seasonal variations, and large variations with periods associated with weather systems. The California Current is a slow and broad equatorward surface flow, branching from the North Pacific Current, and marked by cold subarctic water type. The waters of the various countercurrents may be characterized by their admixture with water of equatorial origin which has relatively high levels of temperature, salinity and phosphate, and relatively low dissolved

oxygen. During the winter months a surface current with poleward flow occurs in nearshore regions off the west coast of the United States. This current, inshore of the California Current, is known as the Davidson Current and is ordinarily found north of Point Conception. The Davidson Current may be a surface manifestation of the California Undercurrent. The Southern California Countercurrent is the name applied to the poleward flow from San Diego to Point Conception; during winter months, this nearshore flow is sometimes continuous with the Davidson Current.

The study of eastern boundary currents is of both theoretical and practical interest. Dynamical models with features of observed eastern boundary currents have been developed since the turn of the century. Ekman (1905) described the effects of a steady wind blowing on an ocean, and stated the concepts now known as the Ekman spiral and the Ekman transport. Sverdrup, Johnson, and Fleming (1941) provided some understanding of the dynamics of the upwelling process. Munk (1950) computed the mass transports in a wind-driven ocean from the curl of the estimated wind stress.

Recent models include the two-dimensional and three-dimensional upwelling models, and sea breeze produced upwelling models reviewed by O'Brien (1977). These models considered the influences of horizontal boundaries, bottom topography, and the variability of wind stress on the

ocean. The first numerical model of coastal upwelling was constructed by O'Brien and Hurlburt (1972); this two-layer model successfully predicted the observed equatorward jet but failed to produce a poleward undercurrent. Suginoohara (1974) used a model with a straight coast and a bottom topography which did not vary in a coastwise direction. His model succeeded in developing a poleward flow in the lower layer. A later review of models is given by Allen (1980). These models permit inferences, such as the effects of shelf width and coastal winds, to be made about shelf-flow motions which have time scales like those of the atmospheric weather systems which drive them. Irregularities of the coastline and bottom topography force three-dimensional motions. However, there has been little theoretical work in this area until recently. An important conclusion from the models is that the currents arise from and are maintained by both local and remote atmospheric forcing. Significantly improved models of coastal upwelling include more realistic wind stress and finer resolution of bottom topography, especially the shelf break and steep bottom slopes.

Complementing models are field experiments which provide the basis for their motivation and verification. Two recent comparisons of models to field observations are Hickey (1980) and Janowitz (1980). Hickey used the two-dimensional, baroclinic, time-dependent model of

Hamilton (1978) and found it to be effective for time periods as long as fifteen days in predicting the displacement of isopycnals off the Oregon coast. Janowitz's comparison of a model of time-dependent quasi-geostrophic upwelling to moored meter data concluded tentatively that the model may have some validity, but further comparisons and verification should be undertaken.

Early observational studies of the California Current System emphasized relatively large-scale motions. Sverdrup and Fleming (1941) utilized T-S relationships to define the origins of water of two sorts (in northern hemispheric eastern boundary flows): northern water with increasing salinity as temperature decreases with depth and southern water with relatively constant salinity as temperature decreases. That the warmer water was a northward-flowing current was also demonstrated by Sverdrup and Fleming (1941) utilizing geostrophy; later, Reid, et al. (1958) showed that geo-strophic shear of the flow at the 200-dbar surface with respect to the 500 and the 1000-dbar surfaces indicates a northward flowing undercurrent. During the fifties and early sixties most Lagrangian current measurements were limited to drift bottle estimates of surface currents. One important exception was the tracking (for a few days) of deep drogues by Reid (1962), which also indicated a northward-flowing undercurrent off the central California coast. It is in the last decade that moored

current meters have provided a means to examine details of the flow over long time-periods. Moored current meters can be positioned to give direct measurements of the currents over extended periods (approximately two months for the Aanderaa meter, if a ten-minute sampling interval is used). Moored meters provide an excellent means for detailed local studies to elucidate better the properties, relationships, and interactions of the several portions of the California Current System. Studies of the California Current System during the 1960's using moored meters were primarily of the coastal waters off Oregon and Washington. While few current measurements have been made in the California Current and reliable wind stations are sparse, continuing studies off Washington and Oregon by Hickey (1979, 1980) and Huyer et al. (1979) show a significant relationship between local wind forcing and currents. Hickey stated that the seasonal variation of the nearshore region of strong flow appears to be related to the seasonal variation of the alongshore component of wind stress at the coast. Huyer et al. show that the transition from the predominantly northward surface currents of the winter oceanographic regime to the predominantly southward surface currents of the spring oceanographic regime over the Oregon continental shelf occurs within a period of several days during a strong southward wind event. Recent work for waters off the central region of the California

coast includes descriptive studies by Wickham (1975), Coddington (1979) and Dreves (1980). Wickham (1975) made salinity-temperature-depth (STD) sections, and parachute drogue observations off Monterey Bay. Wickham found the California Countercurrent to be present 15 km off the coast in August 1972 and in August 1973. Coddington (1979) compared direct current measurements from an array moored off Cape San Martin to indirect measurements from geostrophy. Coddington found the California Countercurrent to be present during the study period from November 1978 to February 1979. Dreves (1980) studied the relationship between local sea level gradient and alongshore flow for the same study period as Coddington. Dreves found that current and sea level gradient energy distributions were in close agreement, showing high energy concentration at the low frequency end of the spectrum.

The region of the central California coast off Cape San Martin (Figure 1) was chosen for study for several reasons: there is relatively little ship traffic or fishing and, consequently, less risk of current meter damage or loss; the bottom topography is relatively devoid of complications, consisting of an extremely narrow shelf, sharp shelf break, and depth contours approximately parallel to the coast; additionally, the close proximity of the study area to Monterey was a logistical convenience.

The current meter data used by Coddington and Dreves,

some six sets of current meter observations spanning six months from 25 July 1978 until 22 January 1979, have been augmented as part of the continuous monitoring of the countercurrent off Cape San Martin. An observational data base of direct current measurements of more than one year's duration now exists.

The objective of this study is to provide a preliminary analysis of current meter data for the period January 1979 to April 1980.

II. DIRECT CURRENT OBSERVATIONS

A. DATA COLLECTION

The data for this study were collected using Aanderaa Model RCM-4 recording current meters, which are self-recording and intended to be anchored in the ocean below the wind wave zone; they record current speed and direction and water temperature.

The meters were deployed off Cape San Martin, California, from August 1978 until July 1980 (see Figure 2). The station locations are shown in Figure 3. The present study covers the period from January 1979 to May 1980. Coddington (1979) and Dreves (1980) have discussed data collected during the period from April 1978 to January 1979. Deployment of the arrays was accomplished with the Naval Postgraduate School's research vessel ACANIA. Each mooring of several meters was launched by being strung out behind the ship, the uppermost meter and flotation devices first and the anchor last. The array's descent was slowed by a small drogue about two meters in diameter attached to the anchor. An array of three meters was used at Station 2 ($35^{\circ} 52.16'N$, $121^{\circ} 33.76'W$) and four meters at Station 7 ($35^{\circ} 51.4'N$, $121^{\circ} 46.54'W$). They were arranged approximately as depicted in Figure 4. The anchor consisted of

one or two railroad wheels attached to an AMF-Sealink Model 242 acoustic release. Benthos 17-inch glass spheres in plastic hard hats (55 pounds net buoyancy each) were used to provide wire tension, with two spheres directly above each current meter and six above the release. The entire array was moored below the region of strong surface wave action and was recovered by acoustically activating the release. Upon recovery the meters were returned to the laboratory for maintenance prior to subsequent redeployment.

B. DATA PROCESSING

The data were recorded on three-inch reels of 1/4-inch audio tape (Scotch Brand number 295) at ten-minute sampling intervals. Conversion of the data from the tapes recorded by the RCM-4 meters into a computer-acceptable format was accomplished with a Hewlett-Packard 9845 computer and an Aanderaa tape translator. The 1/4-inch tape was played back on a Wollensach audio deck and an oscilloscope was used to give a visual confirmation that data were present and of appropriate amplitude. The data were then translated from long and short to high and low voltage pulses and recorded on IBM-compatible 9-track tape on a Kennedy 9-track tape recorder. The Hewlett-Packard 9845 computer was also used to plot and print portions of the data.

Five different programs were used with the Naval Postgraduate School's IBM 360 computer in processing the data. They are listed in Appendix D. The initial program reads in the raw data from the 9-track magnetic tape, allows an initial look at the data if desired, and stores the data in mass storage for quicker, more efficient utilization. The second program applies temperature, speed, and direction calibrations to the data for each current meter. The third program reads in the calibrated output from program two, identifies missing records, and uses established cut-off parameters to suppress noise. Temperatures greater than 12°C , and less than 5°C are discarded, along with current speeds in excess of 100 cm-s^{-1} . Discarded and missing records are filled in by the following process: upon encountering a faulty value, searching continues until a value is found that meets the acceptance criteria. Linear interpolation is used to obtain fill-in values. Initial looks at the data revealed only minimal gaps in the records. Program three, by means of a binomial, converts the data record from ten-minute values to hourly values and then produces four plots. Currents are presented in the form of stickplots, and three other plots display U and V components of the current (respectively, eastward and northward for positive values), and temperature as functions of time. The fourth program reads in the output of program two, fills in missing and

faulty records, and then performs a spectrum analysis of the data. Its output consists of two plots of frequency versus power density for onshore and alongshore components of current. The fifth program uses the hourly records produced in program three to construct progressive vector plots. Two of the current meters used in the study were very noisy and gave unrealistically high indications of the speed. These noisy data are not shown here.

III. STUDY OBJECTIVES

The objective of this study is to provide a preliminary analysis of the current meter data. Questions to be considered are:

1. Do the data reveal seasonal variations of the flow?
2. Do the data reveal differences or similarities in the flow between Stations 2 and 7?
3. Are there indications of mesoscale events?
4. Are such mesoscale events coherent with respect to depth and/or position?
5. Is there a generalization about variation with depth that can be made?
6. How do the currents appear to be related to Bakun's coastal upwelling index (Bakun, 1980)?

IV. DESCRIPTION AND ORGANIZATION OF GRAPHICS

To highlight the salient features of the variations, and to examine them in the framework of Section III the data are presented in several ways. There are seven different graphical representations in Appendixes A, B, and C. These plots are:

1. Time series of Bakun's coastal upwelling index (Bakun, 1980).
2. Time series of current vectors.
3. Time series of eastward components of the current vectors.
4. Time series of northward components of the current vectors.
5. Time series of temperature.
6. Spectrum analyses of alongshore flow and on/offshore flow.
7. Progressive vector diagrams.

The plots are organized chronologically according to deployment date of the meters, beginning 5 January 1979 and ending in March 1980.

In Appendix A there are sets of time series. For example, Figure 8 and those like it contain time series of Bakun's coastal upwelling index (UI), and current series

(stickplots), in this case for the meters deployed on 5 January 1979 at Station 7, permitting visual comparison of one aspect of local forcing and the associated motions. The coastal upwelling indices are indicative of onshore-offshore Ekman transport, as estimated from wind stress at the position in the vicinity of Point Sur indicated in Figure 1. The procedure for calculating upwelling indices is presented in detail by Bakun (1973). The stickplots are graphical depictions of current speed and current direction. Time-scales are indicated along the top and bottom of Figure 5, and the units of measurement for the ordinates are shown on the left side of the figure. Pertinent information on the figures of this type include: station number, date of deployment, meter serial number, and depth of meter deployment.

Another type is represented by Figures 6 and 7. They depict U, V, and T for the two current meter records represented in Figure 8, where U (positive) is the eastward component of the current vector, V (positive) is the northward component of the current vector, and T is the temperature. Again, time scales and pertinent station information are given in the figure. The time series of these variables are complementary to the progressive vector diagrams found in Appendix C since they accentuate higher frequency events such as inertial and tidal oscillations.

The figures in Appendix B contain spectrum analyses of

alongshore flow and on/offshore flow for each current meter. The abscissa (frequency) and the ordinate (power density function) are clearly labeled, and each figure also lists station number, meter serial number, meter deployment depth, and date of deployment. The spectrum analyses indicate regions of high energy in the frequency domain and suggest forces at work.

Appendix C contains the progressive vector diagrams (PVD). The vertical and horizontal scales are equal (kilometers), and true North is indicated. Crosses are positioned at 3-day intervals, and the letter "F" indicates the final plotted position. In addition to station number, meter number, meter depth, and period of computation, the mean speed and mean direction for the entire period are indicated. The PVD's depict well the low frequency variations, so-called "events", such as eddies.

Appendix D contains the listings of the computer programs used to process and plot the current meter data.

V. ANALYSIS

A. RELATION BETWEEN CURRENT AND LOCAL WIND FORCING

The coastal mountains of California tend to deflect the low level winds so that they blow equatorward parallel to the coast. Consequently, the average Ekman transport is offshore (Stewart 1967). In the simple Ekman model, the offshore flow lies generally above the level at which our current meters are moored. But there are strong vertical motions (up-and-downwelling) and other intense mesoscale exchange mechanisms in the area of study which negate the application of the simple Ekman model to observed cross-slope flow and suggest the possibility of a deeper "virtual" Ekman layer extending well into the pycnocline.

In this section qualitative relations between current and local wind forcing are examined through use of the time series of stickplots and upwelling index and also by referring to Figure 5. These relations will first be examined separately at each mooring station, and then for the time period July - August 1979, when current meters were deployed at both Station 2 and Station 7. Finally, seasonal and geographical variations will be considered.

1. Analysis at Station 2

The corresponding UI and current velocity for Station 2, the inshore station, are shown in Figure 11 for the period from 23 April to mid-June. There are event-scale (ca. one week) changes in current direction and speed that appear to be coherent with depth. The upwelling index is positive all during the months of May and June with nearly periodic episodes of great intensity. It is reasonable that there be upwelling in this period of strong positive upwelling index ($\bar{U}I=+138$). The mean cross slope flow (\bar{U}') for this period (Table II) is small and positive, which indicates that the meters are below the Ekman layer. The poleward alongshore flow shown by the stickplots indicates the presence of a countercurrent at 169 and 241 m. Strong equatorward winds (positive UI) seem to correlate well with strong poleward flow of the countercurrent during this time period, especially at the level nearest the surface. Also, very large drops in the index are associated with a slightly lagging decrease in the poleward current speed, and increased variability in current direction during intervals centered on 21 May, 1 June, and 9 June (Figure 11).

Continuing at Station 2 in the period 21 July - 12 September 1979 (Figure 18), there is also an overall tendency for poleward flow associated with positive upwelling index especially at the level nearest the surface. The mean cross-slope flow (Table II) for this

period of strong upwelling index ($\overline{UI}=+125$) is negative; if an extended Ekman layer is postulated, this cross-slope flow can be interpreted as lying within a layer which includes both meters. The magnitude of UI declines during the latter part of this period. On a shorter time-scale (about 9 days) the rise and fall of the upwelling index is accompanied throughout the record, beginning about 10 August, by poleward currents during periods of high upwelling index, and equatorward or diminished poleward currents during periods of reduced upwelling index. Thus, decreases in the upwelling index clearly relate to decreases in, or disappearance of, the counter current on these time scales (ca. 9 days), especially at the greater depth, 237 m.

In the following period, 24 November 1979 through 18 January 1980, as shown in Figure 24, the upwelling index is further reduced ($\overline{UI}=-20$), becoming dominantly negative after mid December. The meter at 194 m (Figure 24) is suspect due to lack of direction changes. This could be the result of a stuck vane, or a malfunction in the sensor. The alongshore current at depth 266 m alternates between poleward and equatorward flows with durations between three and ten days. There is a marked change in currents after 23 December; they become weak and variable following a strong surge in the downwelling index at that time.

2. Analysis at Station 7

First consider the winter period January - February 1979, illustrated in Figure 8. The mean flow at both levels (152 m and 223 m) is predominantly poleward; but there are important event-scale variations. There are also alternating periods of positive and negative upwelling index during this period. The significant current variations and the upwelling index changes do not seem correlated. For example, from 5 to 10 January 1979 the currents at both depths were toward the southwest and during the next 15 to 17 days rotated clockwise. While the upwelling index varied erratically about zero, a similar rotation of the currents and unrelated variation of the upwelling index continued until about mid-February, when predominantly poleward flow again resumed, and the currents flowed in this direction for the remainder of the record, approximately twelve days. A fair conclusion for this period, when wind forcing is inconsistent and weak, is that there is no simple relation between the local upwelling index and the observed behavior of the currents on time scales of tens of days, and that some other mechanism than local forcing is involved.

During July and August 1979 (Figure 14), the index is positive and the flow at Station 7, is also predominantly poleward at 158, 231, and 356 m, especially in July. Large events involving reversals in the currents can be seen on

about 7 August and 24 August at all three observed levels. These events appear to occur at all depths almost simultaneously, which suggests that they are not directly related to the local wind.

During October and November 1979 (Figure 21) there is again a period of generally weak upwelling index when that index has no obvious relation to the currents. These currents were equatorward from 12 until to 30 October, followed by a reversal to become poleward from 1 through 21 November while the upwelling index again varied erratically near zero.

During the period 3 March through 12 April 1980 (Figure 27) poleward and equatorward flow alternate until about mid-March, while the upwelling index remains low. Following a rise in the upwelling index at that time (mid-March) and its persistence at high levels for nearly three weeks, predominantly poleward flow begins and persists for the remainder of the recorded period, some three weeks.

The meter at 113 m (Figure 27) is suspect due to lack of direction changes and small magnitude, and its data will be ignored.

3. Comparision of Stations 2 and 7

Current meter arrays were deployed at both Stations 2 and 7 during the period from 21 July to the end of August, providing an opportunity for examining horizontal

variations. As mentioned above, the currents at Station 2 (depicted in Figure 18) appear to respond with little or no lag to local forcing for this entire period. The response of the currents to local winds is not so clear at Station 7 (Figure 14). The currents at Station 7 may respond differently to local winds than currents at Station 2 because of the increased distance from the controlling boundary (coast). It is also possible that the response of the currents at Station 7 to local forcing may be masked by other influences. Certainly, there is no longer a nearly in-phase response of the current (note, for example, that on 27 August flow at Station 2 is predominantly poleward while flow at Station 7 is predominantly equatorward). If flow at Station 7 is being driven by local winds, the response must lag the wind.

Seasonally, the countercurrent was strongest during the spring months of 1979 at Station 2 (Figure 11). Geographically, the major discernable difference is the closer correlation between the current and the local forcing at Station 2 (inshore) than at Station 7 (offshore).

In summary, there are four important conclusions to the analysis of the currents and their relation to the upwelling index:

1. The entire record from January 1979 to April 1980 indicates currents are predominantly poleward at both stations, especially while Bakun's coastal upwelling index is high and positive.

2. Throughout the period, many events with time scales of tens of days occur at all recorded depths.

3. Current response to local forcing is more apparent at Station 2.

4. The countercurrent runs most strongly during the periods of high upwelling index at the nearshore station (Station 2).

B. SPECTRUM ANALYSIS

The current meter data are subjected to spectrum analysis in order to identify regions of high energy in the frequency domain, and consequently suggest forces at work in the study area.

The information from spectrum analysis, in this case via a program using Fast Fourier Transform (FFT), depends upon the record length and the sampling interval. The parameters used in the spectrum analysis program are:

Record length = TR = 1024 h

Sampling interval = Δt = 1 h

No. of points per record = N = 1024

Resolution = Δf = .0098 h^{-1}

Nyquist frequency = f_N = .5 h^{-1}

No. of frequencies resolved = M = $f_N/\Delta f$ = 512

No. of degrees of freedom = N/M = 2

The records available are typically about 50 days (1200 h) long; the maximum resolution attainable by FFT is, therefore, obtained from data sets of length 1024 hours.

For a fixed record length, however, high resolution is paid for at the expense of stability. The resolution with no averaging of spectral estimates over frequency is $\Delta f = 1024^{-1} \text{ h}^{-1}$; and for single spectra (with no ensemble averaging) the estimates of variance have only two degrees of freedom (and are thus uncertain indicators of the variance distribution).

For time series defined at equal time-intervals Δt , the highest frequency component discernable is given by $N_f = (2\Delta t)^{-1}$, the "Nyquist frequency". The variance of frequencies higher than this are attributed, spuriously, to lower frequencies. Such misread ("aliased") variance is thought to be of minor concern in the data sets of this study except for those few (discarded) with high frequency instrumental noise. Among forces known to be at work in the ocean which are likely to contribute to energetic currents are tidal and (possibly) inertial forces. Some of the most important components are the semi-diurnal tide-producing forces (Sverdrup, et al., 1942):

Name	Symbol	Period(h)	Frequency(h^{-1})
Principal lunar	M_2	12.42	.0805
Principal solar	S_2	12.00	.0833
Luni-solar	K_2	11.97	.0835

The inertial frequency and period, calculated with the average latitude (35.8°) of Station 2 and Station 7, are $f(i) = .0487 \text{ h}^{-1}$, and $T(i) = 20.5 \text{ h}$.

The spectral estimates consistently indicate energetic components at tidal and inertial frequencies as well as at periods of approximately 10 days. The dominant tidal components present are the semi-diurnal, with the most significant peaks appearing to be the luni-solar. In Table I are shown the approximate values of the low frequency, inertial, and semi-diurnal tidal peaks for both alongshore, and onshore/offshore motion. These values in Table I are taken from the spectrum analysis plots to show what, if any, relation there is between high energy and depth, season, and proximity of the shore. In general the spectra indicate greater energy for tidal, inertial, and low frequencies at the upper meters. It appears that motions at these frequencies are also more energetic in winter than in summer. Finally, tidal and low frequency energy are greater near shore, while energy in the inertial frequency is greater offshore.

C. INFERENCES FROM PROGRESSIVE VECTOR DIAGRAMS

The PVD's are helpful in observing low frequency variations and the mean currents which are summarized in Table II. As a meander, eddy, or wave in the countercurrent moves through a stations position the boundary between the poleward flow and equatorward flow moves about, with the current meters alternating between either side of that boundary. Such an occurrence is reflected in the PVD's as a current reversal.

TABLE I
COMPARISON OF HIGH ENERGY PEAKS (1000 CM. SQ. HOUR)

STATION	START DATE	DEPTH	LOW FREQ. (10 DAY)		INERTIAL		S.D. TIDAL	
			ALONG SHORE	ON/OFF SHORE	ALONG SHORE	ON/OFF SHORE	ALONG SHORE	ON/OFF SHORE
2	23 APR 79	169	5.3	0.5	1.0	0.5	8.0	6.5
		241	4.0	SMALL	1.0	0.5	11.0	5.0
2	21 JUL 79	165	17.0	0.5	1.0	0.3	3.0	1.7
		237	8.0	0.5	SMALL	0.2	3.0	1.2
2	24 NOV 79	194*	0.3	0.5	SMALL	SMALL	SMALL	0.1
		266	45.0	1.0	2.0	1.0	11.0	17.0
7	5 JAN 79	152	6.8	7.0	1.8	2.3	1.8	2.0
		223	1.5	5.4	0.6	0.5	1.4	0.8
7	7 JUL 79	158	2.6	17.0	0.2	SMALL	1.6	2.0
		231	2.0	5.1	0.4	SMALL	1.3	1.8
		356	0.8	1.0	0.9	0.7	0.5	0.6
7	7 OCT 79	127	1.0	1.6	4.5	3.4	3.7	3.8
		200	1.3	1.1	2.0	2.3	3.0	2.6
		113*	0.2	0.1	0.1	0.1	0.3	0.1
7	3 MAR 80	186	1.8	1.1	1.4	1.5	2.6	2.0
		311	0.9	0.2	1.8	1.8	5.0	1.2

S.D. = Semi-Diurnal

* = Meter is suspect

TABLE II
COMPARISON OF MEAN CURRENT AND TEMPERATURE

STATION	TIME	PERIOD	DEPTH	(azim. $\bar{\theta}$)	(°T)	\bar{V} (cm/sec)	(° cent.)	V' (cm/sec)	\bar{U}' (cm/sec)
2	23 APR	79	169	341.2	16.0	8.5	+ 16.0	+ 0.34	
	thru		241	340.4	11.1	8.0	+ 11.1	+ 0.08	
2	16 JUN	79	165	325.1	6.1	9.0	+ 5.89	- 1.57	
	thru		237	314.3	1.5	8.5	+ 1.35	- 0.65	
2	21 JUL	79	165	325.1	6.1	9.0	+ 5.89	- 1.57	
	13 SEP	79	237	314.3	1.5	8.5	+ 1.35	- 0.65	
2	24 NOV	79	194*	279.8	6.2	9.0	+ 3.08	- 5.38	
	thru		266	003.1	2.7	8.0	+ 2.48	+ 1.06	
2	18 JAN	80	152	354.8	4.6	9.4	+ 4.58	+ 0.39	
	9 JAN	79	223	16.6	4.3	8.6	+ 3.84	+ 1.93	
7	28 FEB	79	158	312.2	4.5	8.7	+ 3.56	- 2.76	
	9 JUL	79	231	330.6	5.8	8.3	+ 5.47	- 1.93	
7	30 AUG	79	356	338.6	2.8	7.4	+ 2.74	- 0.55	
	9 OCT	79	127	68.1	5.1	9.3	+ 1.05	+ 4.99	
7	29 NOV	79	200	70.6	4.1	8.4	+ 0.67	+ 4.05	
	4 MAR	80	113*	310.5	4.4	9.0	+ 3.40	- 2.80	
7	thru		186	328.7	3.4	8.0	+ 3.17	- 1.24	
	15 APR	80	311	8.2	2.7	7.0	+ 2.56	+ 0.84	

\bar{U}' = Mean cross-slope current
 \bar{V}' = Mean alongshore current
* = Meter is suspect

Two interesting features readily seen in the progressive vector diagrams Figures 47 through 62, are current reversals of long duration, and the mean current for the duration of the mooring. The mean current direction (θ), given as azimuth, speed (V), cm-s^{-1} , and temperature (T), degrees Celsius, for each current meter for the entire study period are shown in Table II; and they are also shown on the individual plots. Also shown in Table II are the mean onshore and alongshore current components respectively. The alongshore direction in this case is defined as 340° T for Station 2, and 350° T for Station 7, which represent the azimuths of the mean contours at those sites.

For both Stations 2 and 7 over the entire period, the seasonal and depth variations will be considered. The mean alongshore current is always poleward at all observed levels (from 127 m to 356 m) and at both stations. Mean alongshore current speeds were greater nearshore at Station 2, than offshore at Station 7. Mean alongshore current speed at the upper levels appears to vary only slightly seasonally at both stations, approximately 4 to 6 cm-s^{-1} , with the exception of the upper meter at Station 2, 23 April to mid-June, i.e., the counter current appears weak at observed depths, except in late spring.

The PVD's indicate predominantly unidirectional flow at the near-surface levels of Station 2, while at the deeper,

lower meters there were often current reversals and oscillations possibly associated with meanders, waves, and eddies. Current reversals occurred in greater numbers and were present at all depths at Station 7 which may possibly be due to Station 7 being near a boundary between north and south currents. The semidiurnal components of the currents are at times apparent in the PVD's as for example in Figures 49 and 57.

Shorter term variations are also indicated by the PVD's, in particular reversals. No apparent current reversals are present at the upper meter of Station 2, 24 April to mid-June (Figure 49), and only two minor reversals can be seen near the end of the record for the lower meter (Figure 50). At the same station from 23 July to mid-September, two current reversals of short duration are evident at the upper layer (Figure 54); and more than half a dozen current reversals of from three to twelve days in duration can be seen for the current at greater depth (Figure 55). Current reversals are not present at the upper level of Station 2 (Figure 58), 27 November 1979 to mid-January 1980, but several current reversals of approximately three to nine days duration can be seen at depth (Figure 59).

A single current reversal is present at both meters of Station 7 (Figures 47 and 48), 9 January to the end of February 1979. At the same station, 9 July to the end of

August 1979, three current reversals are apparent at the upper two meters (Figures 51 and 52), and two reversals can be seen in the lower meter (Figure 53). These reversals all appear to be of a relatively long duration, 15 to 20 d. Two current reversals are present at both meters of Station 7 (Figures 56 and 57), 9 October to 29 November 1979. For the period 4 March to 15 April 1980 at the same station, no reversals are seen in the upper meter (Figure 60), but several oscillations and reversals are seen in the two lower meters (Figures 61 and 62).

D. CROSS-SLOPE CURRENT

The mean cross-slope currents from Table II are plotted against time in Figure 5. The dominant feature of these currents is an annual variation with onshore flow in winter months and offshore in spring and summer. This annual variation correlates with the strong upwelling occurring in the spring and summer, and the weak upwelling index in the winter.

Qualitatively, the relation between the upwelling index and the cross-slope current means is consistent with a thick layer influenced by a modified surface Ekman regime.

E. TIME SERIES

The time series plots of U (positive-east) and V (positive-north) components were primarily used as an aid in interpreting the stickplot data. They are also useful for their resolution of high frequency variations. The

semidiurnal components of the currents are evident as well as the larger scale current oscillations indicated in the stickplots.

The temperature versus time plots also indicate the semidiurnal components and large-scale oscillations found in the stickplots. Approximate mean temperatures for the current meters at Station 2 and 7 throughout the record are shown in Table II. The temperature decreased with depth at all stations. The mean temperatures at Station 2 at all depths (Figure 6) became increasingly warmer during the period from April 1979 to January 1980, while the mean temperatures at Station 7 at all depths (Figure 7) became increasingly cooler. This is consistent with existing wind stresses, which would tend to uplift the isotherms at the nearshore station (Station 2) in the spring (strong upwelling index) and depress them in winter (weak upwelling index). The cooling continues at Station 7 at all depths from December 1979 until April 1980, and no simple explanation is apparent.

IV. CONCLUSIONS

A northward flowing current was found for the entire period of this study. It was strongest at the upper levels, roughly between 100 and 200 m. Seasonally, this countercurrent was strong during spring and substantially weaker during winter. The speed and direction of the countercurrent at any given time may differ markedly from the average flow. There were events on scales of tens of days which appeared to be qualitatively coherent between stations and also between depths at a given station. Frequent current reversals and oscillations occurred, consistent with the weak, poorly defined, broad flows associated with eastern boundary currents.

Bakun's coastal upwelling index is an indicator of possible wind-driven coastal upwelling. The coastal upwelling index is, in the mean, consistent with the observations of a deep cross-slope flow (Ekman layer), a large upwelling index corresponding to thickening of the Ekman layer. The countercurrent is present during the entire study, and the low frequency alongshore current is never equatorward.

Relatively high-energy peaks at semidiurnal tidal frequencies and inertial frequencies occurred in the

majority of the current records. Additionally, low frequency energy peaks were found at periods of about 10 d.

At Station 2, (nearshore), the alongshore component of these three frequencies tends to be greater than the on/offshore component, and generally speaking, the low frequency energy peak ($T = 10$ d) is dominant. At Station 7 (offshore), the on/offshore component of these three frequencies is noticeably greater, but there is no obvious pattern to the energy distribution.

The countercurrent was present at the study site, but it was not possible to unequivocally identify and correlate local forcing with the countercurrent. The vertical migration of the frontal boundary between equatorward and poleward flow was observed at both stations, but less often at the nearshore Station 2 than at Station 7. Hydrographic data from the study area for this time period were not examined at all, and deserve future consideration. Correlation of currents and wind or upwelling index, comparision of observed currents with predicitons of various models, and the relation of metered currents to those inferred from hydrographic data are recommended for future studies.

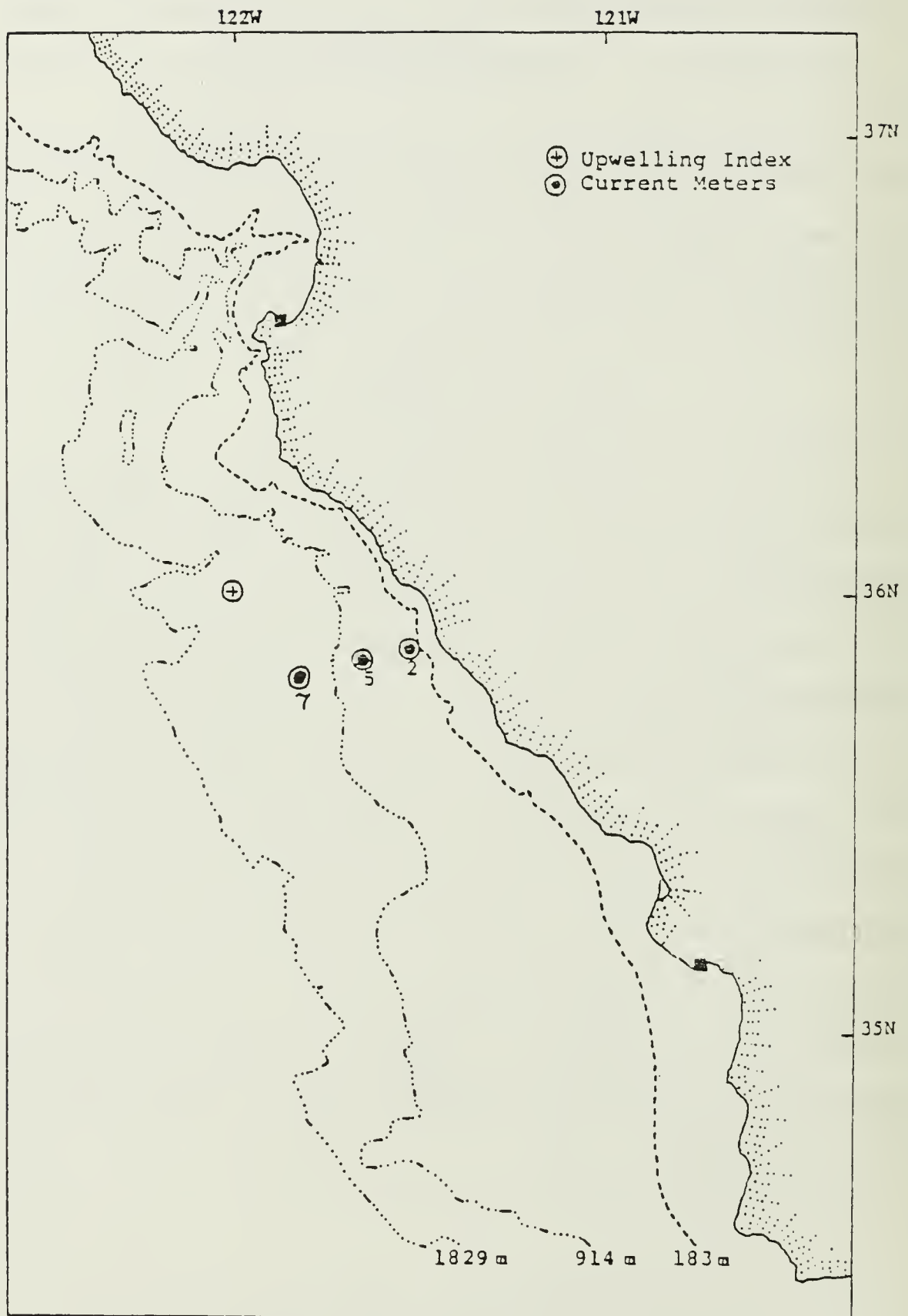


Figure 1. The study area.

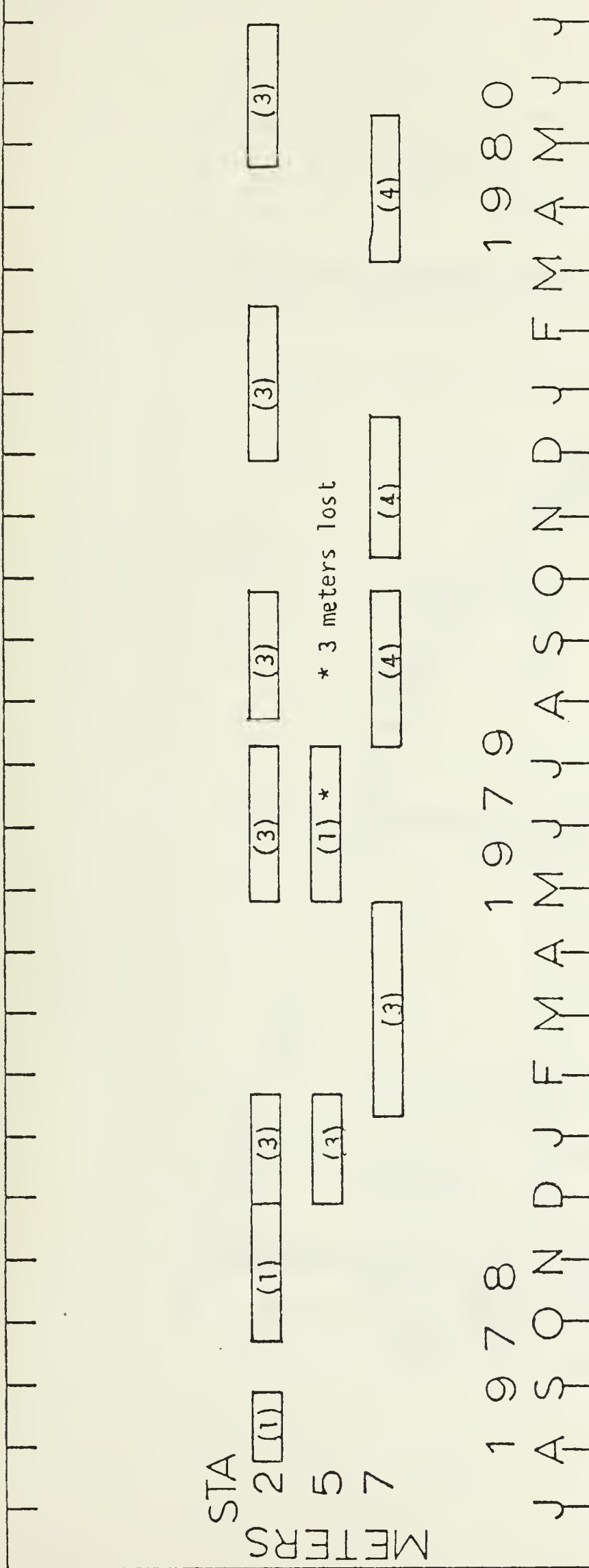


Figure 2. Chronology of current meter deployment.

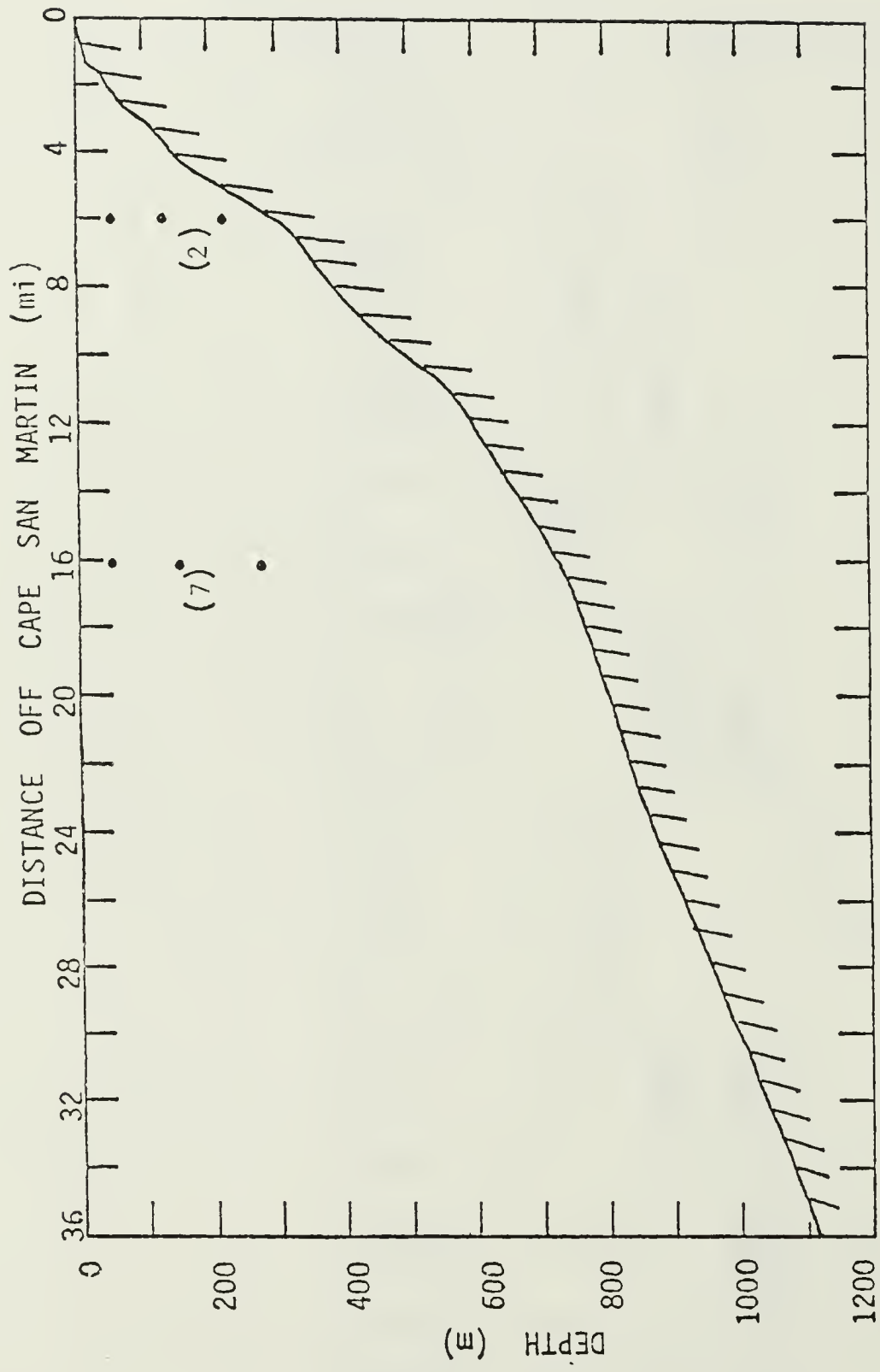


Figure 3. Vertical section showing representative locations of current meters off Cape San Martin, California.

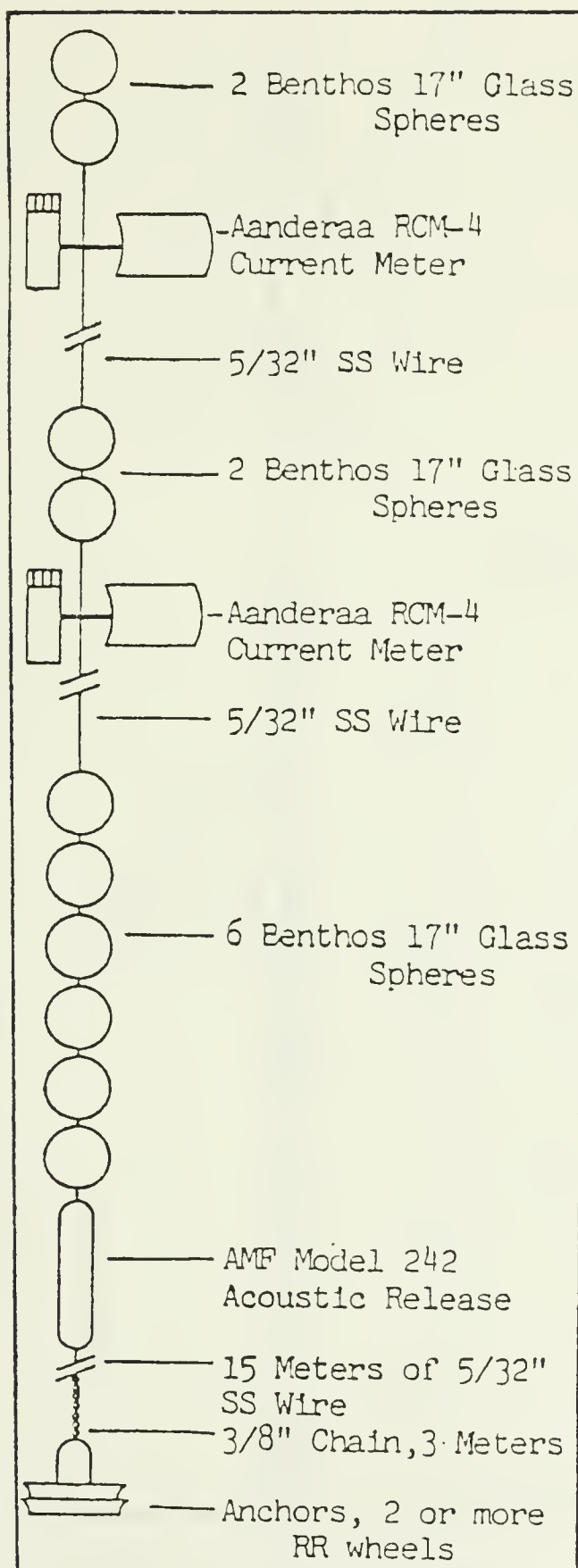


Figure 4. Current meter array.

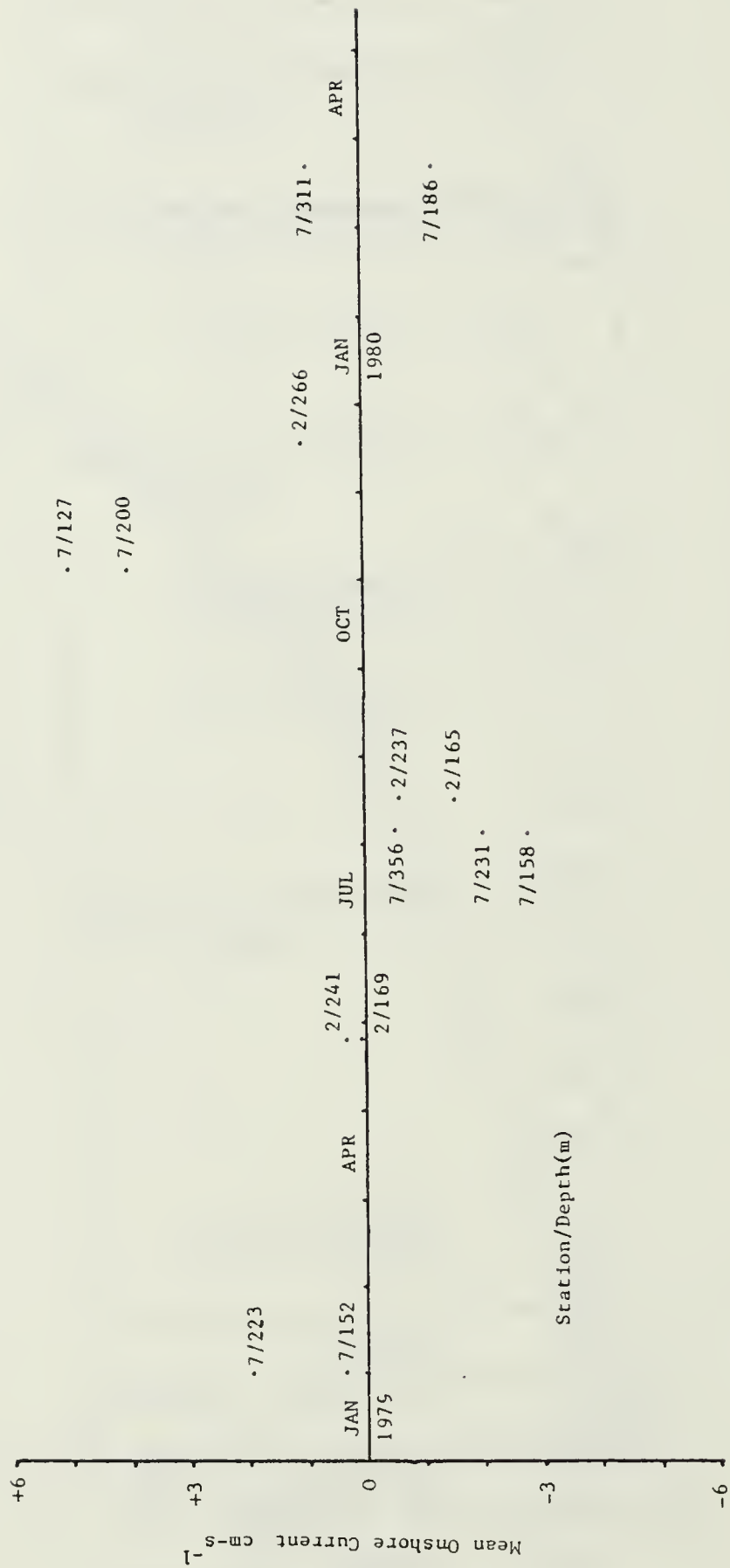


Figure 5. Mean onshore currents.

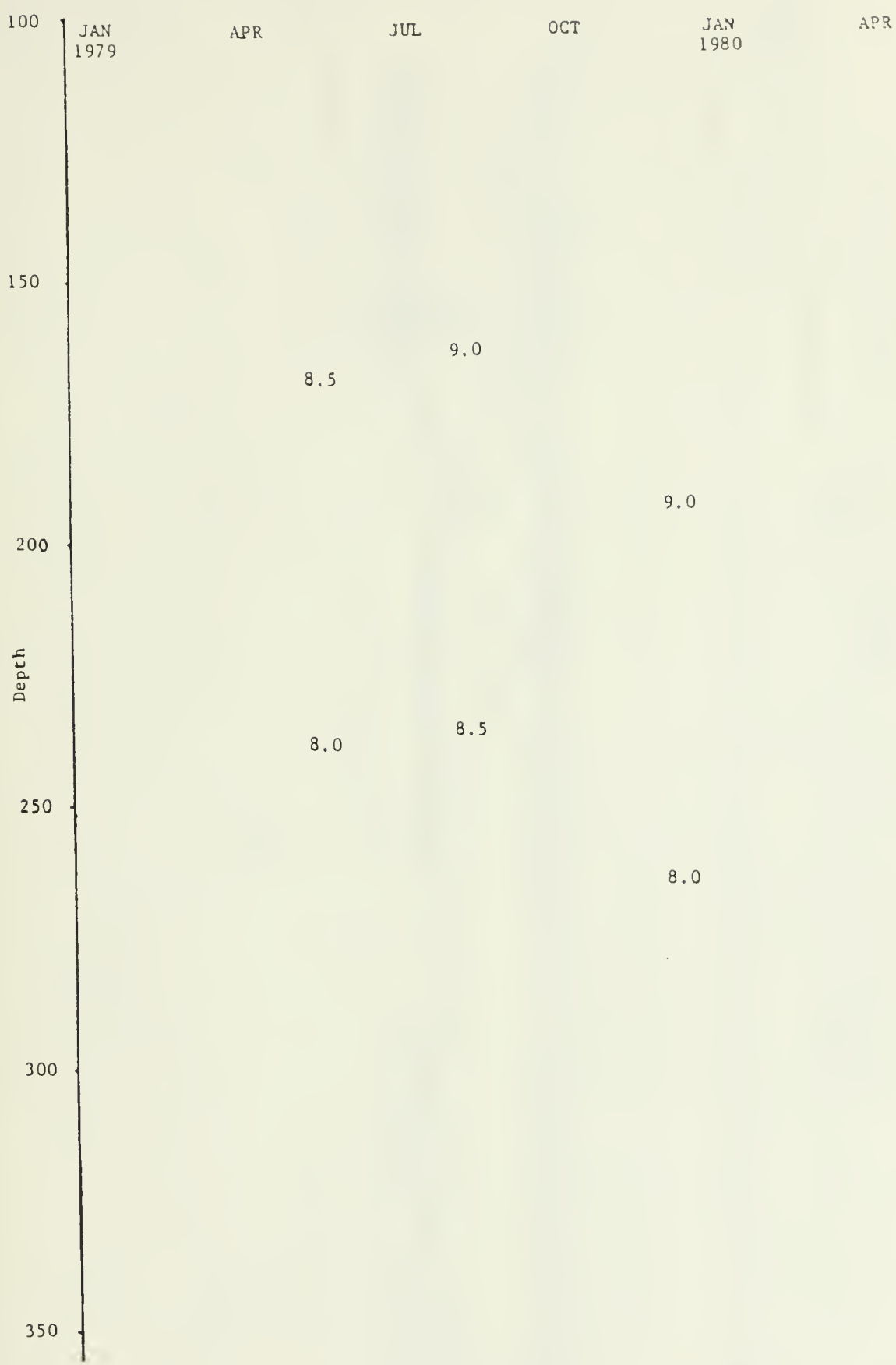


Figure 6. Mean temperatures at Station 2.

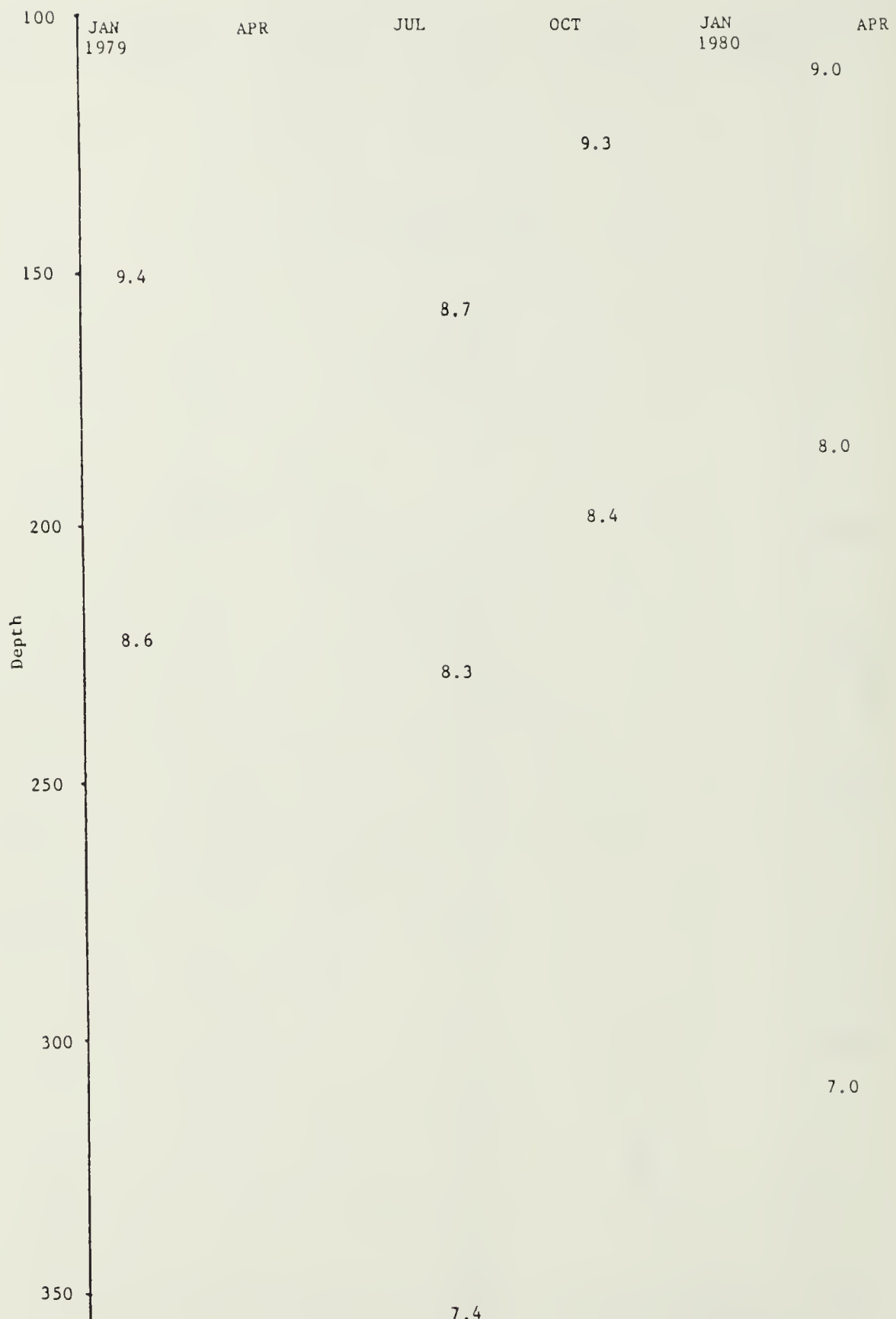


Figure 7. Mean temperatures at Station 7.

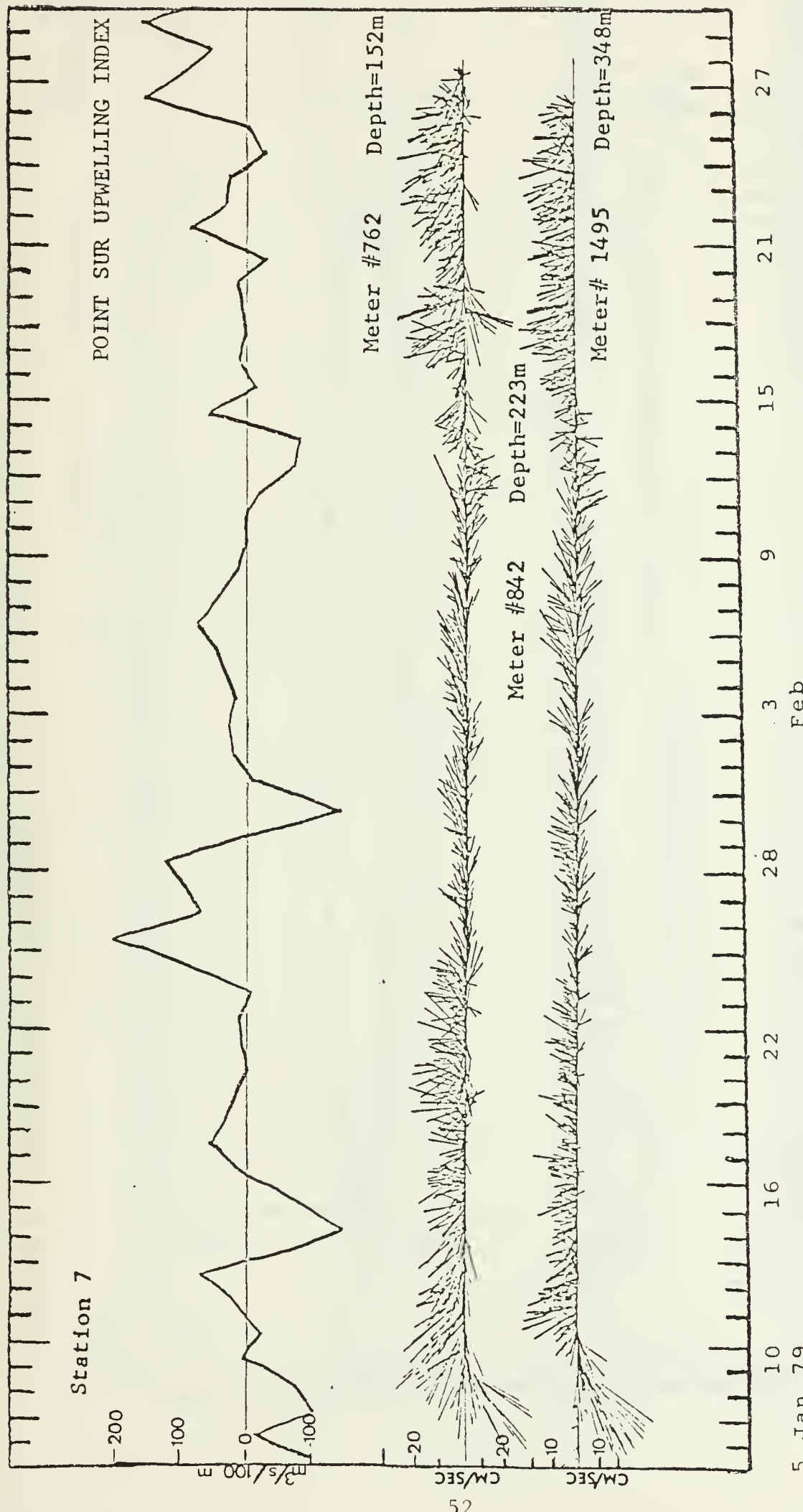


Figure 8. Point Sur Upwelling Index and stickplots of hourly current vectors for the current meters at Station 7 deployed on 5 January 1979.

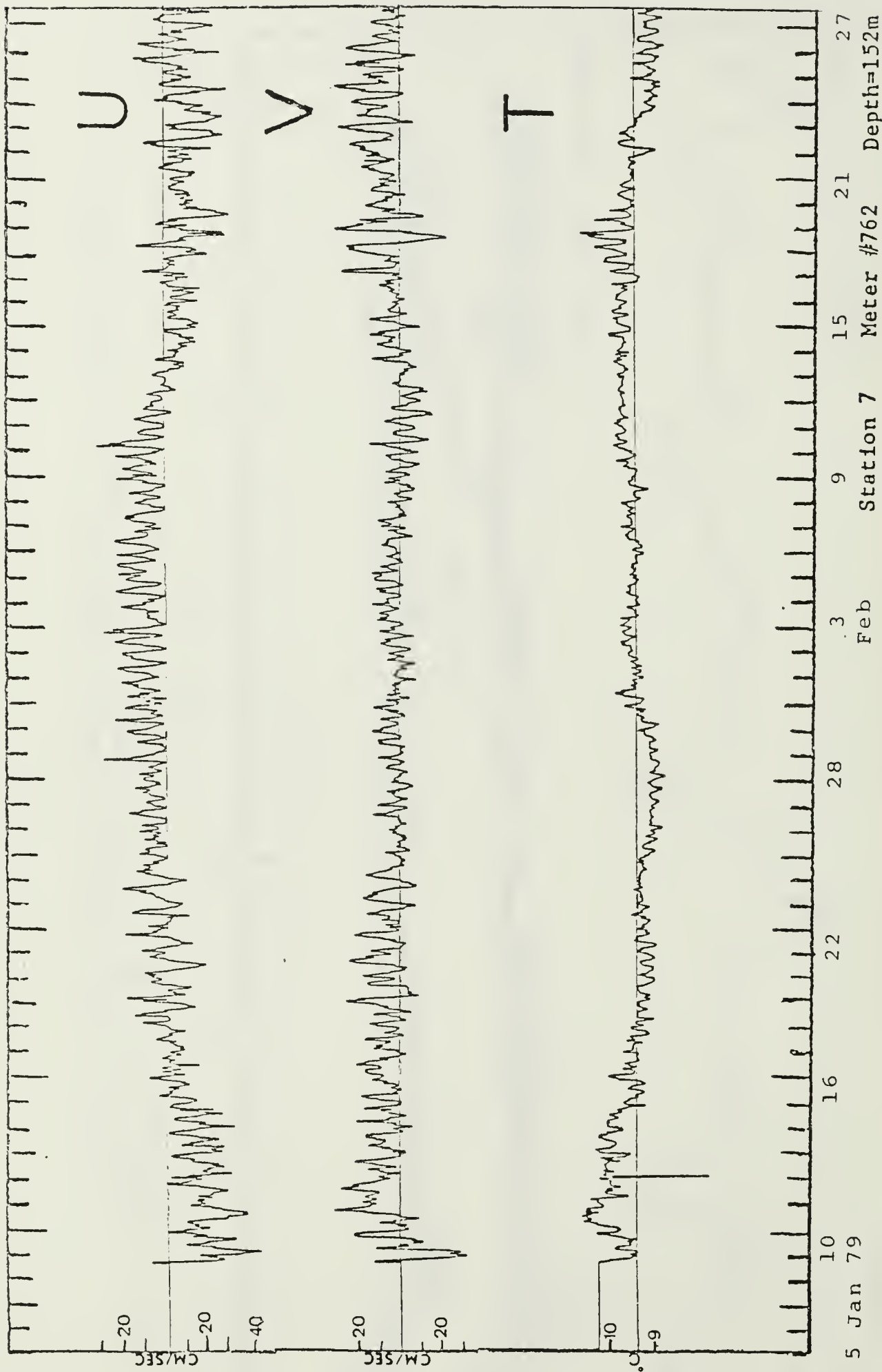


Figure 9. U component, V component, and temperature plots versus time for the current meter at 152 m depth at Station 7 deployed on 5 January 1979.

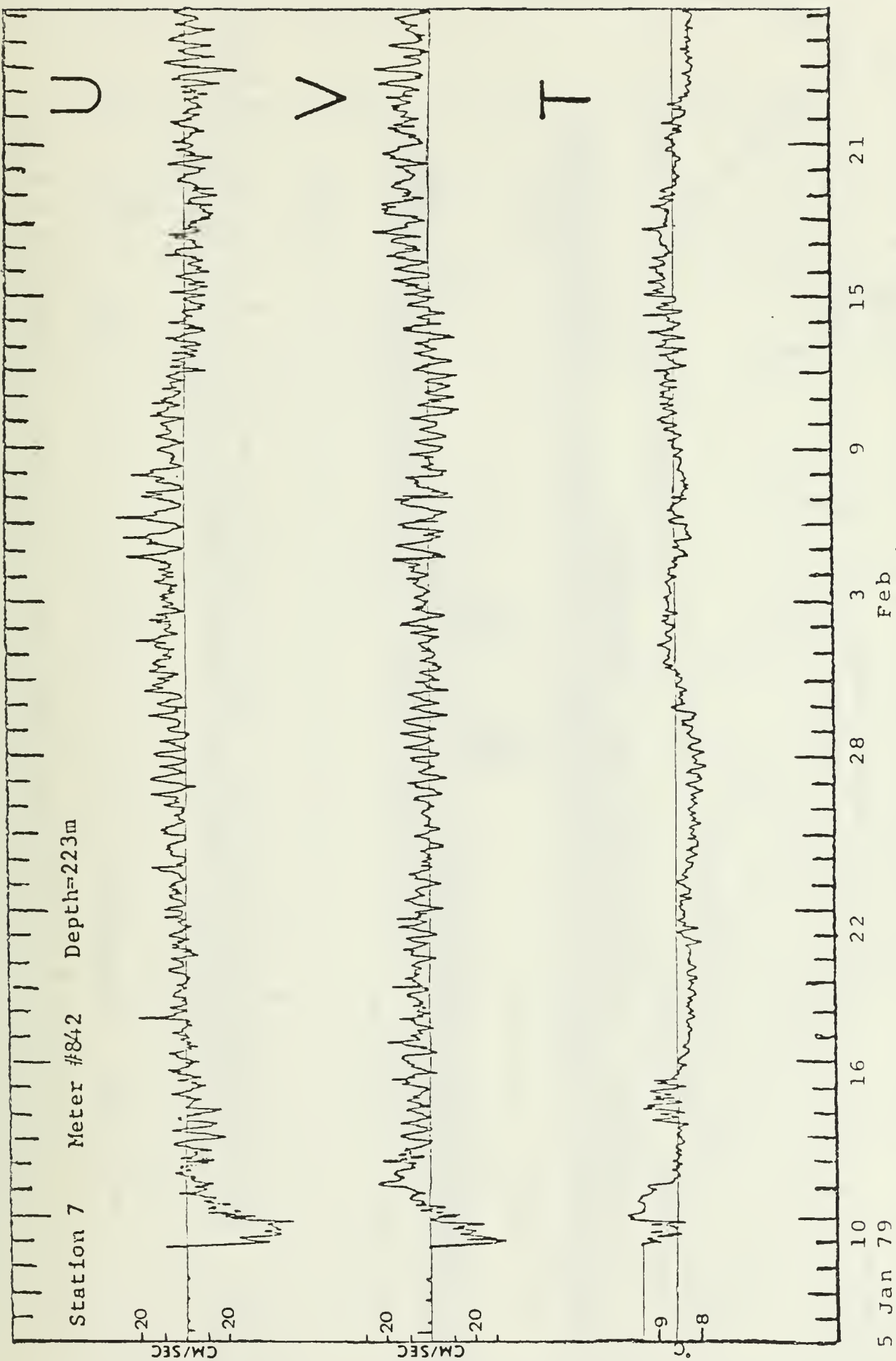


Figure 10. U component, V component, and temperature plots versus time for the current meter at 223 m depth at Station 7 deployed on 23 April 1979.

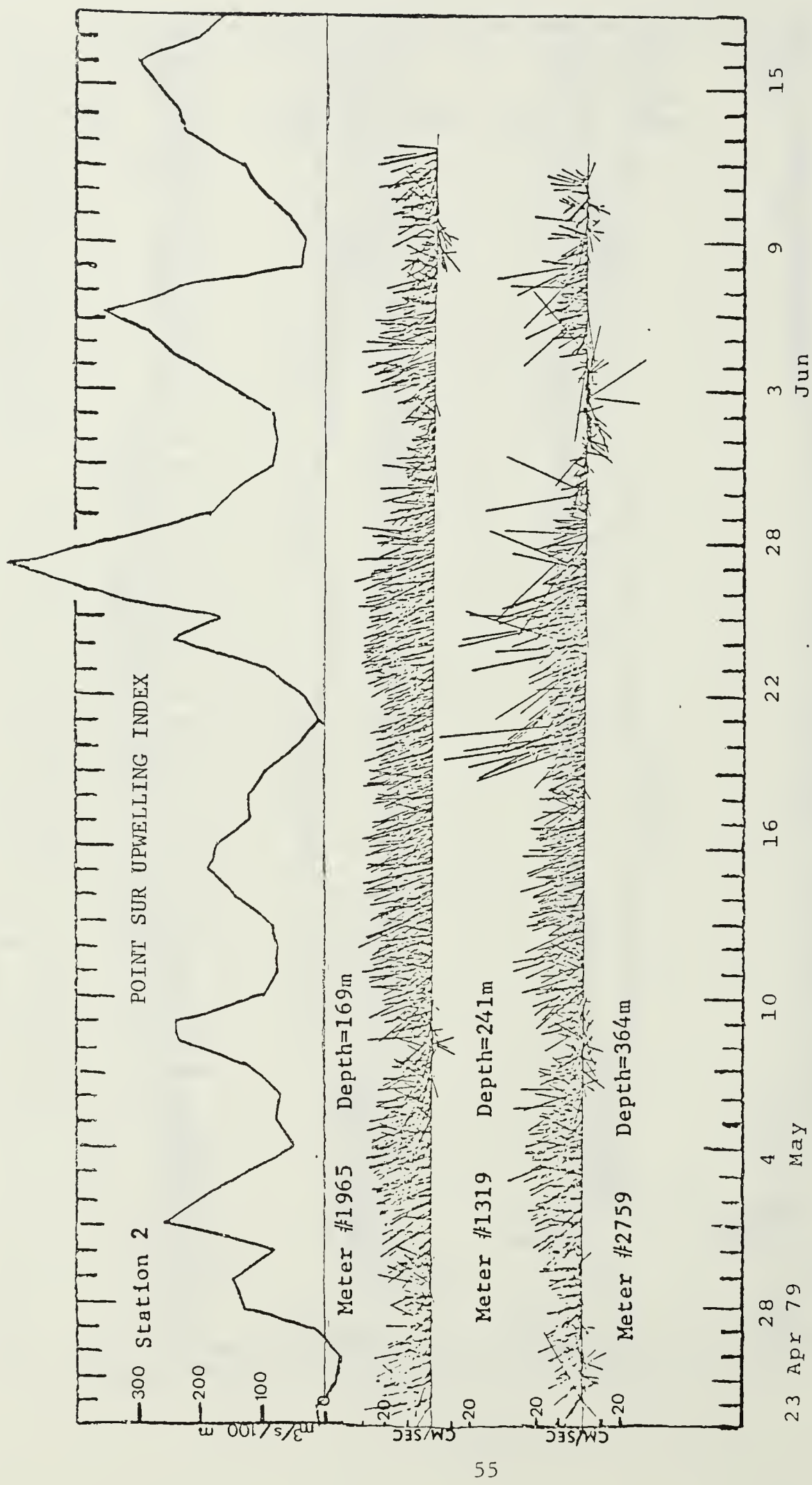


Figure 11. Point Sur Upwelling Index and stickplots of hourly current vectors for the current meters at Station 2 deployed on 23 April 1979.

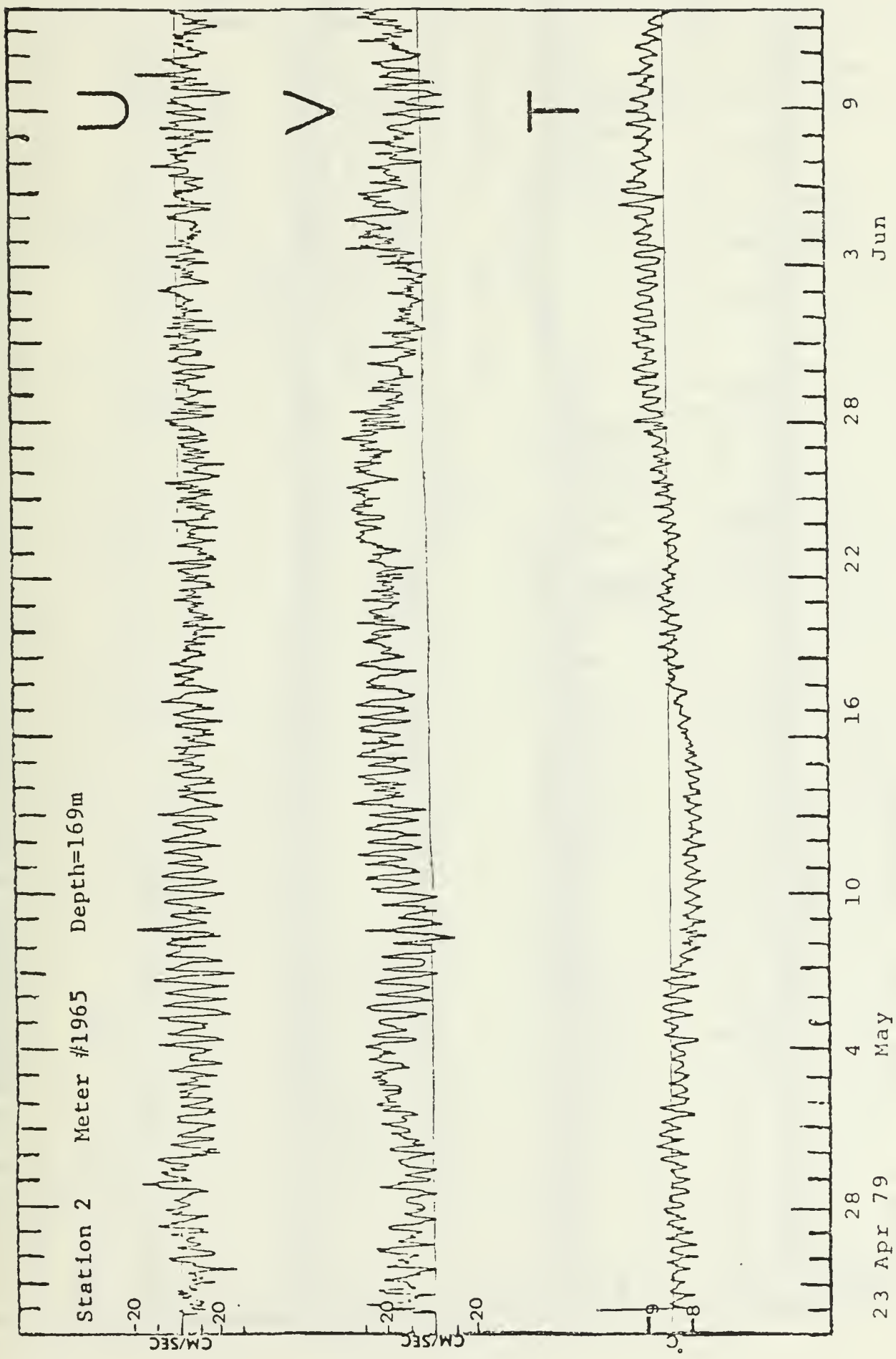


Figure 12. U component, V component, and temperature plots versus time for the current meter at 169 m depth at Station 2 deployed on 23 April 1979.

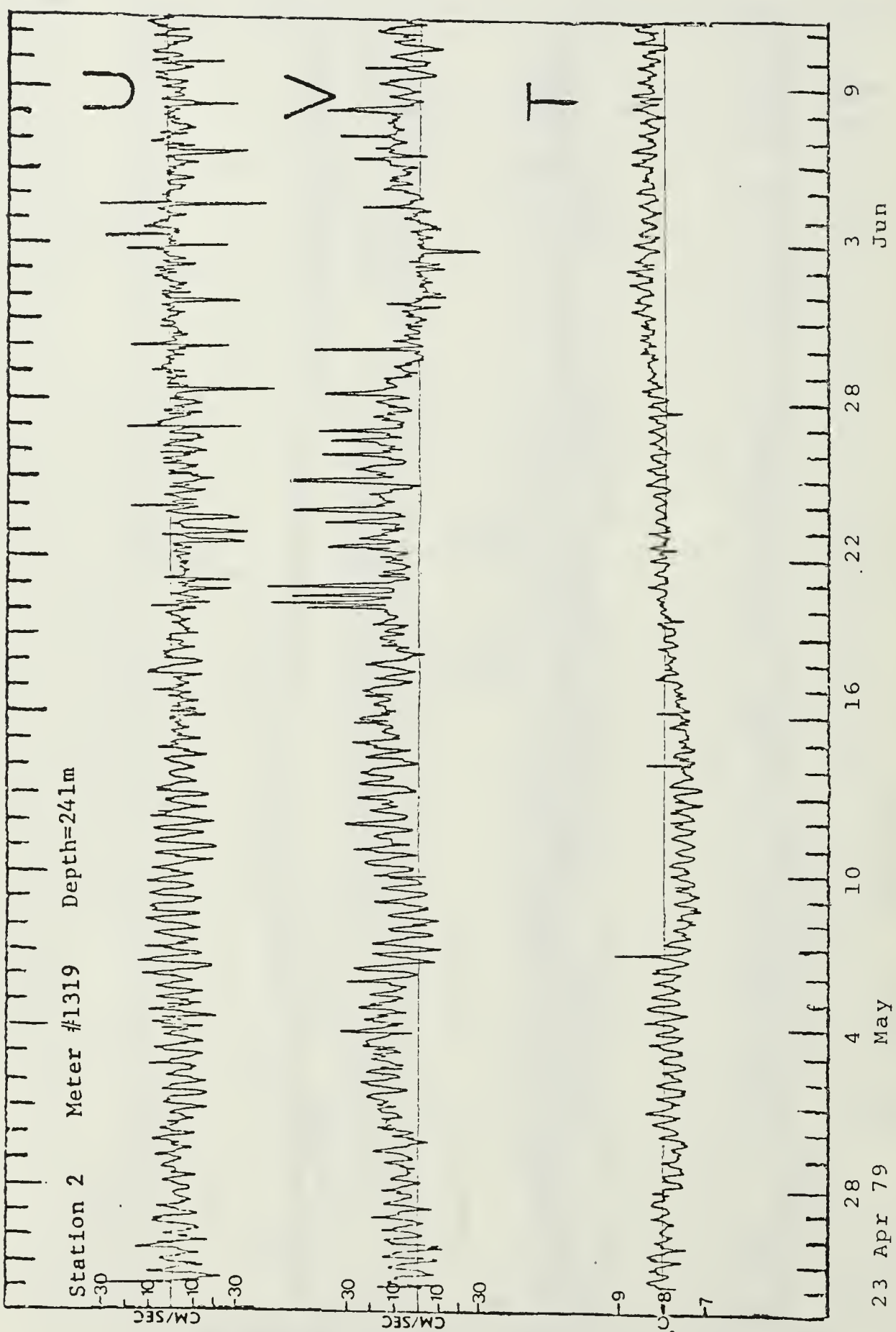


Figure 13. U component, V component, and temperature plots versus time for the current meter at 241 m depth at Station 2 deployed on 23 April 1979.

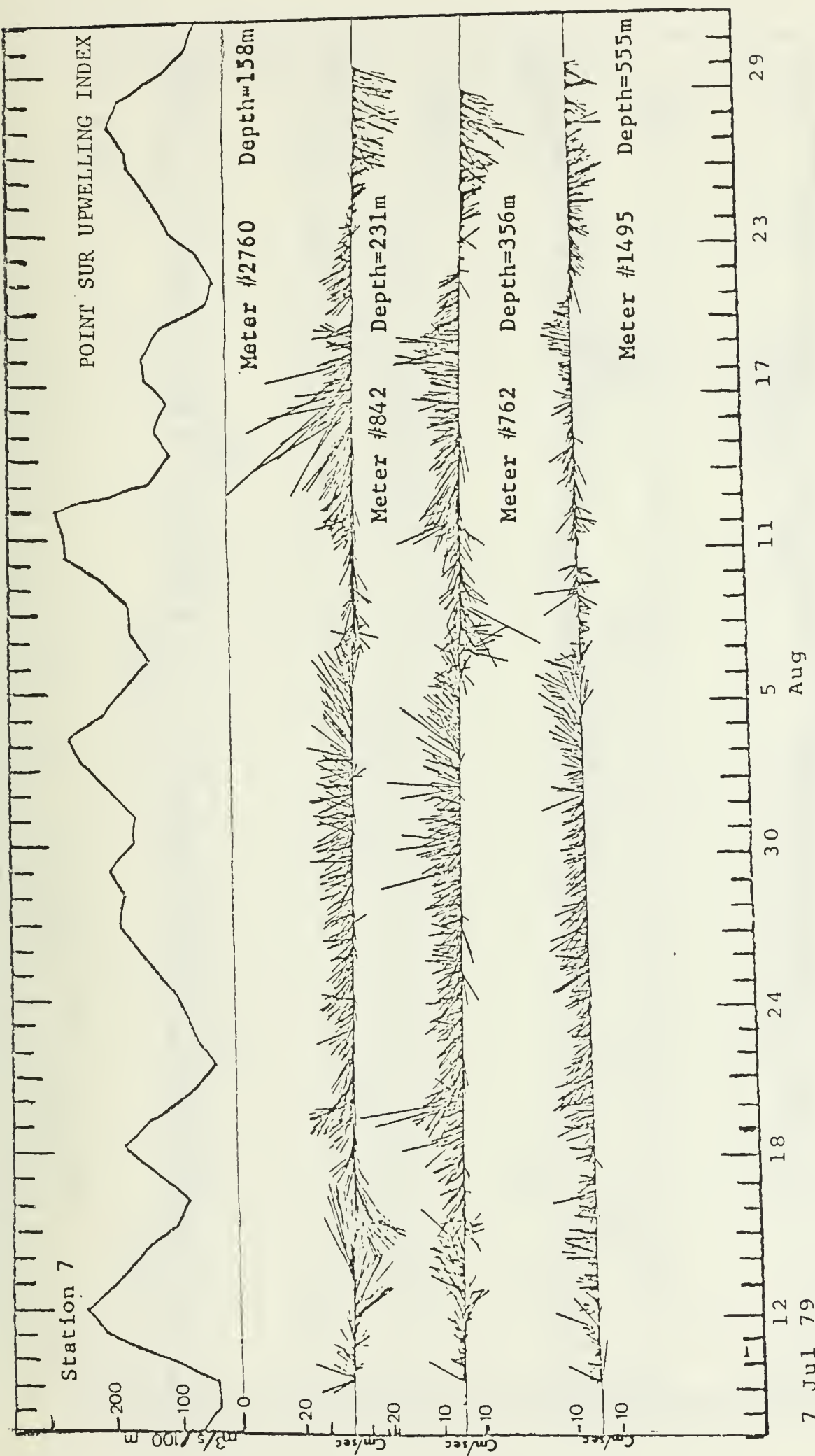


Figure 14. Point Sur Upwelling Index and stickplots of hourly current vectors for the current meters at Station 7 deployed on 7 July 1979.

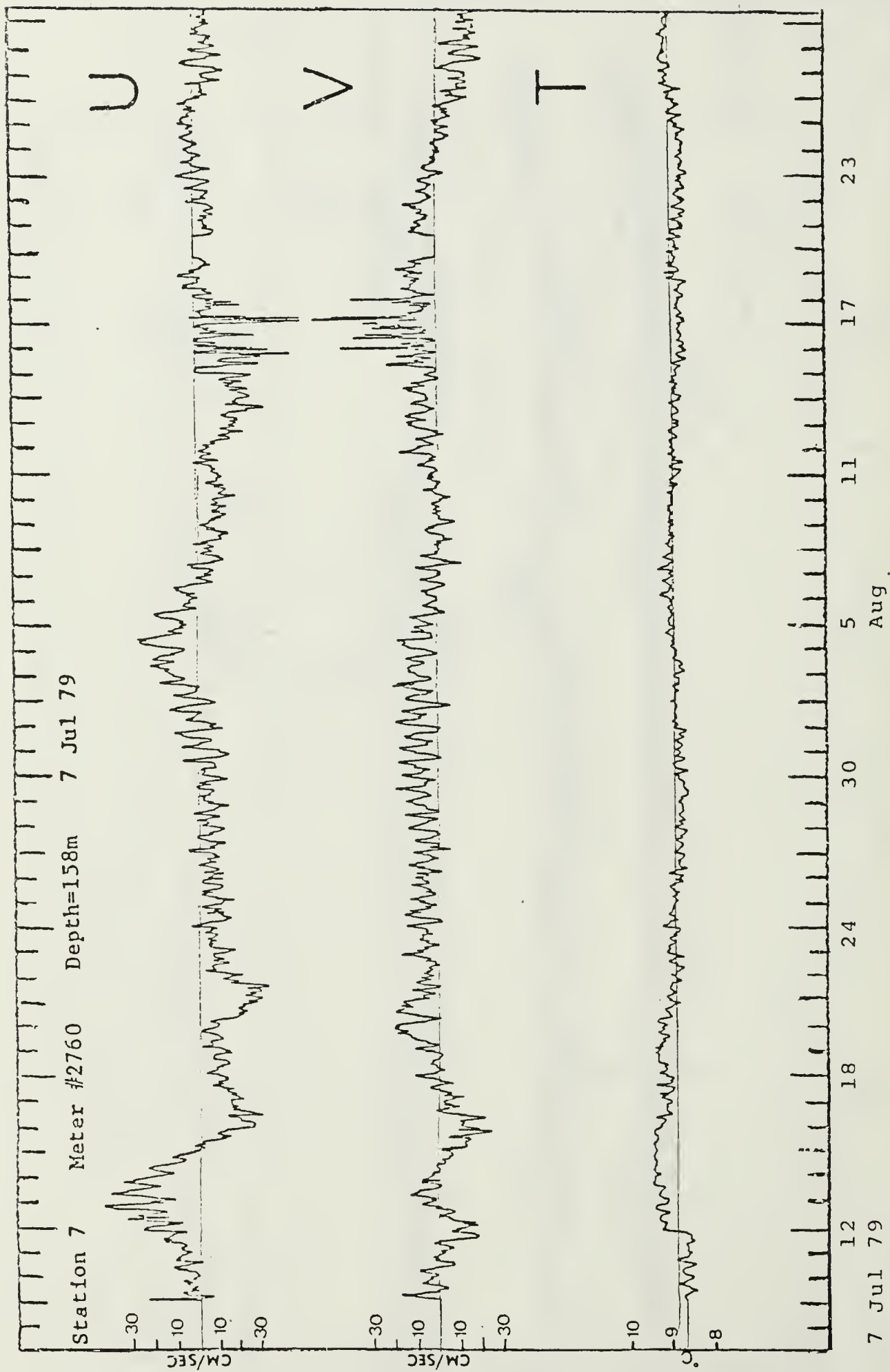


Figure 15. U component, V component, and temperature plots versus time for the current meter at 158 m depth at Station 7 deployed on 7 July 1979.

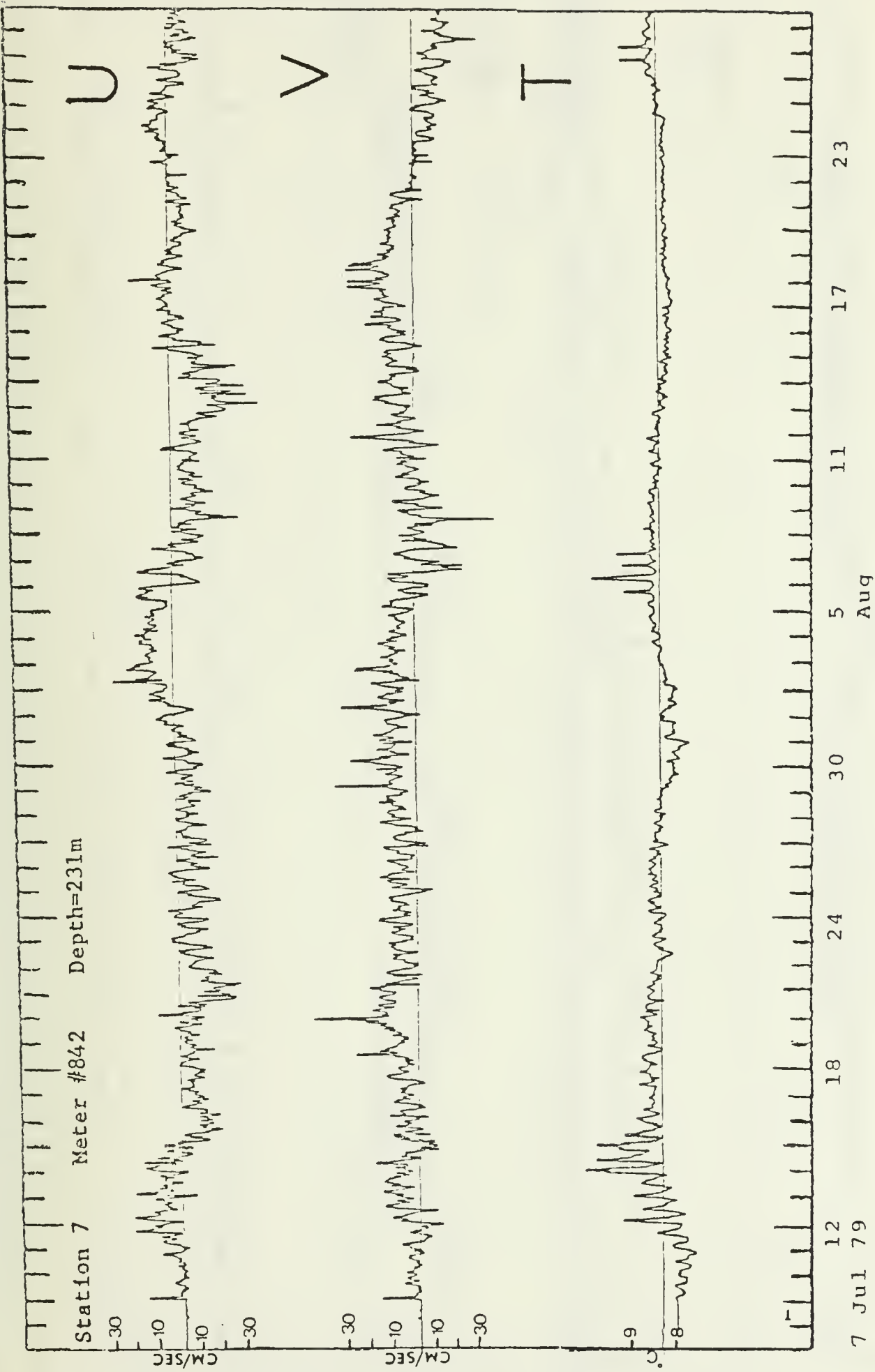


Figure 16. U component, V component, and temperature plots versus time for the current meter at 231 m depth at Station 7 deployed on 7 July 1979.

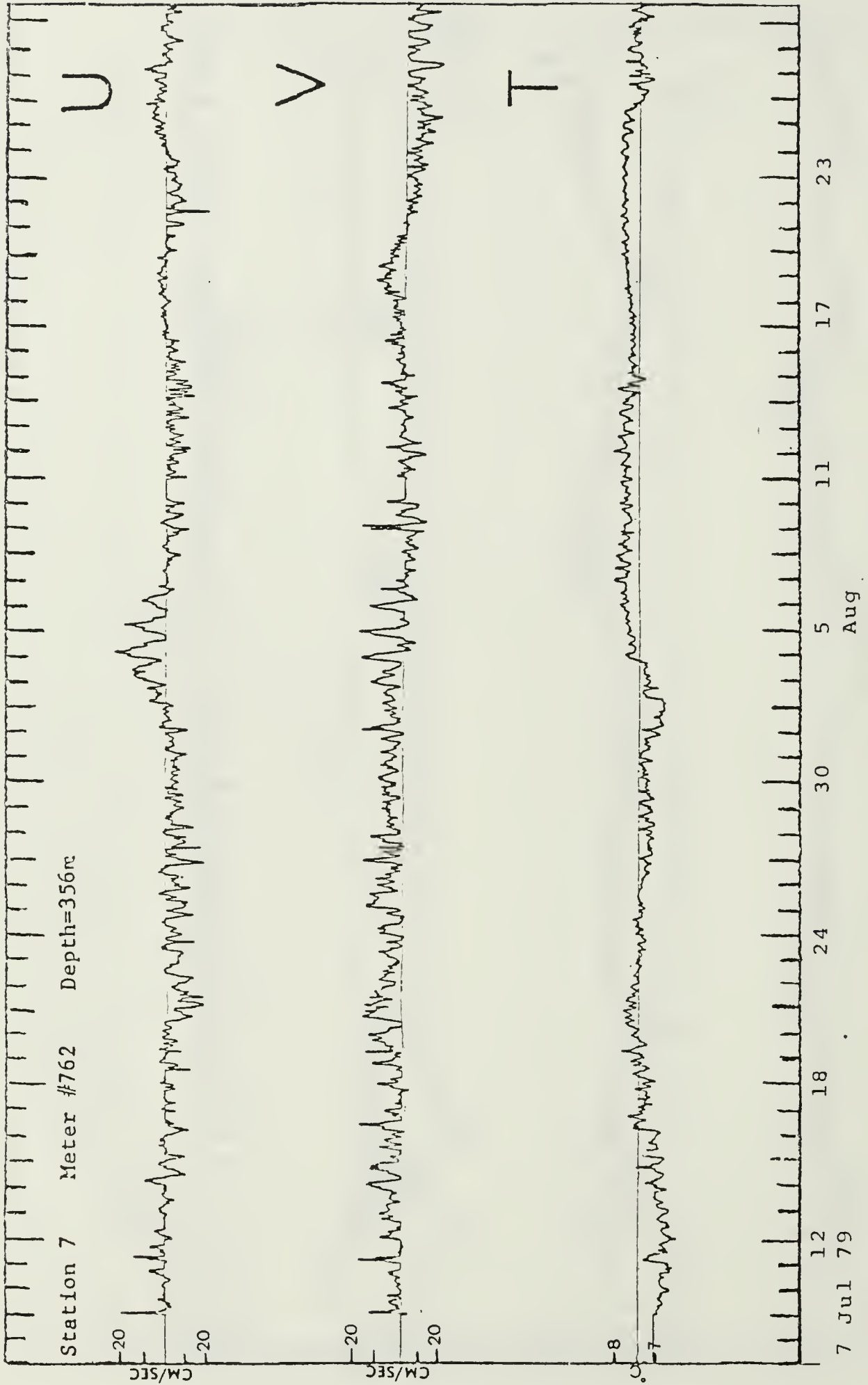


Figure 17. U component, V component, and temperature plots versus time for the current meter at 356 m depth at Station 7 deployed on 7 July 1979.

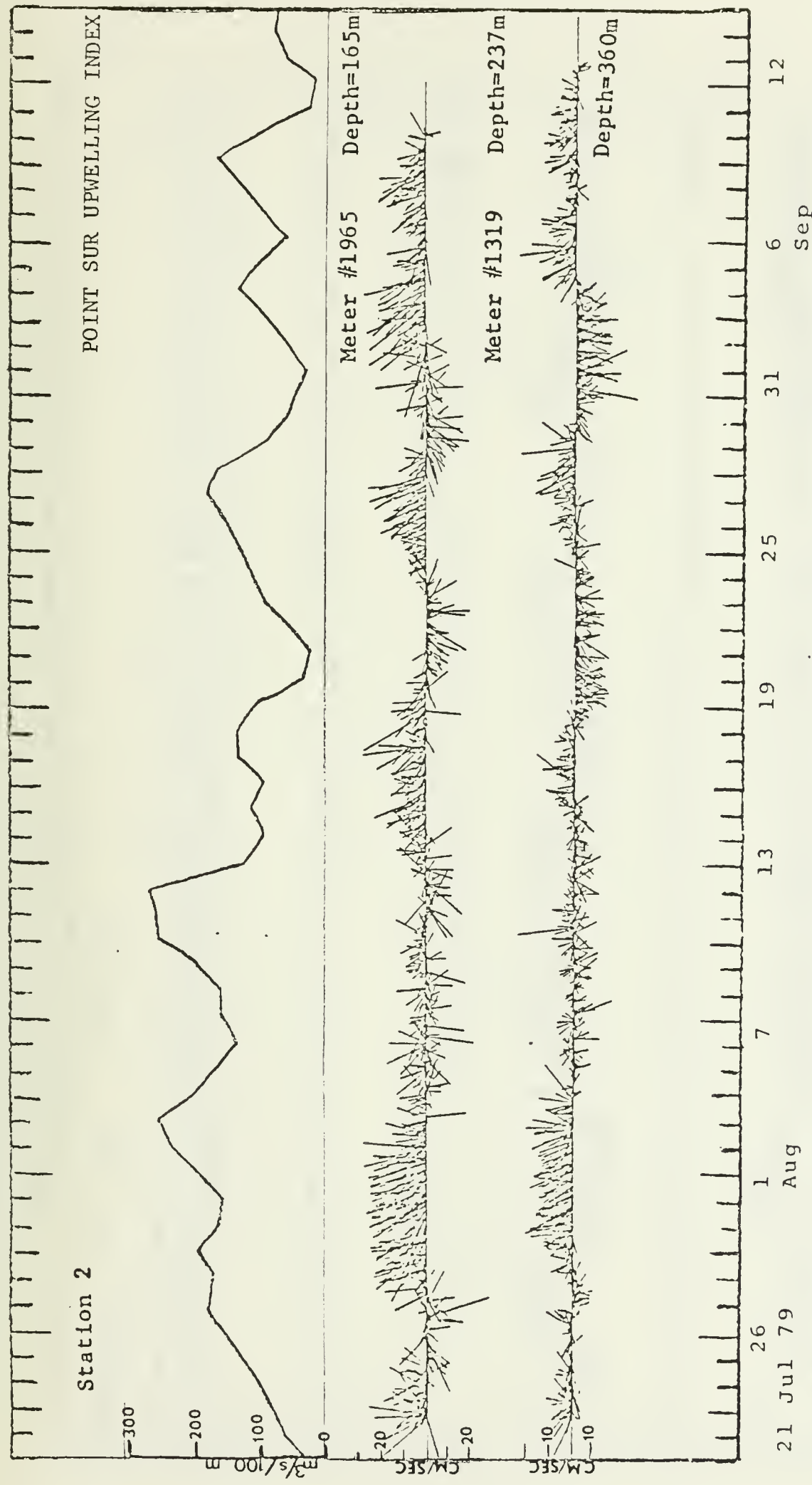


Figure 18. Point Sur Upwelling Index and stickplots of hourly current vectors for the current meters at Station 2 deployed on 21 July 1979.

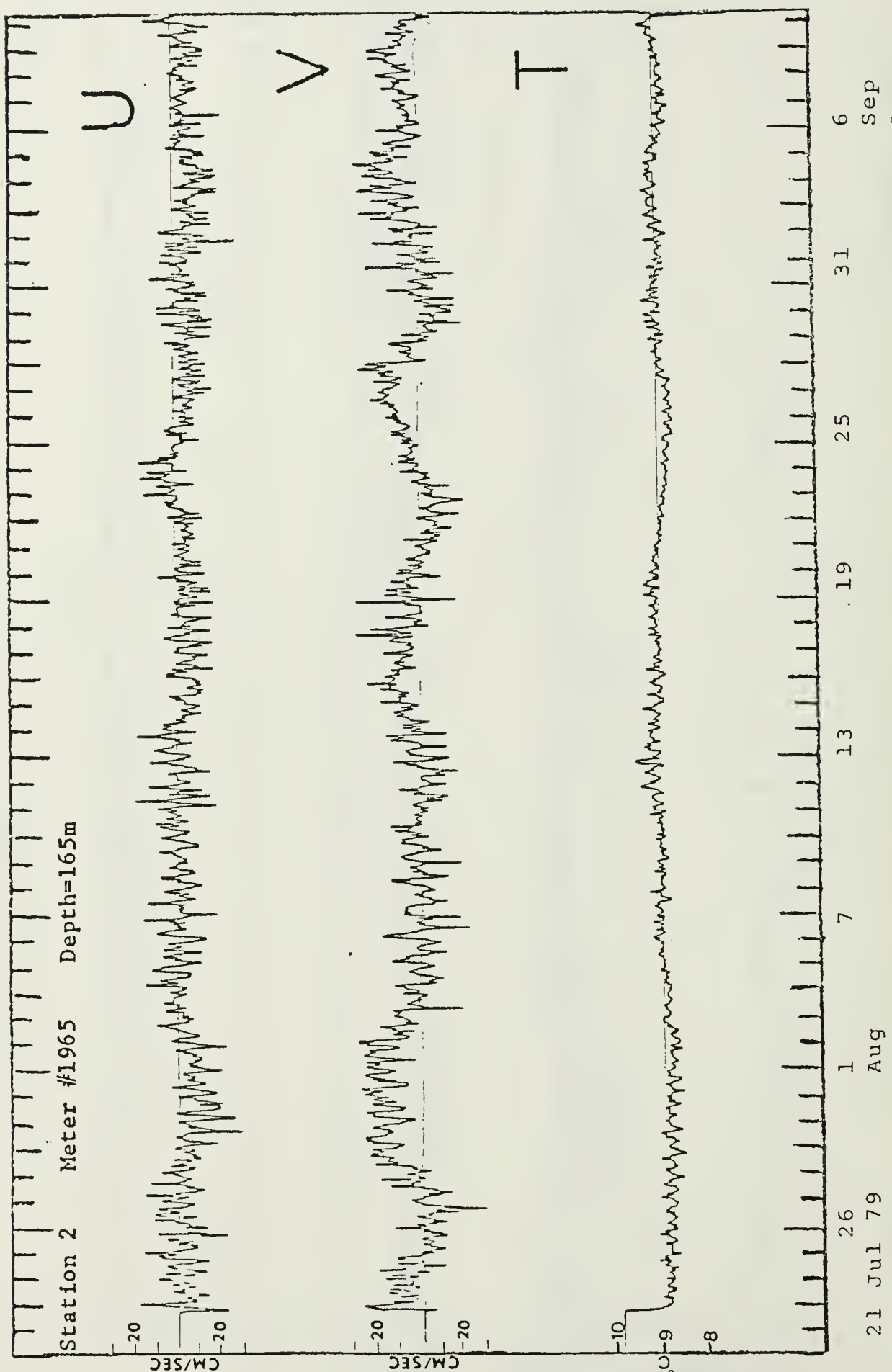


Figure 19. U component, V component, and temperature plots versus time for the current meter at 165 m depth at Station 2 deployed on 21 July 1979.

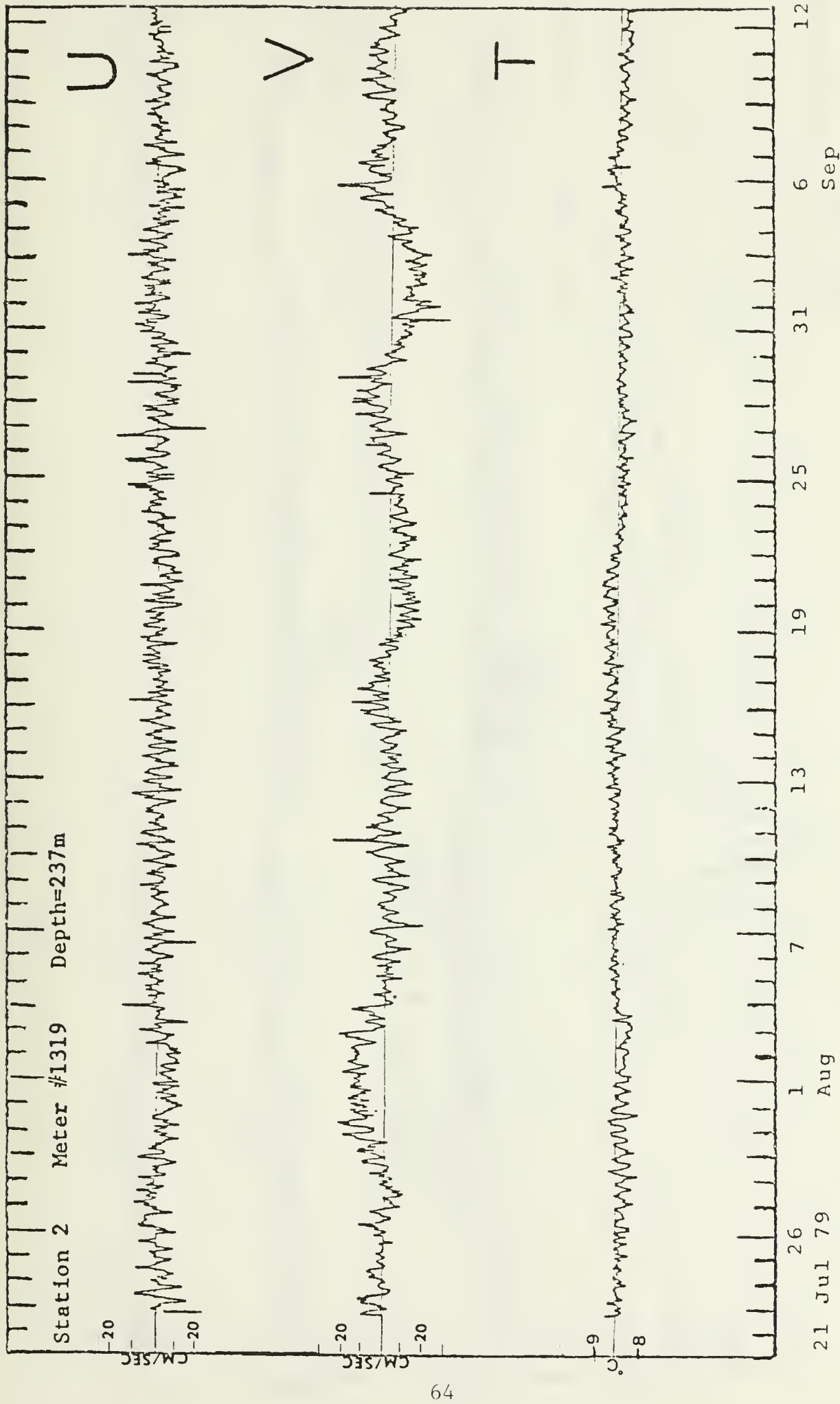


Figure 20. U component, V component, and temperature plots versus time for the current meter at 237 m depth at Station 2 deployed on 21 July 1979.

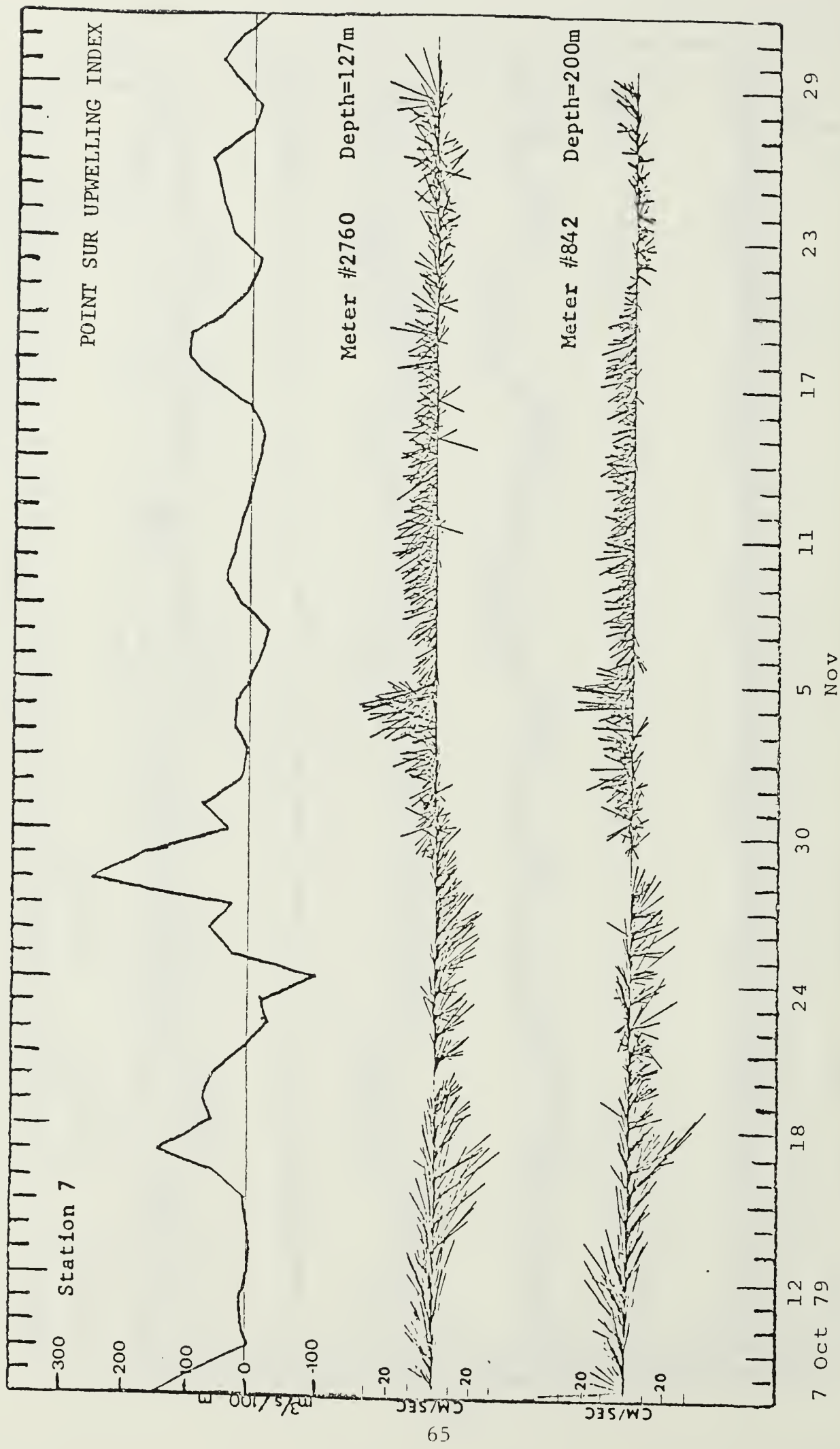


Figure 21. Point Sur Upwelling Index and stickplots of hourly current vectors for the current meters at Station 7 deployed on 7 October 1979.

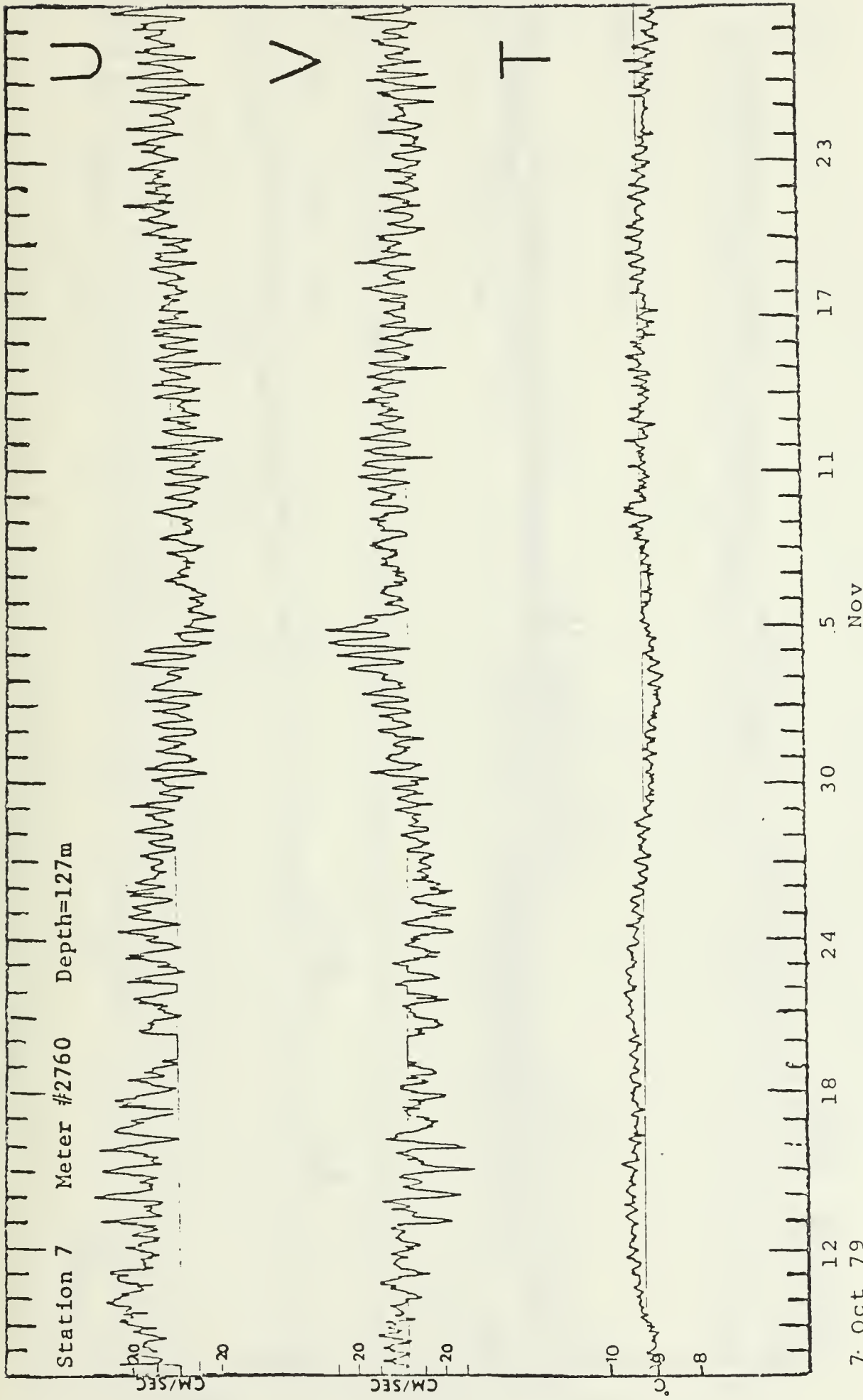


Figure 22. U component, V component, and temperature plots versus time for the current meter at 127 m depth at Station 7 deployed on 7 October 1979.

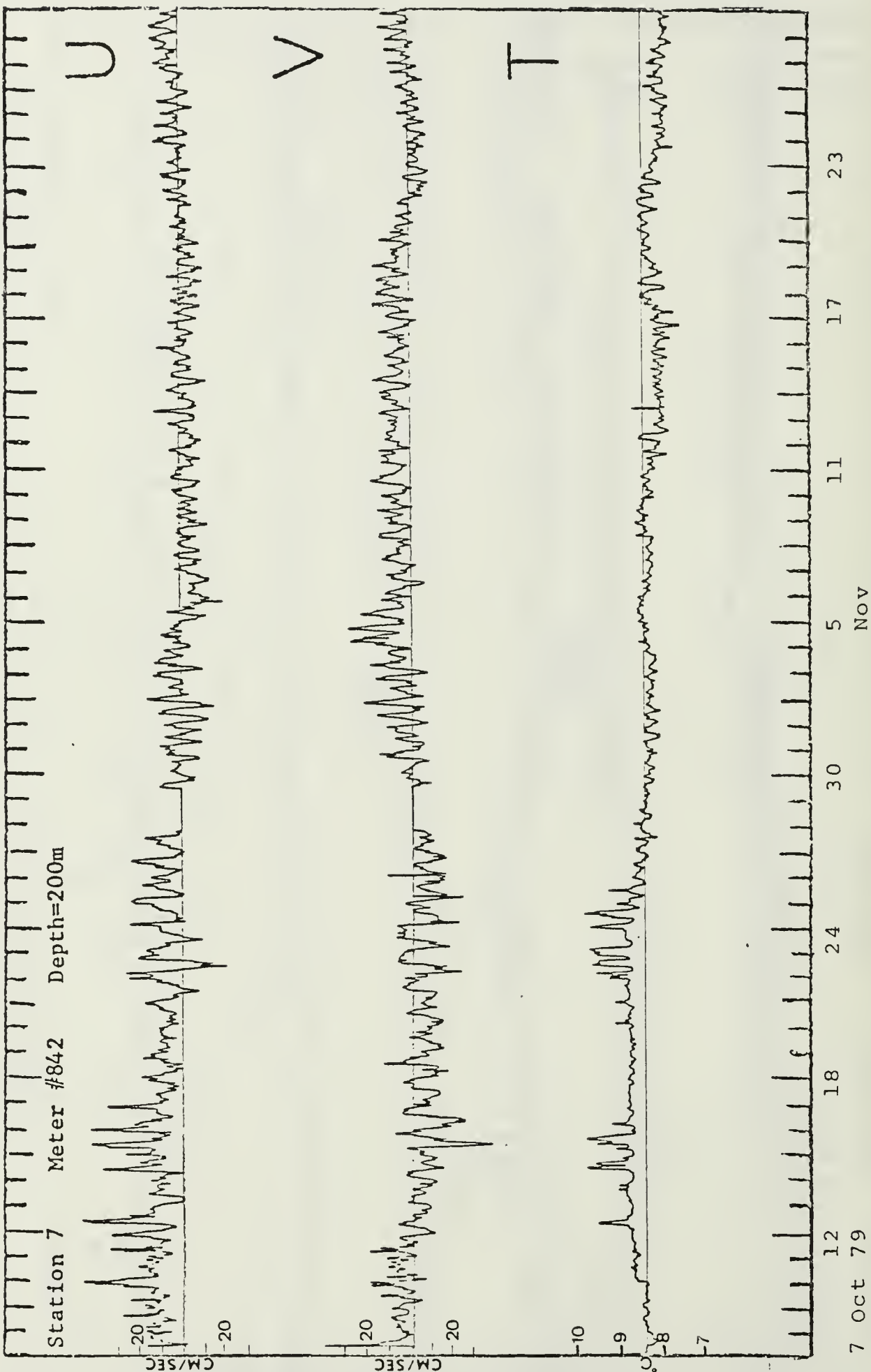


Figure 23. U component, V component, and temperature plots versus time for the current meter at 200 m depth at Station 7 deployed on 7 October 1979.

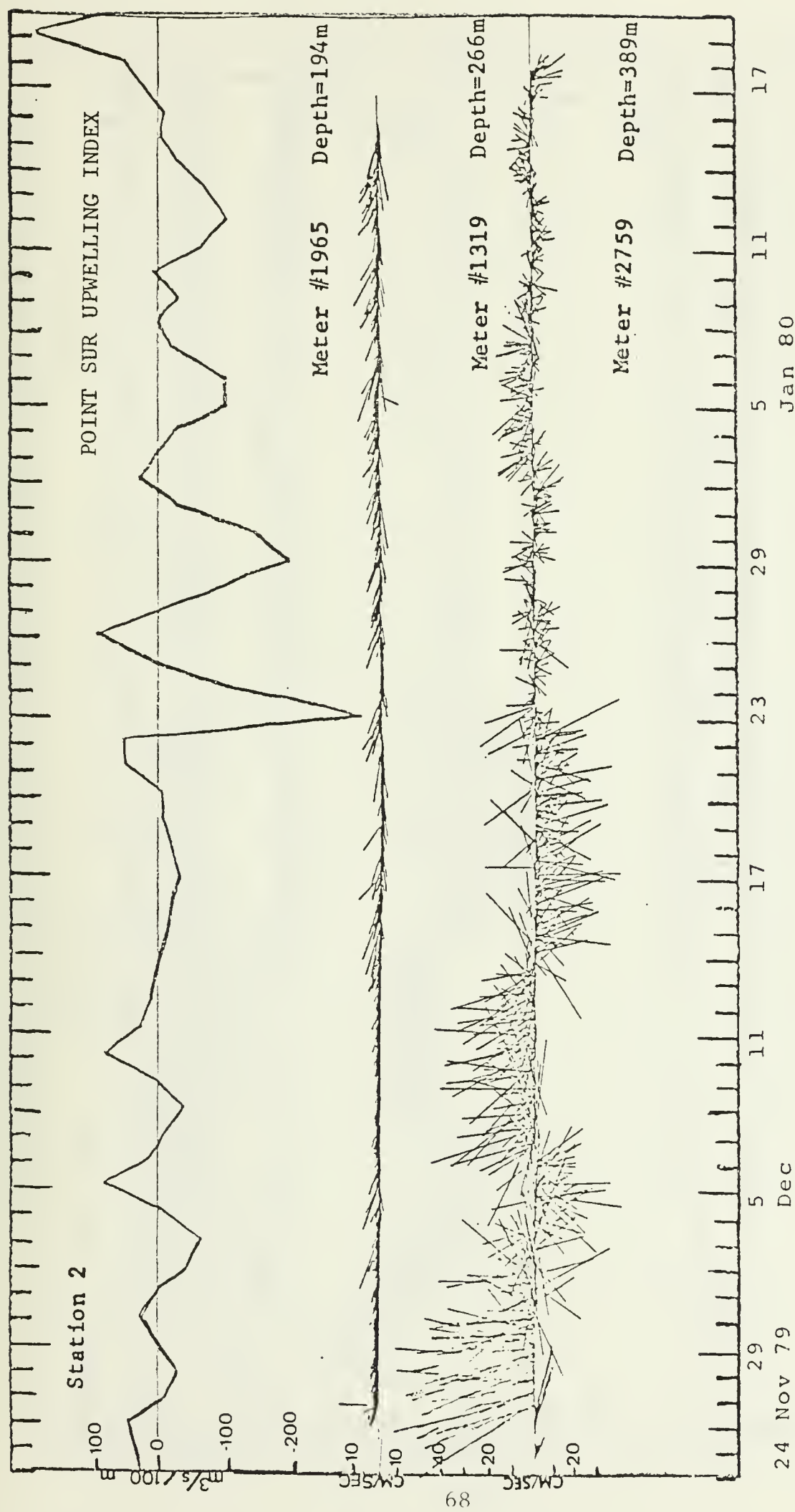


Figure 24. Point Sur Upwelling Index and stickplots of hourly current vectors for the current meters at Station 2 deployed on 24 November 1979.

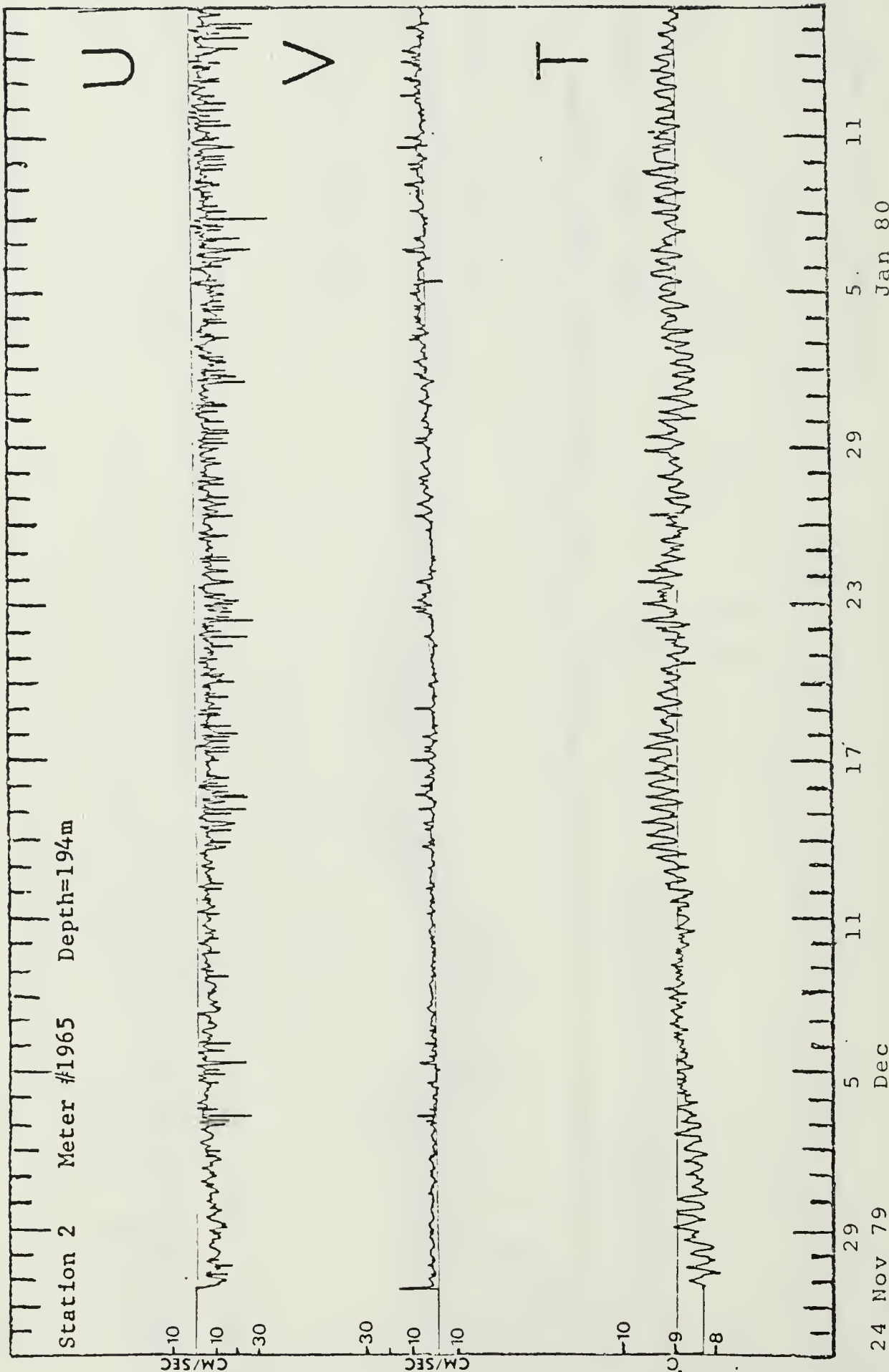


Figure 25. U component, V component, and temperature plots versus time for the current meter at 194 m depth at Station 2 deployed on 24 November 1979.

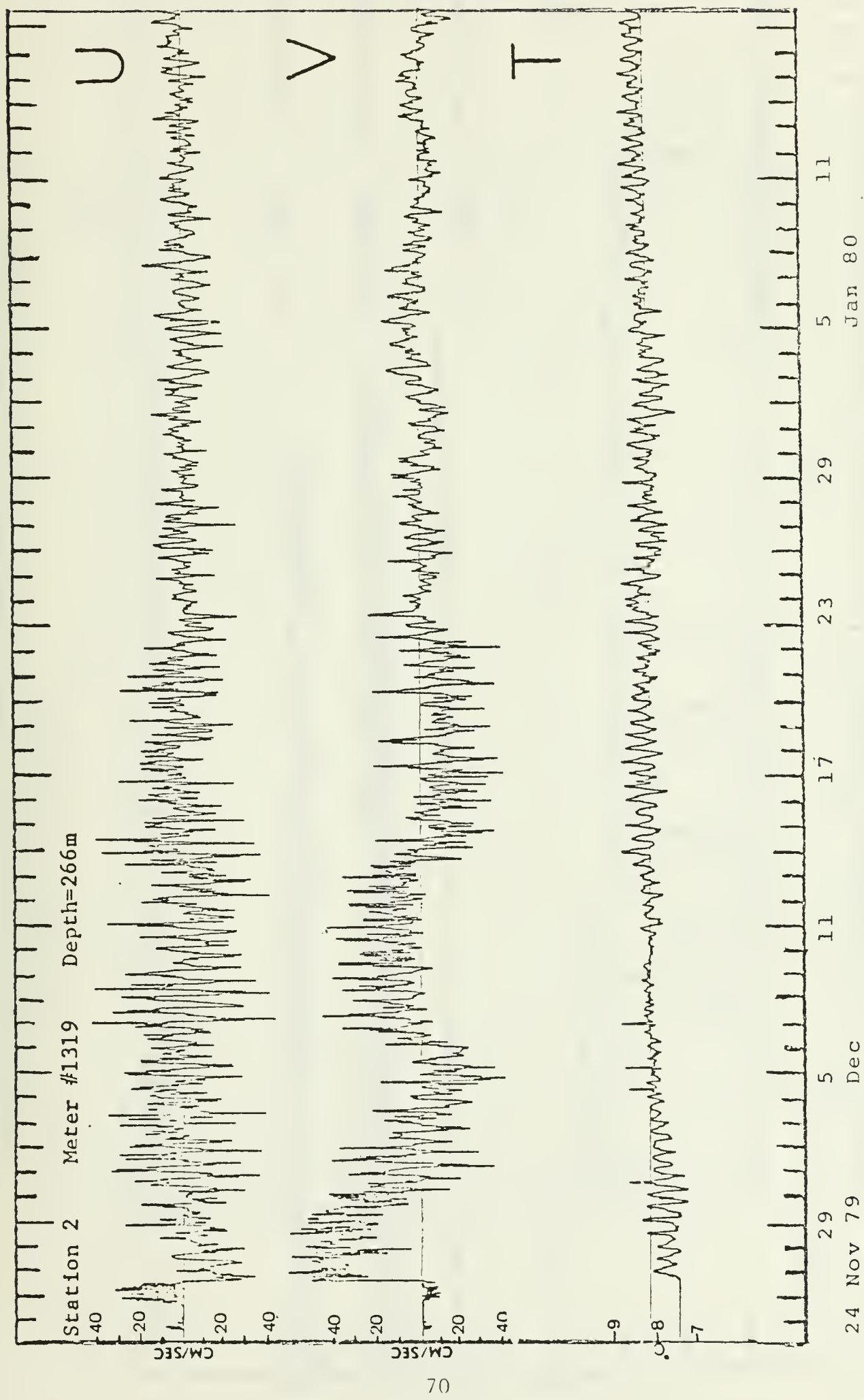


Figure 26. U component, V component, and temperature plots versus time for the current meter at 266 m depth at Station 2 deployed on 24 November 1979.

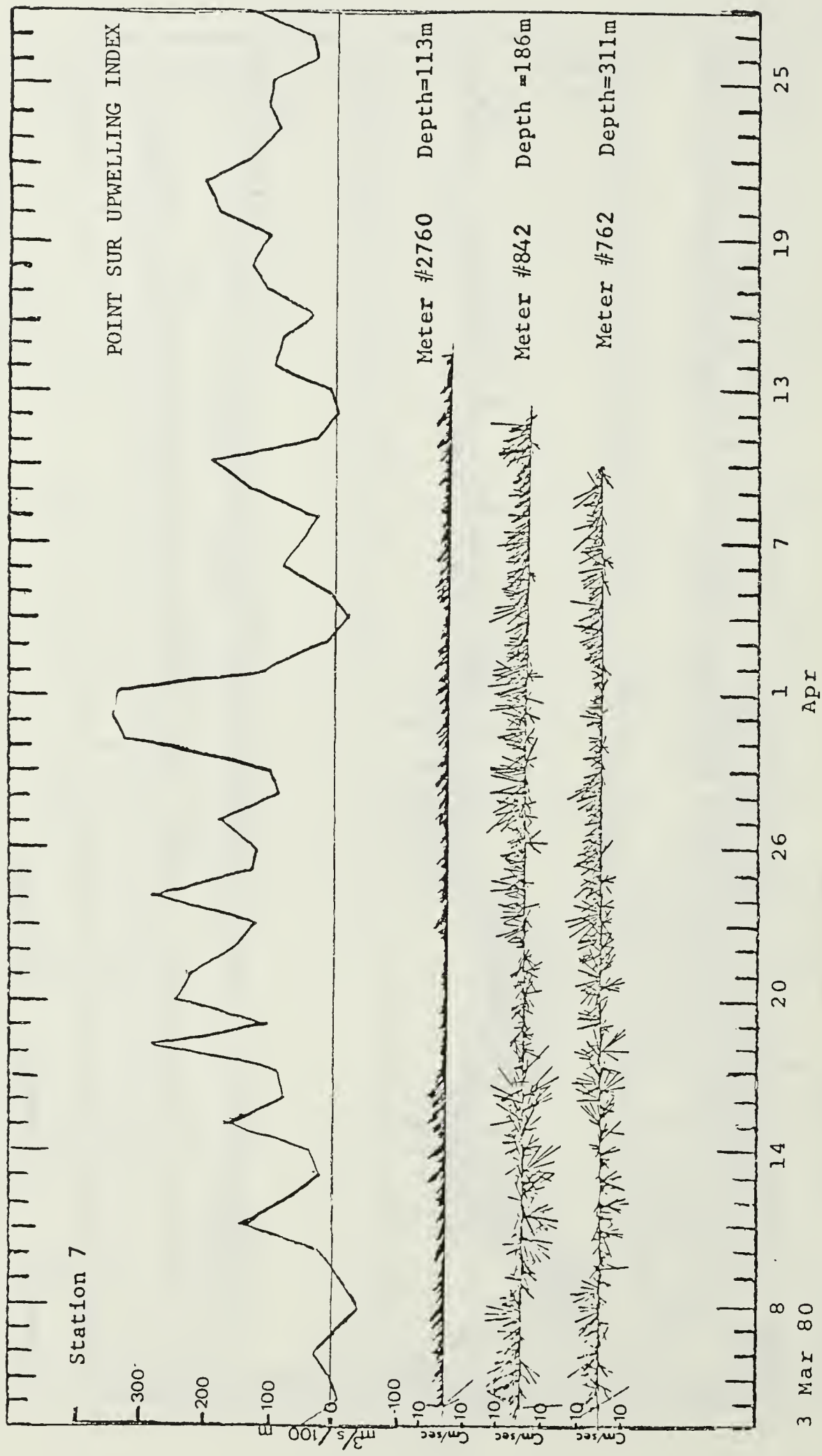


Figure 27. Point Sur Upwelling Index and stickplots of hourly current vectors for the current meters at Station 7 deployed on 3 March 1980.

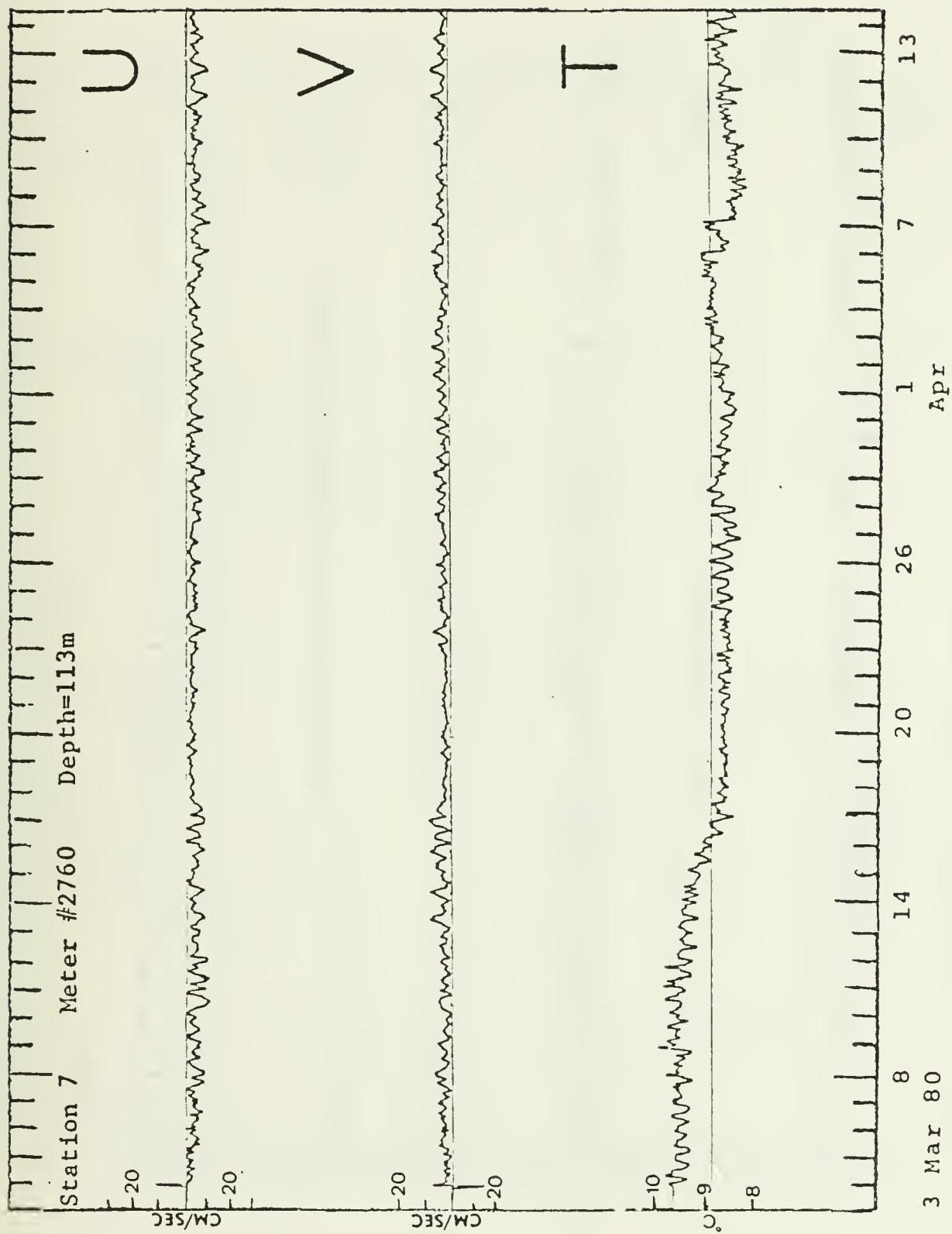


Figure 28. U component, V component, and temperature plots versus time for the current meter at 113 m depth at Station 7 deployed on 3 March 1980.

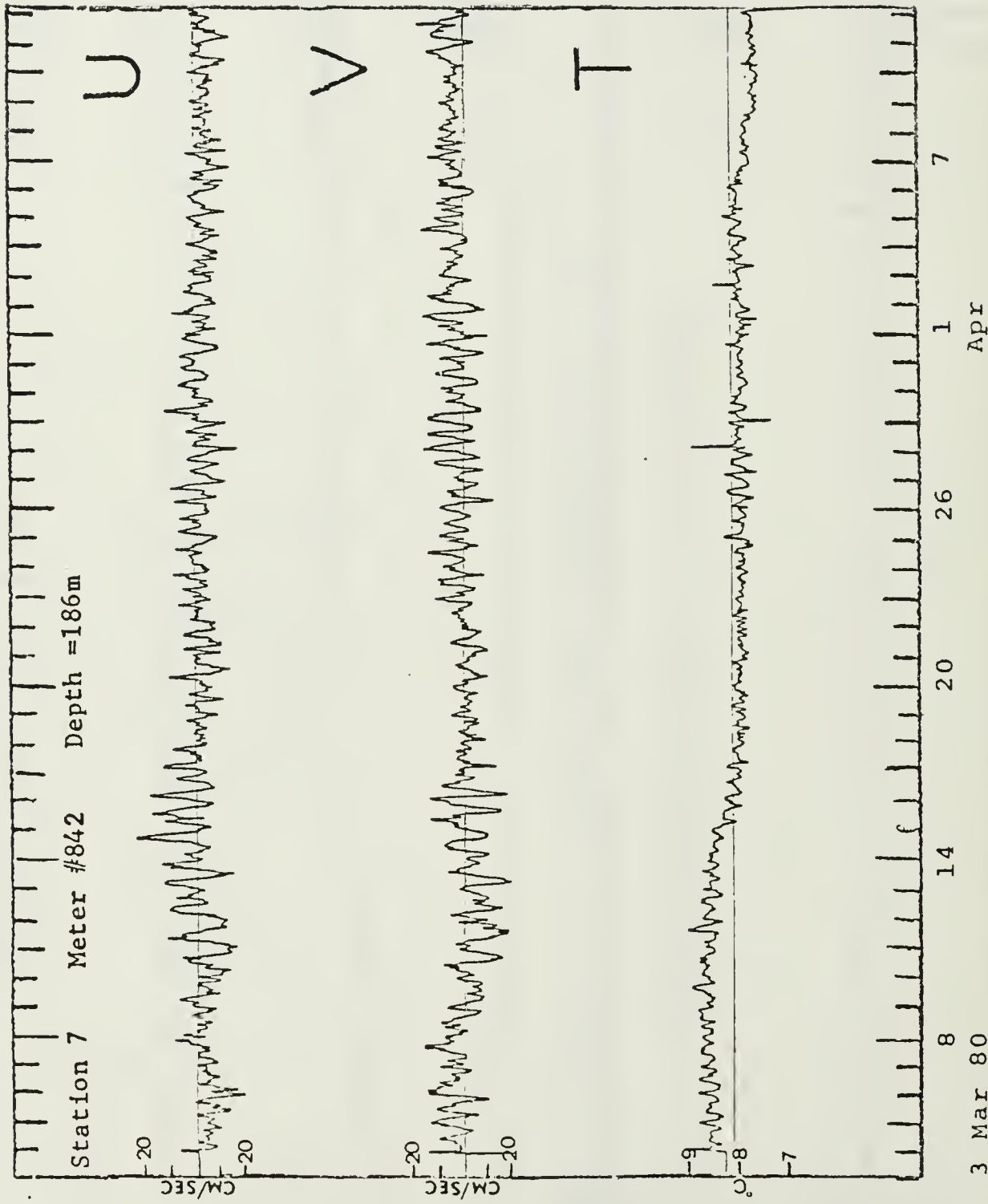


Figure 29. U component, V component, and temperature plots versus time for the current meters at 186 m depth at Station 7 deployed on 3 March 1980.

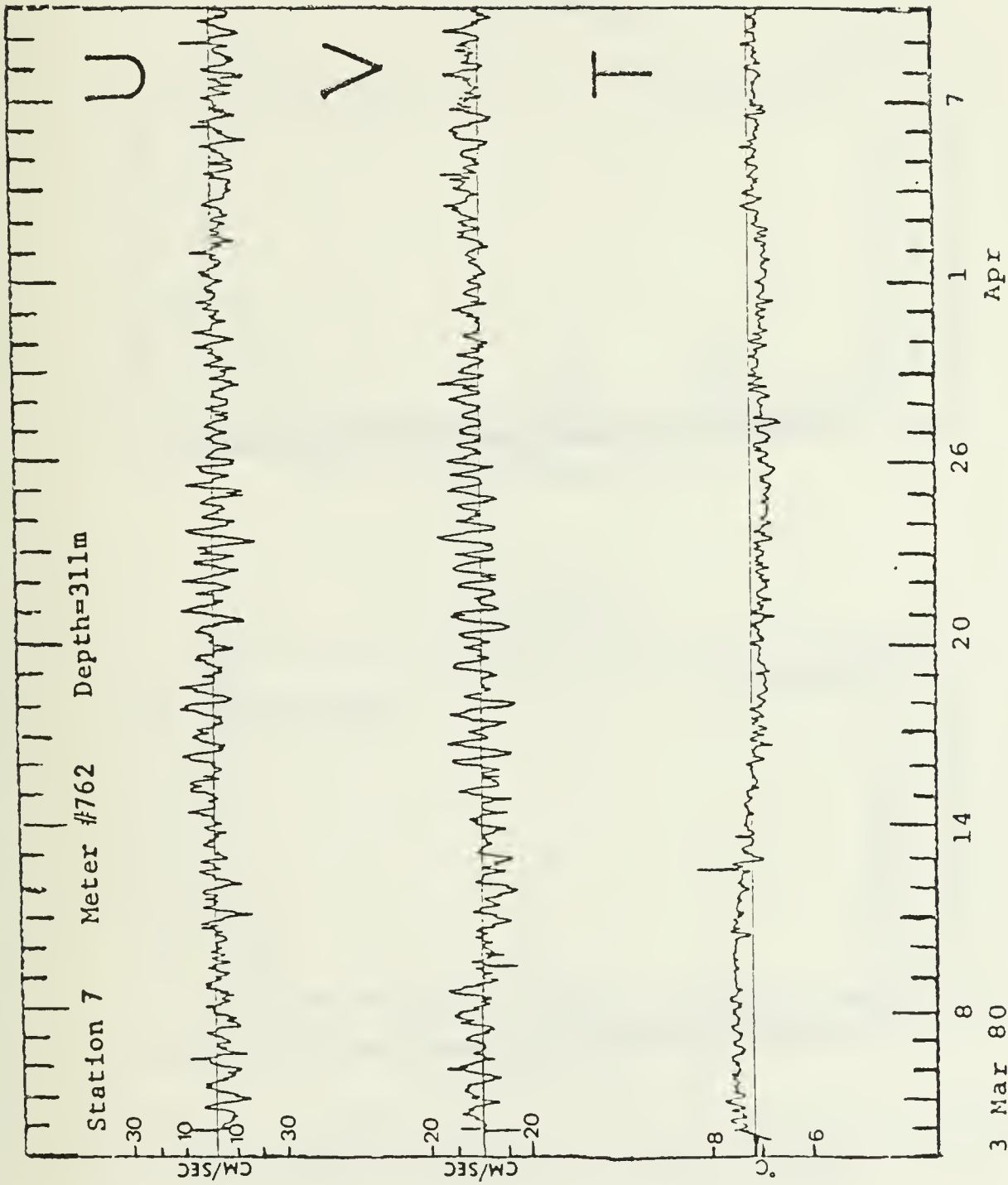


Figure 30. U component, V component, and temperature plots versus time for the current meter at 311 m depth at Station 7 deployed on 5 January 1979.

APPENDIX B: SPECTRUM ANALYSES OF ALONGSHORE FLOW AND
ON/OFFSHORE FLOW

Station 7 Meter #762 Depth=152m 5 Jan 79

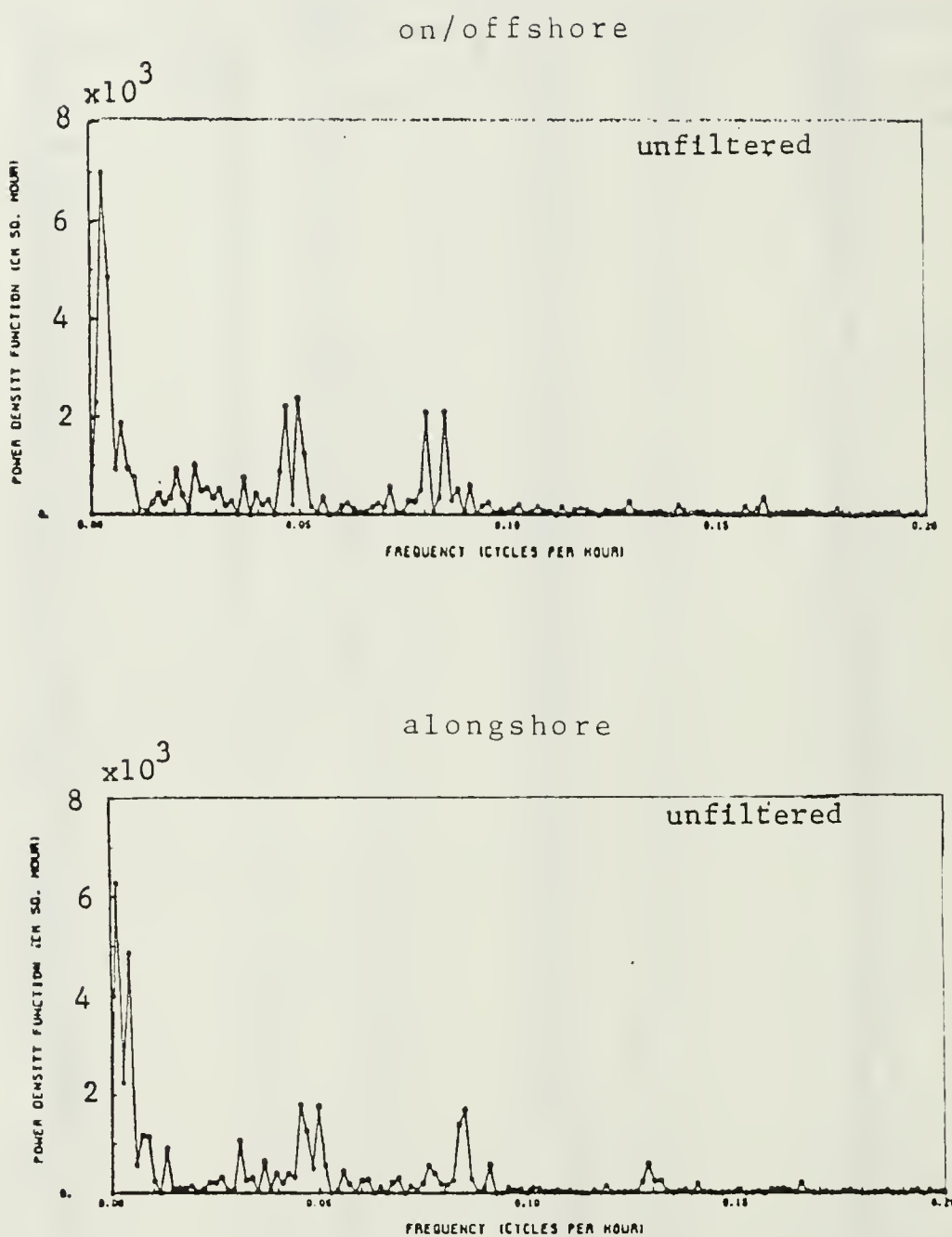


Figure 31. Energy density spectrum of current meter at 152 m depth at Station 7 deployed on 5 January 1979.

Station 7

Meter #842

Depth=223m

5 Jan 79

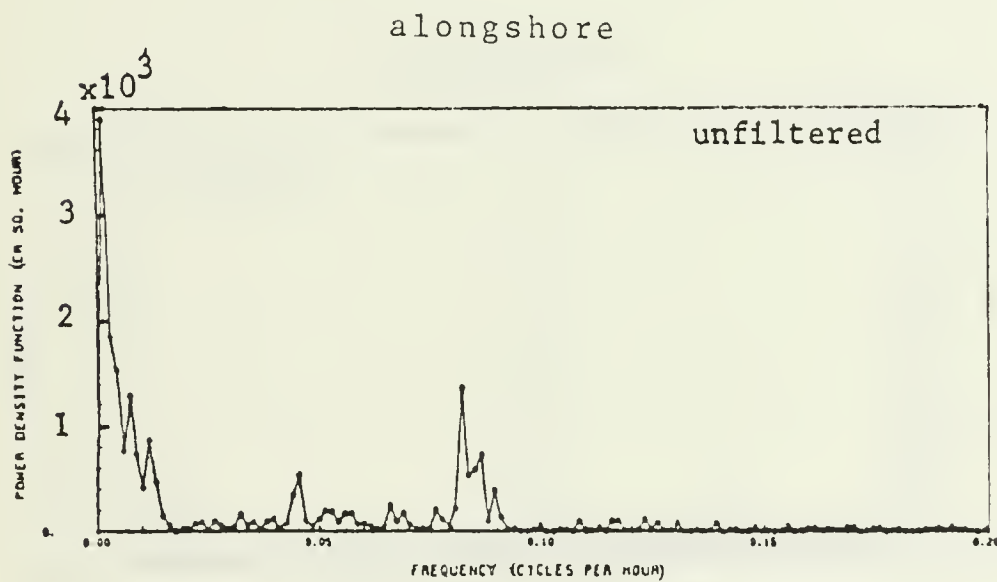
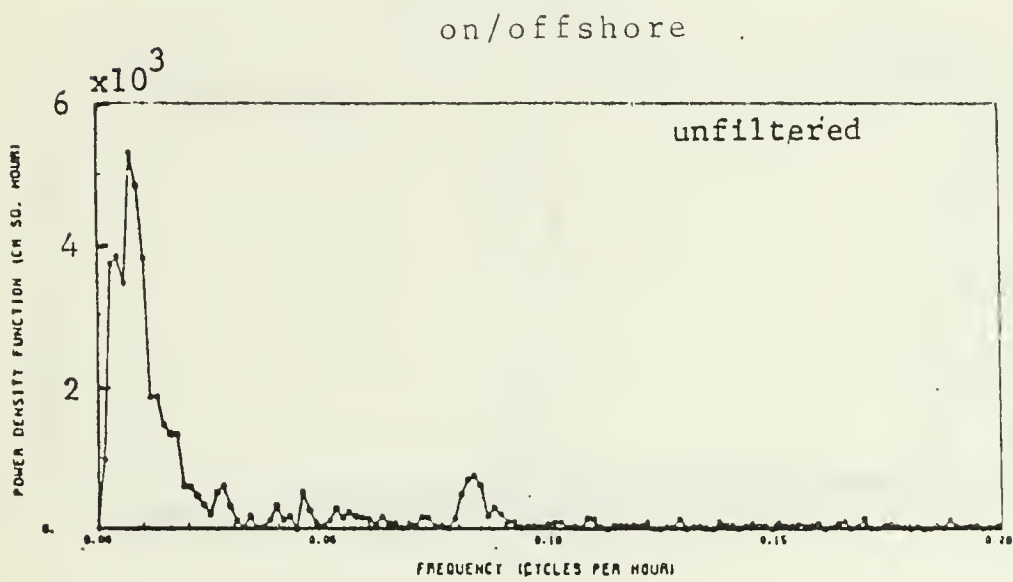


Figure 32. Energy density spectrum of current meter at 223 m depth at Station 7 deployed on 5 January 1979.

Station 2 Meter #1965 Depth=169m 23 Apr 79

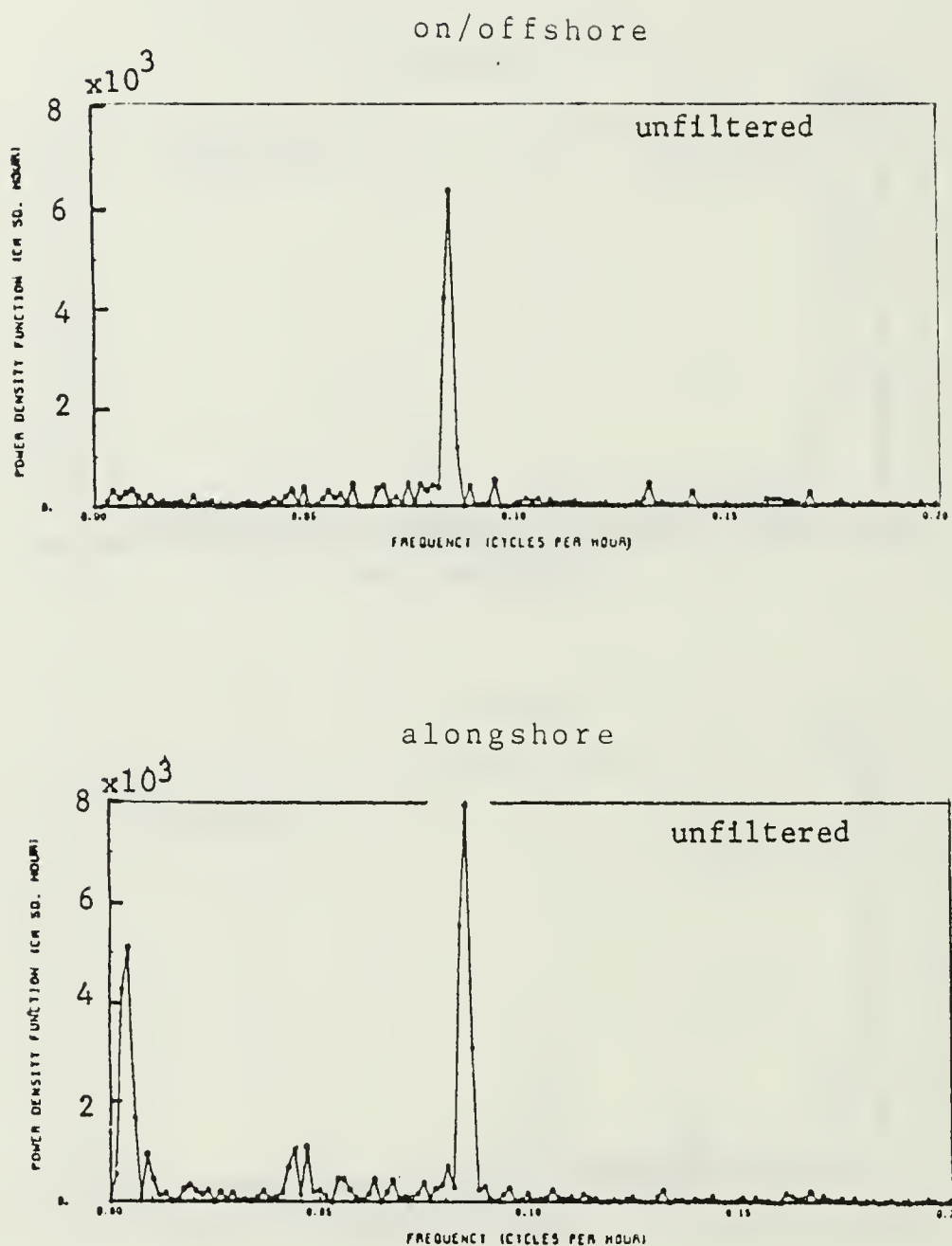


Figure 33. Energy density spectrum of current meter at 169 m depth at Station 2 deployed on 23 April 1979.

Station 2 Meter #1319 Depth=241m 23 Apr 79

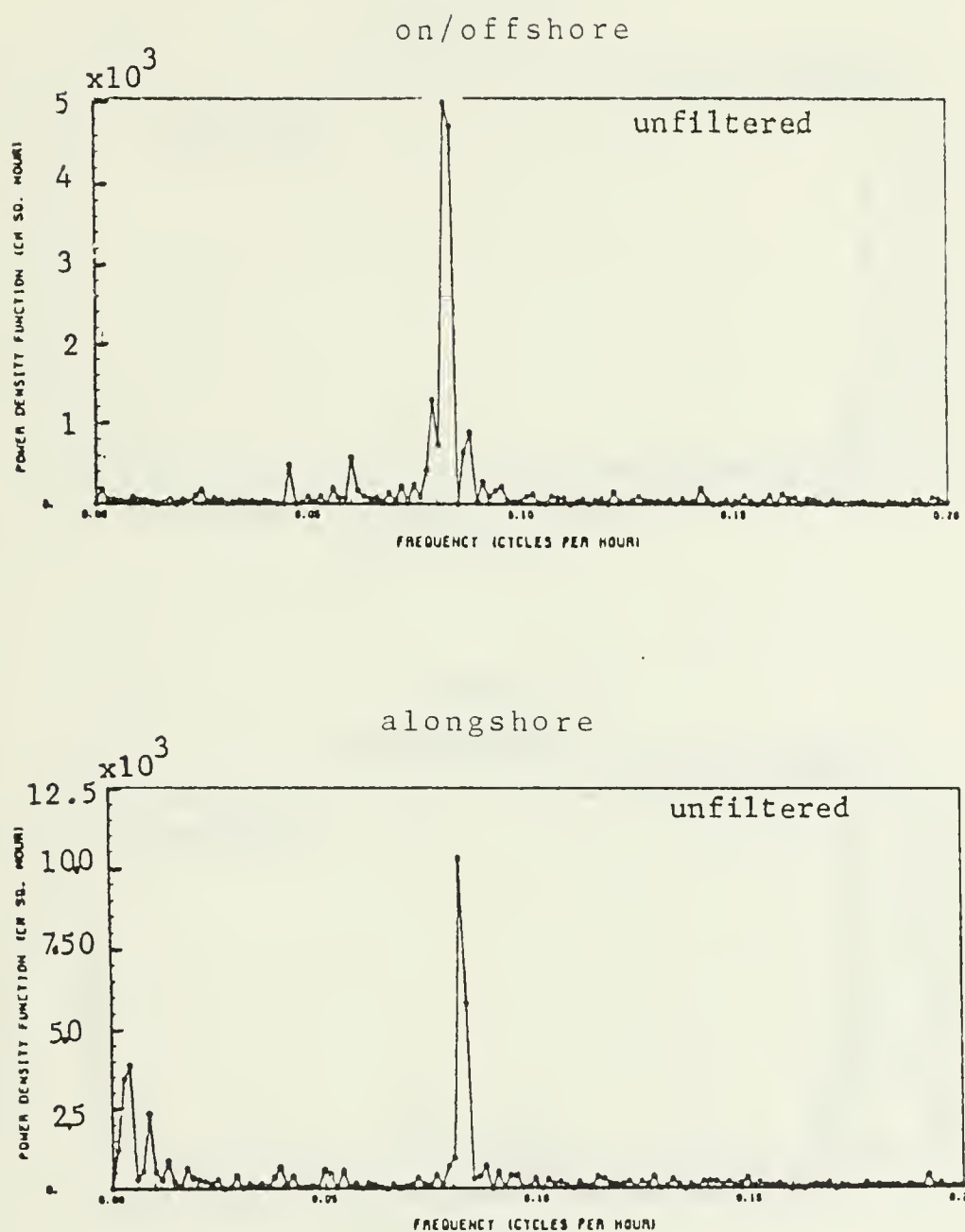


Figure 34. Energy density spectrum of current meter at 241 m depth at Station 2 deployed on 23 April 1979.

Station 7 Meter #2760 Depth=158m 7 Jul 79

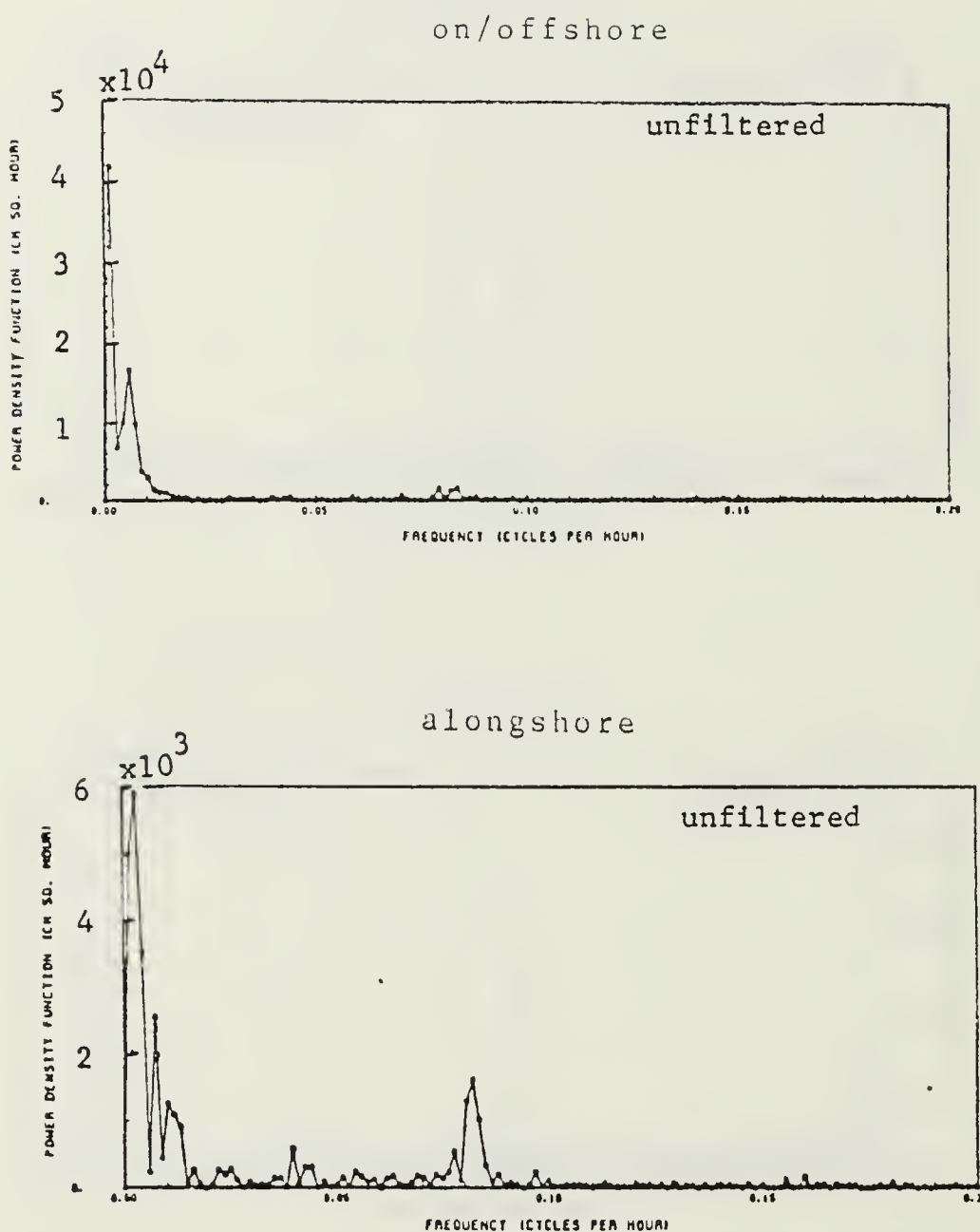


Figure 35. Energy density spectrum of current meter at 158 m depth at Station 7 deployed on 7 July 1979.

Station 7 Meter #842 Depth=231m 7 Jul 79

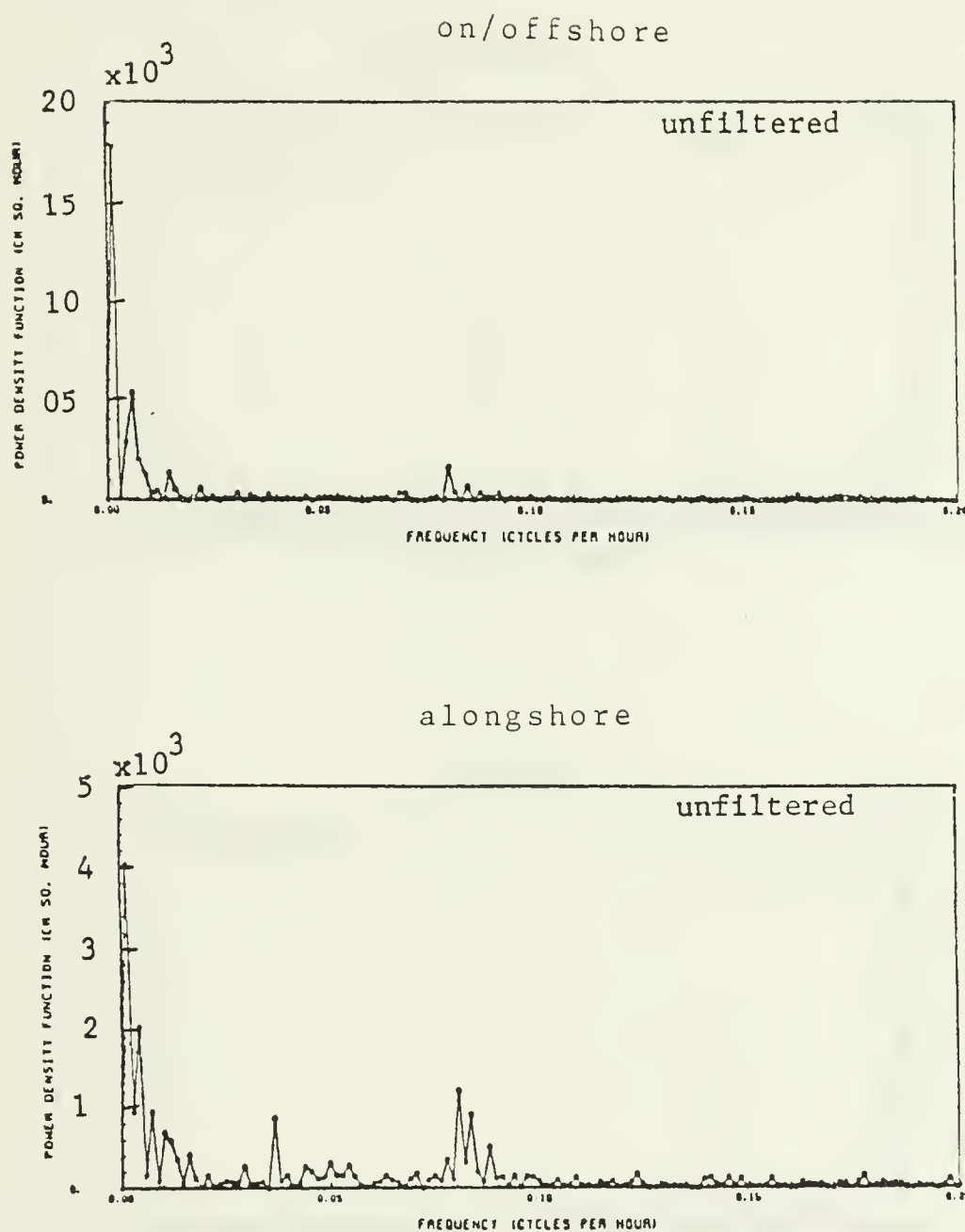


Figure 36. Energy density spectrum of current meter at 231 m depth at Station 7 deployed on 7 July 1979.

Station 7 Meter #762 Depth=356m 7 Jul 79

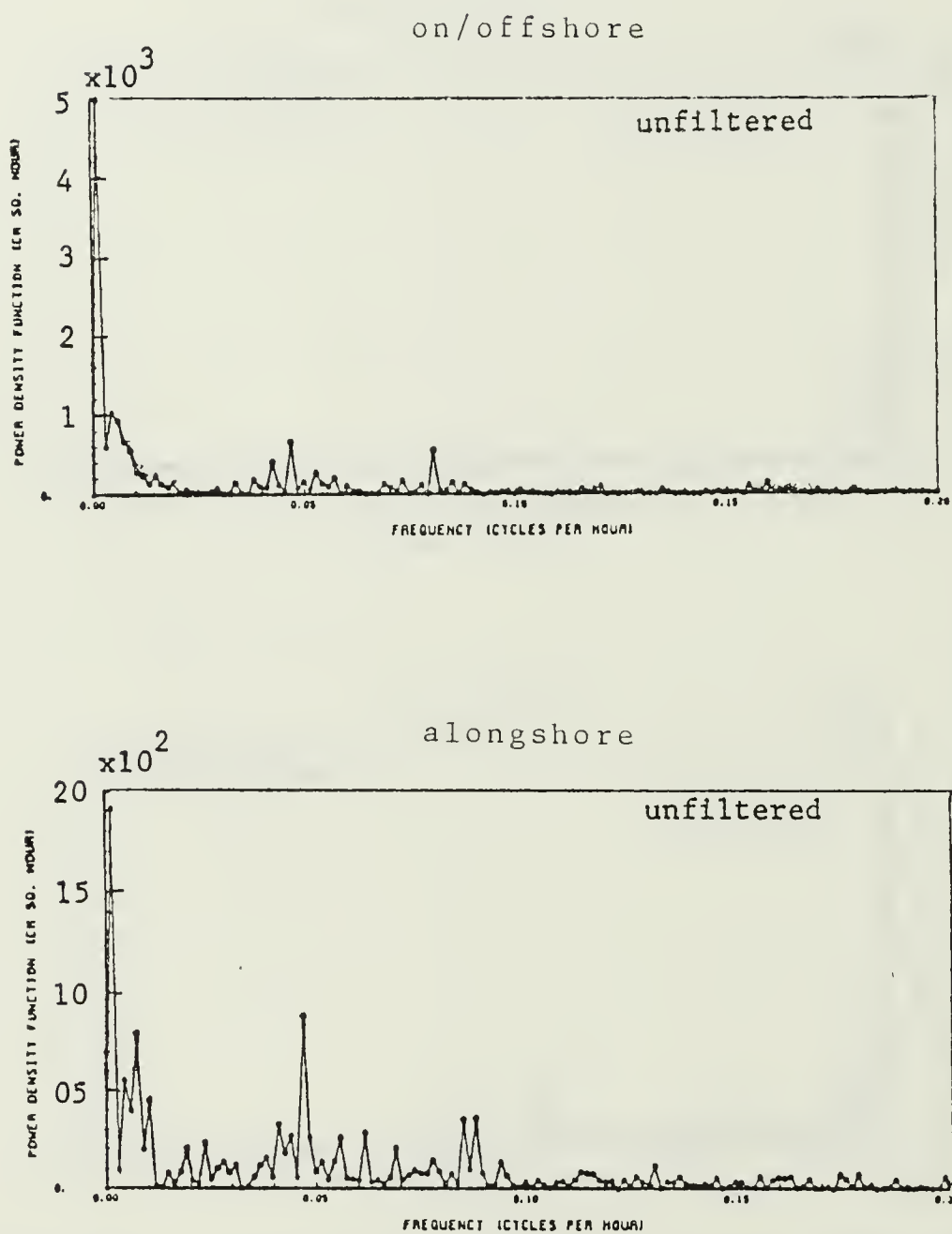


Figure 37. Energy density spectrum of current meter at 356 m depth at Station 7 deployed on 7 July 1979.

Station 2 Meter #1965 Depth=165m 21 Jul 79

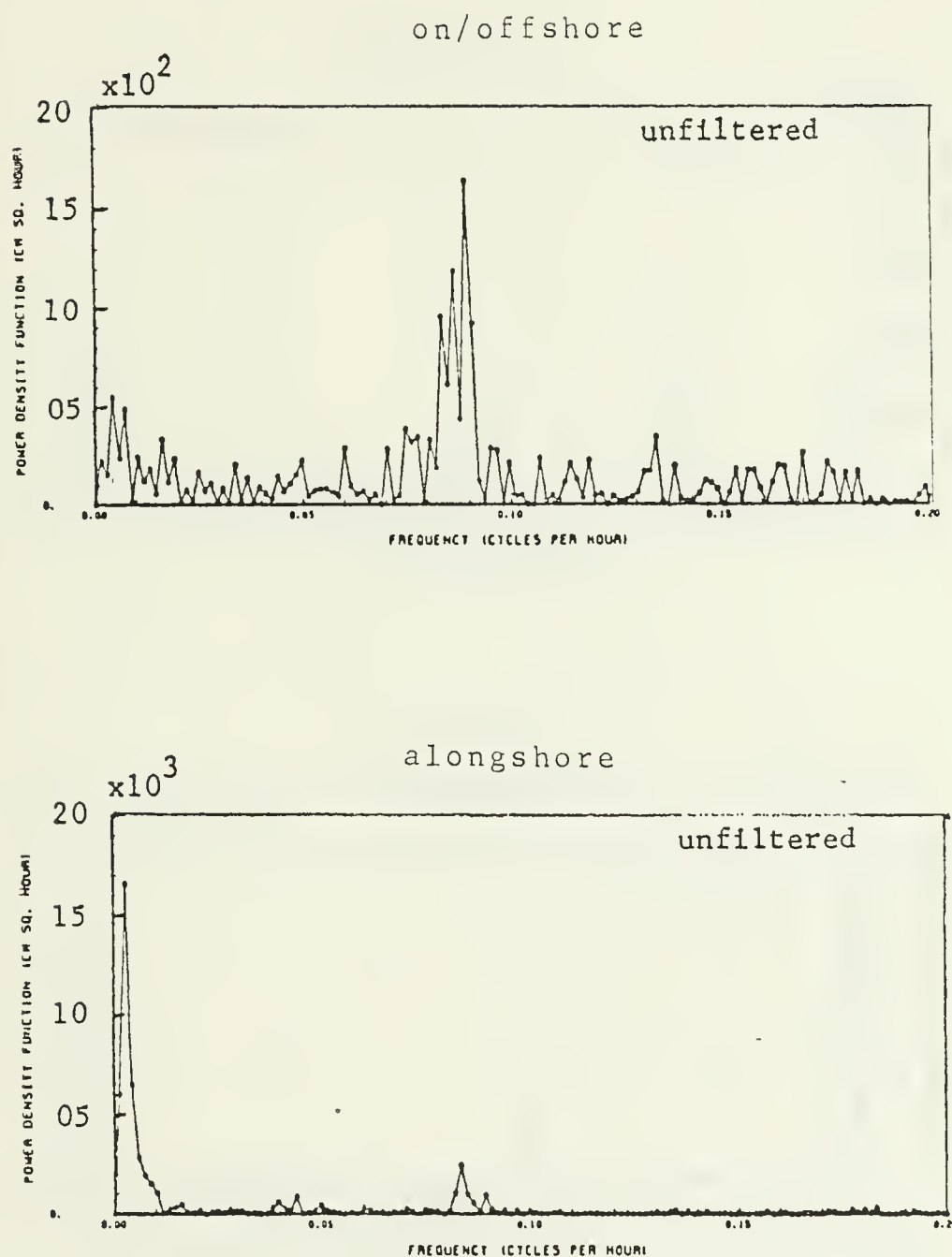


Figure 38. Energy density spectrum of current meter at 165 m depth at Station 2 deployed on 21 July 1979.

Station 2 Meter #1319 Depth=237m 21 Jul 79

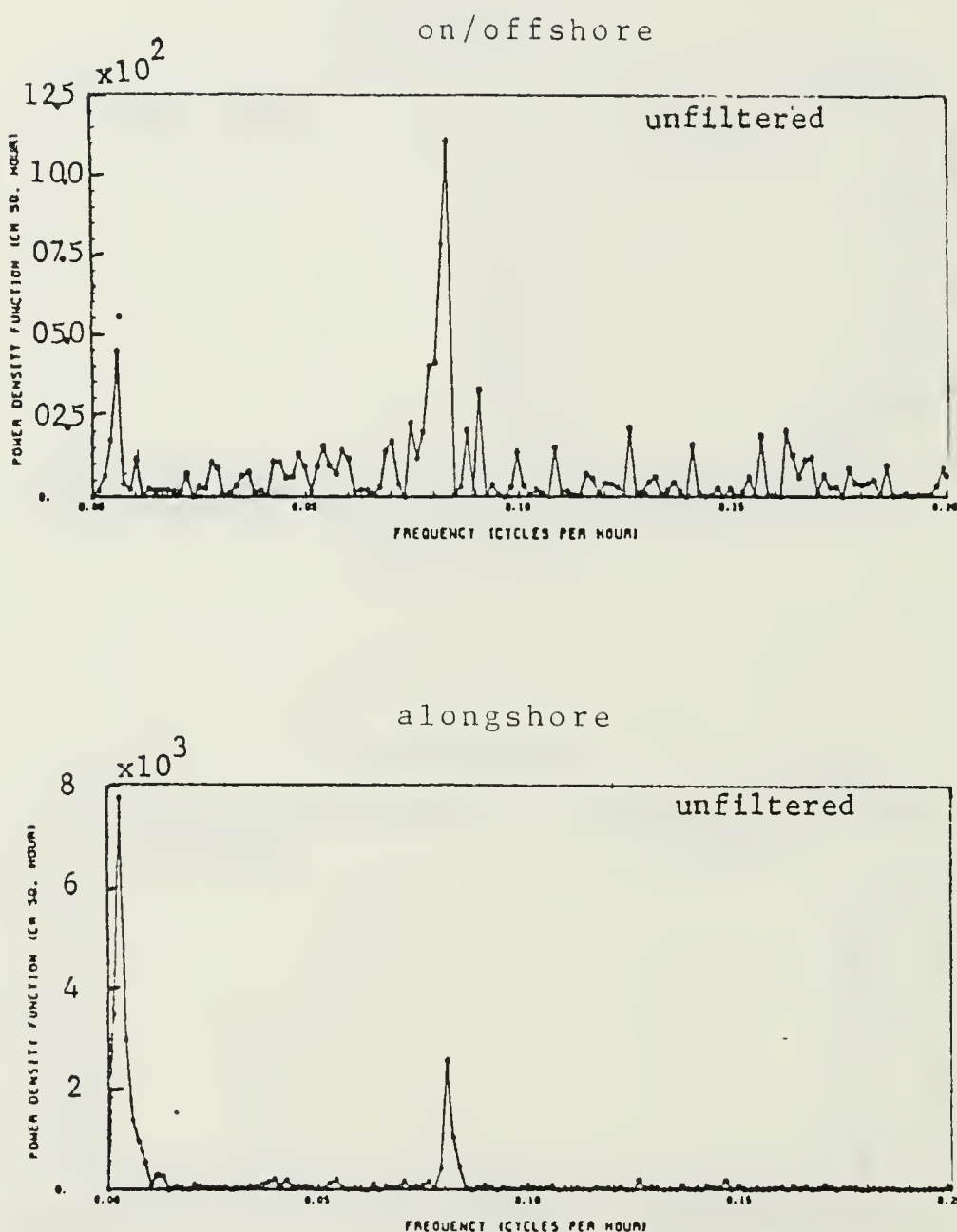


Figure 39. Energy density spectrum of current meter at 237 m depth at Station 2 deployed on 21 July 1979.

Station 7 Meter #2760 Depth=127m 7 Oct 79

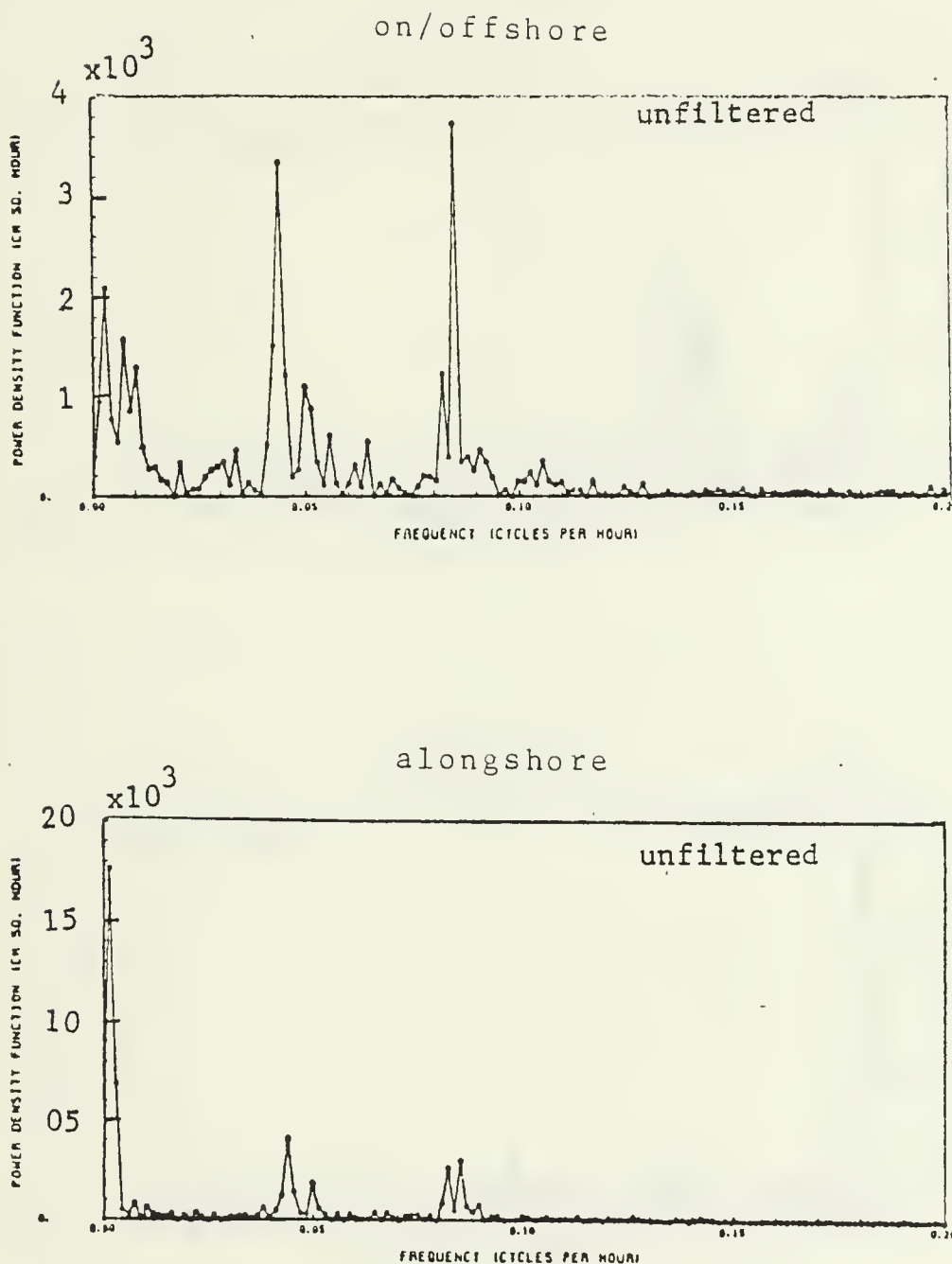


Figure 40. Energy denisty spectrum of current meter at 127 m depth at Station 7 deployed on 7 October 1979.

Station 7 Meter #842 Depth=200m 7 Oct 79

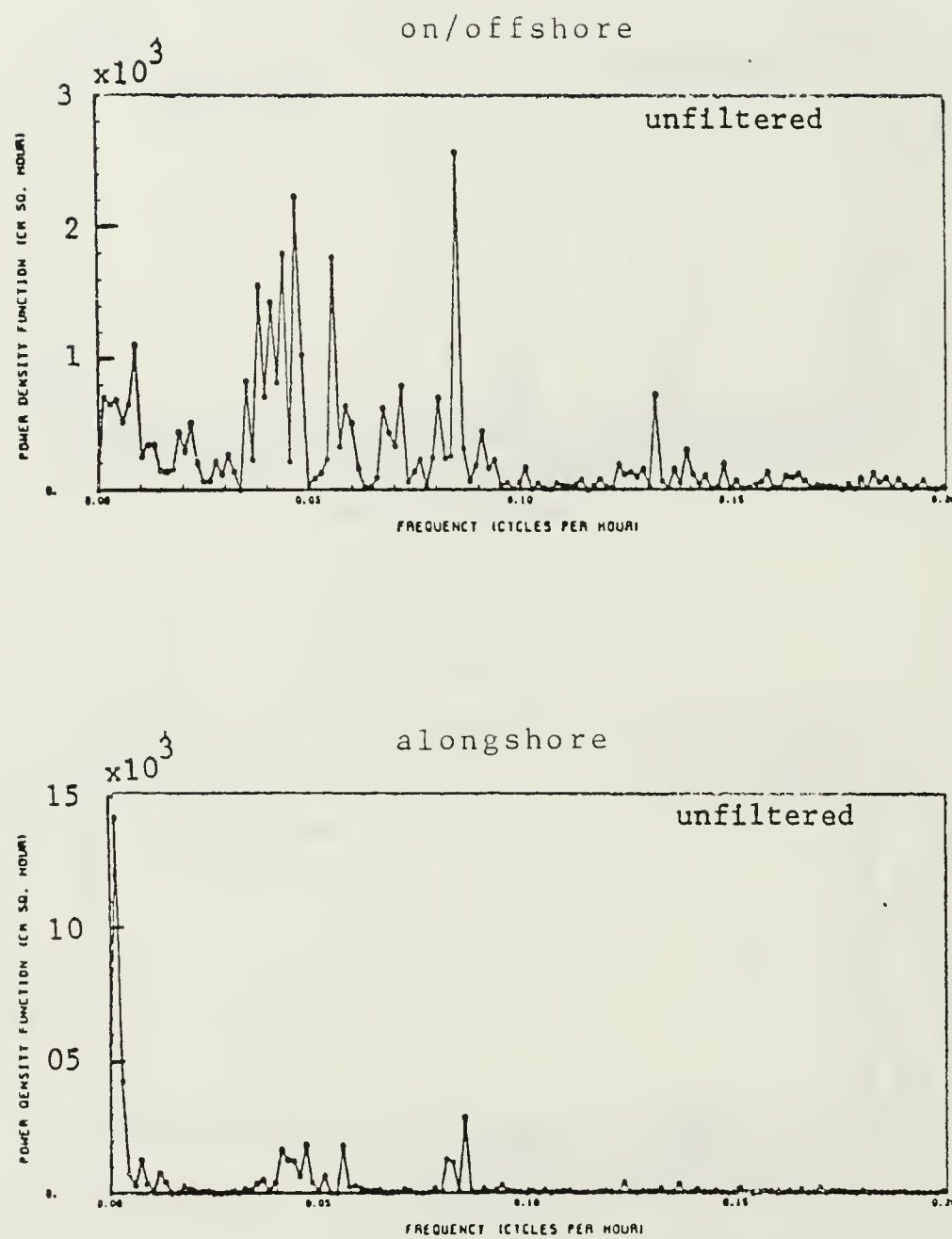


Figure 41. Energy density spectrum of current meter at 200 m depth at Station 7 deployed on 7 October 1979.

Station 2 Meter #1965 Depth=194m 24 Nov 79

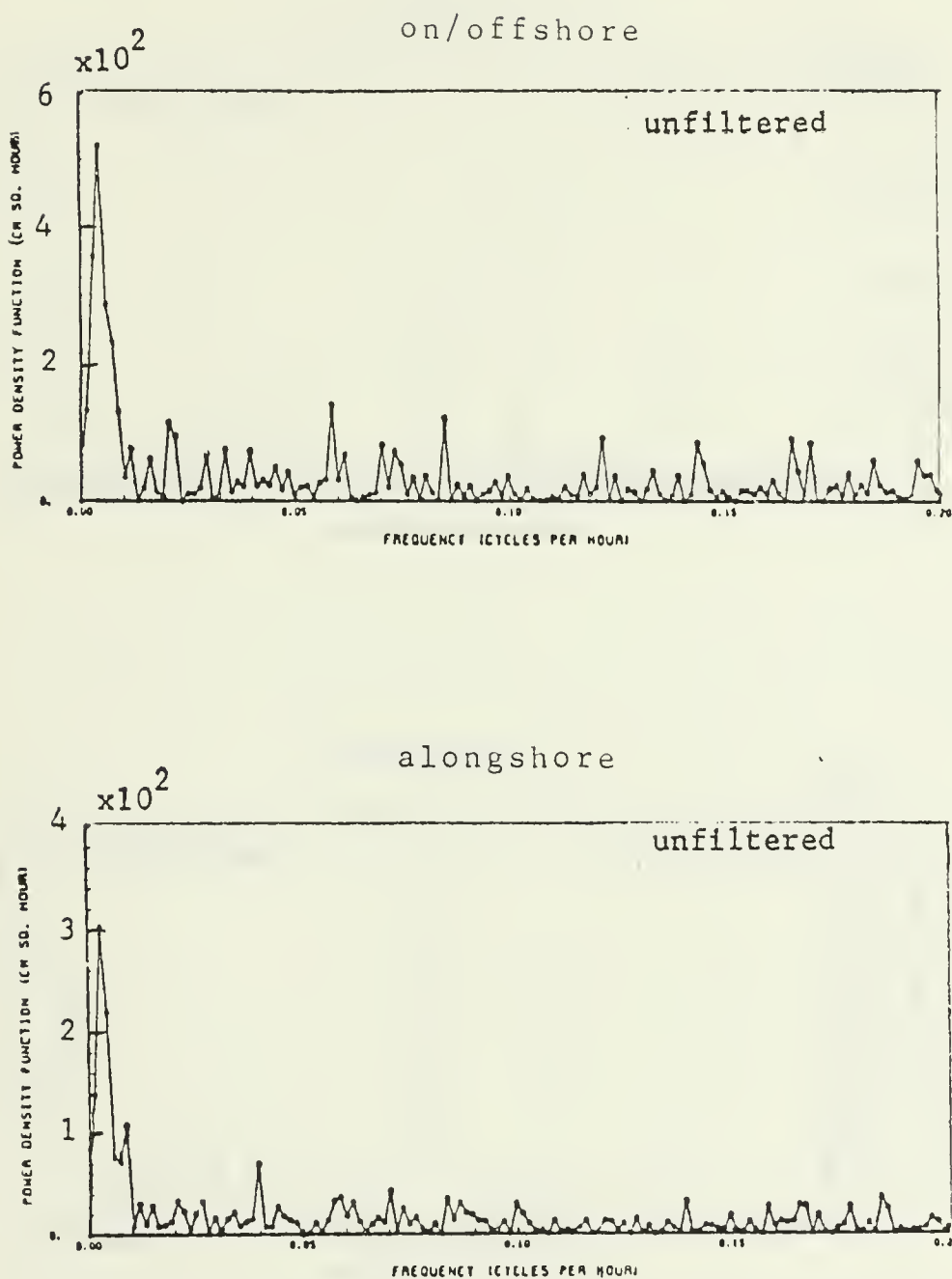


Figure 42. Energy density spectrum of current meter at 194 m depth at Station 2 deployed on 24 November 1979.

Station 2 Meter #1319 Depth=266m 24 Nov 79

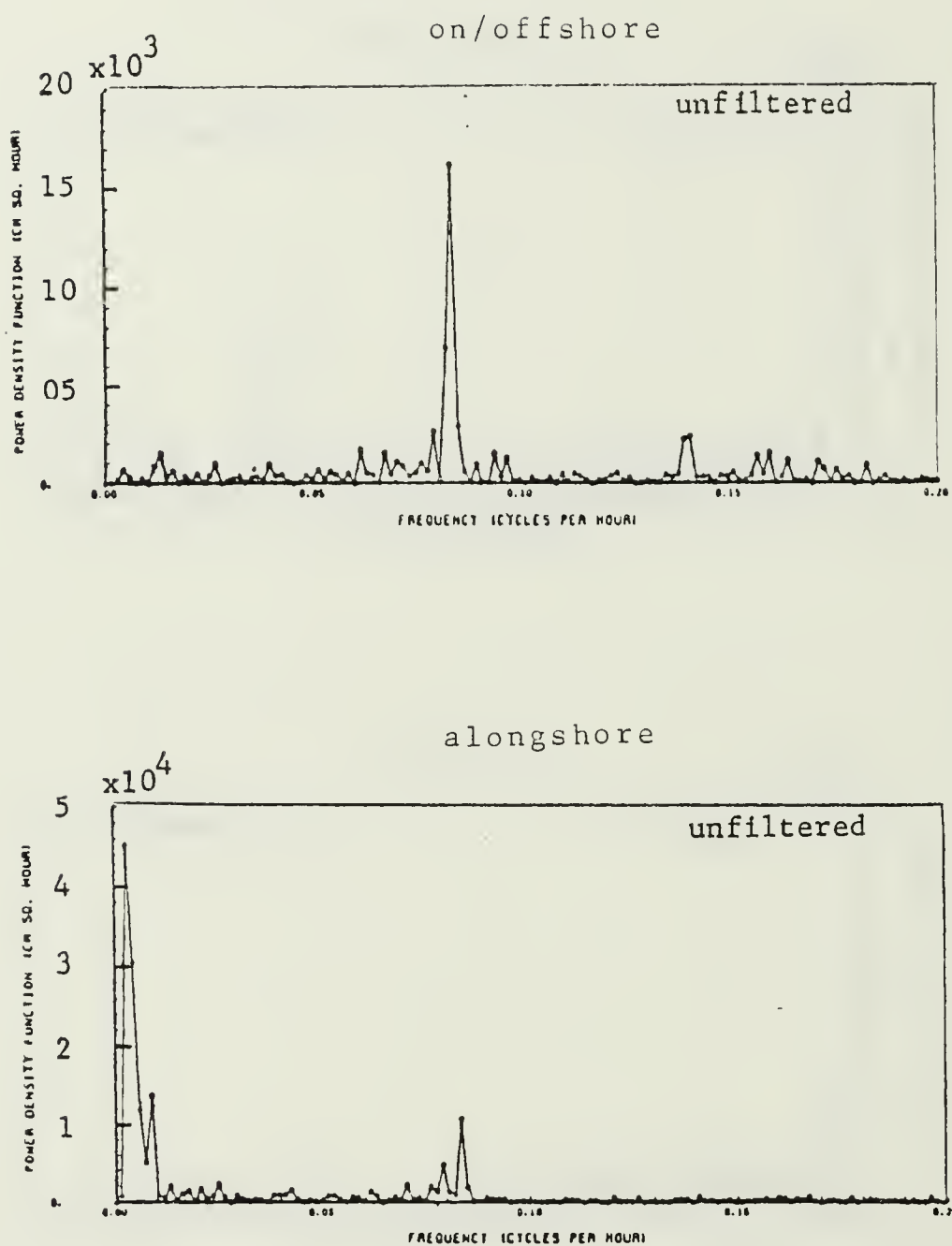
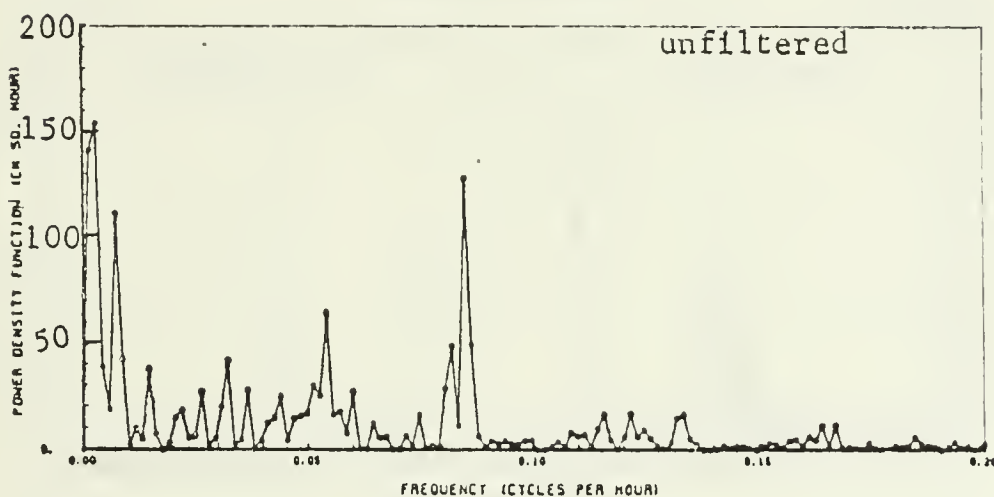


Figure 43. Energy density spectrum of current meter at 266 m depth at Station 2 deployed on 24 November 1979.

Station 7 Meter #2760 Depth=113m 3 Mar 80

on/offshore



alongshore

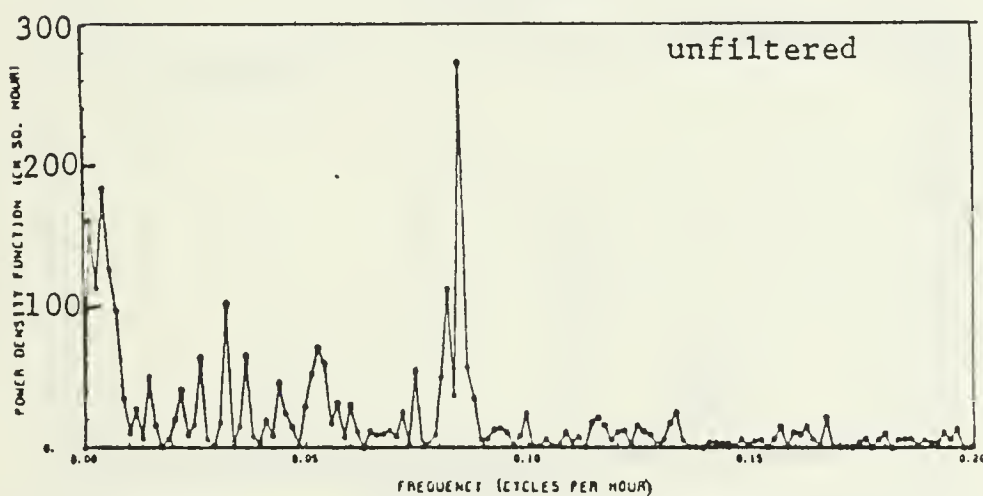


Figure 44. Energy density spectrum of current meter at 113 m depth at Station 7 deployed on 3 March 1980.

Station 7 Meter #842 Depth = 186m 3 Mar 80

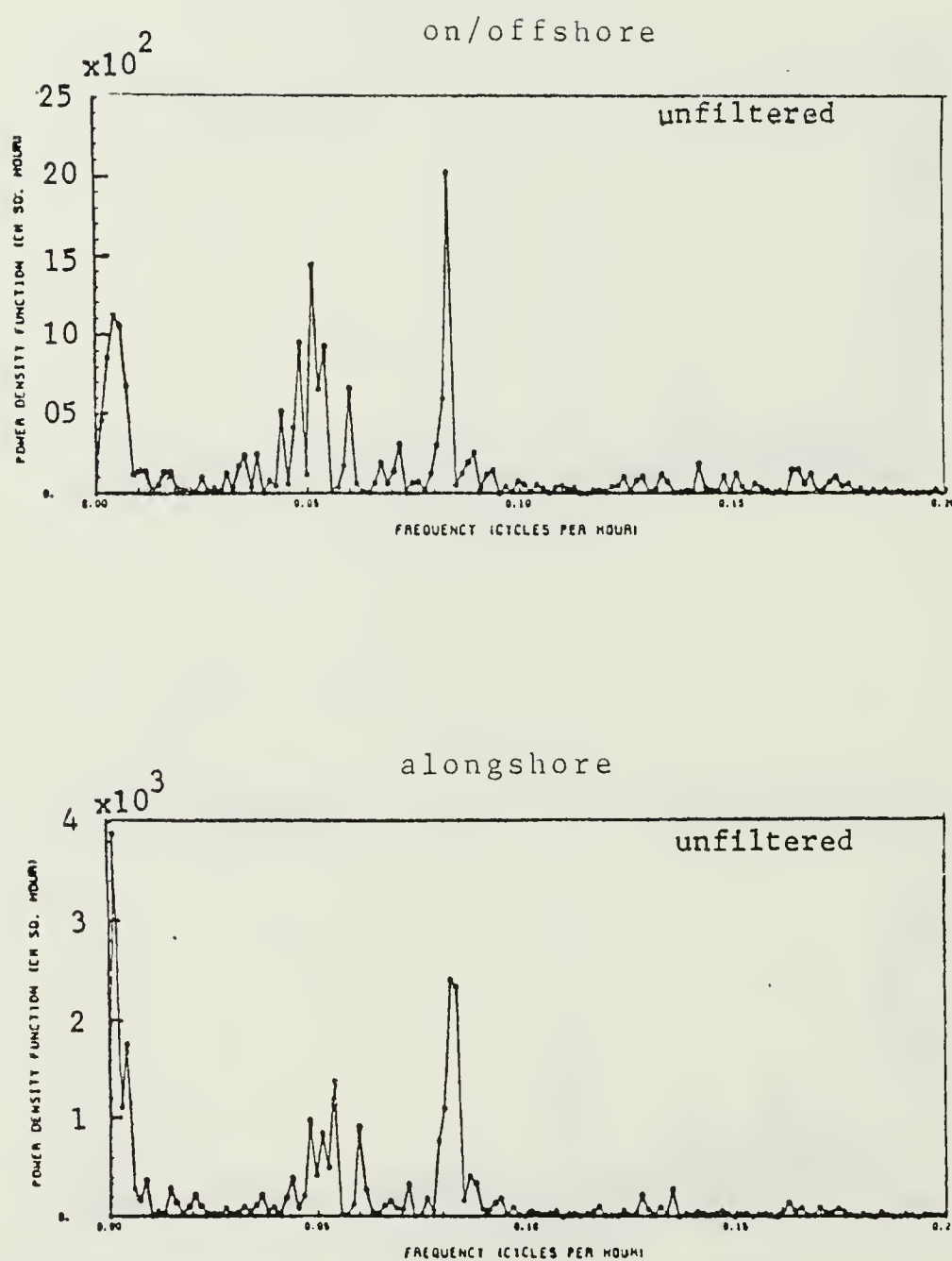


Figure 45. Energy density spectrum of current meter at 186 m depth at Station 7 deployed on 3 March 1980.

Station 7

Meter #762

Depth=311m

3 Mar 80

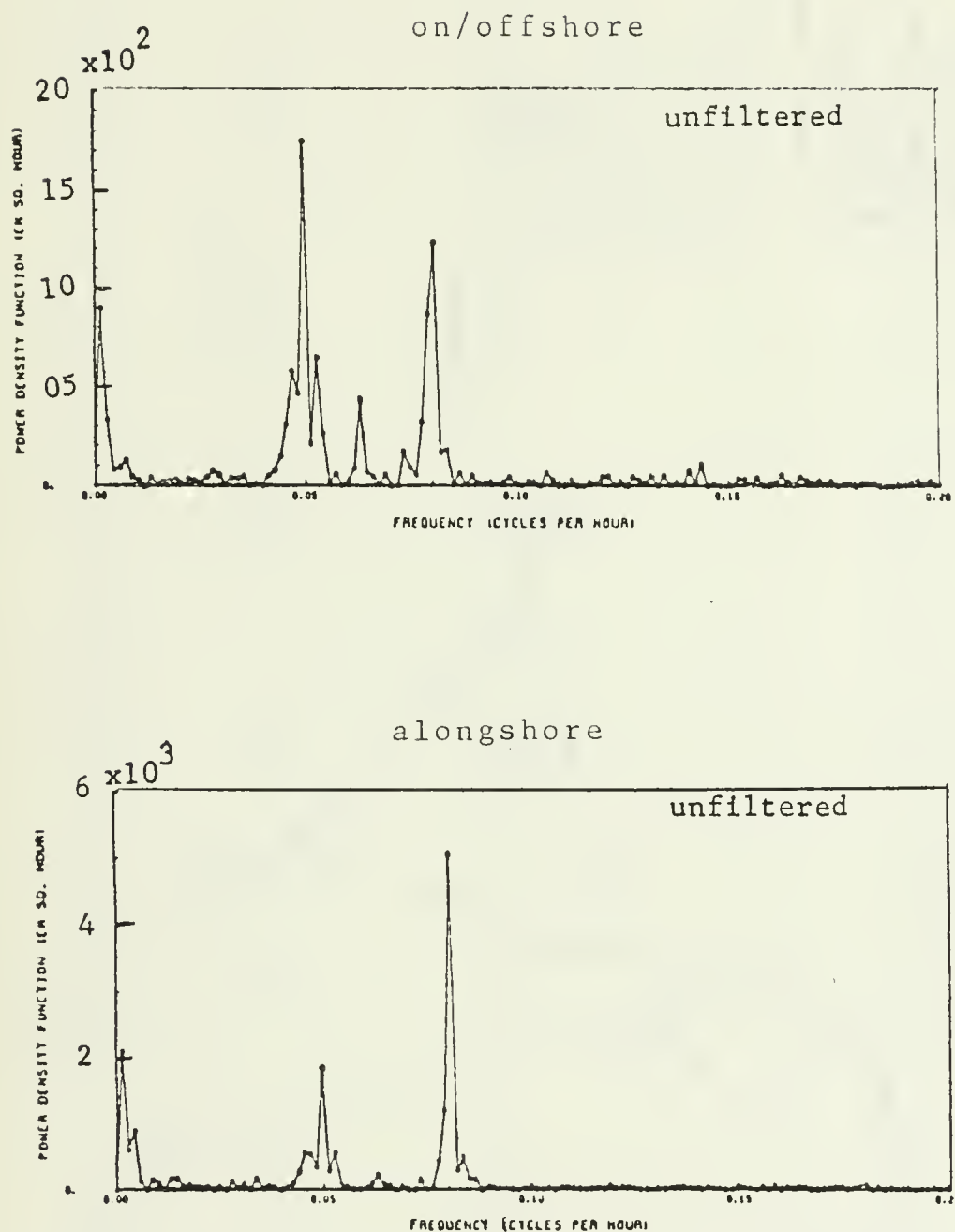


Figure 46. Energy density spectrum of current meter at 311 m depth at Station 7 deployed on 3 March 1980.

APPENDIX C: PROGRESSIVE VECTOR DIAGRAMS

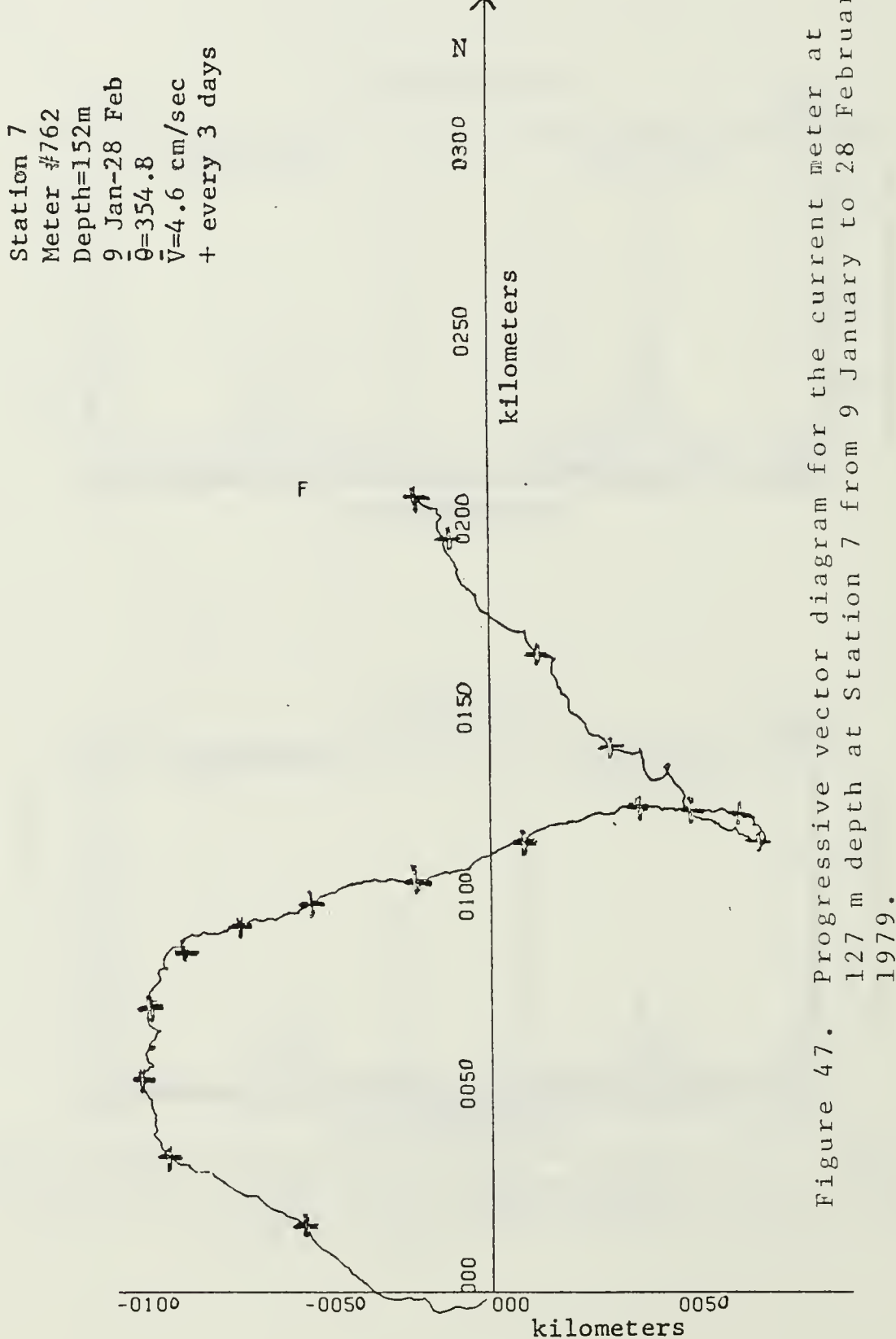


Figure 47. Progressive vector diagram for the current meter at 127 m depth at Station 7 from 9 January to 28 February 1979.

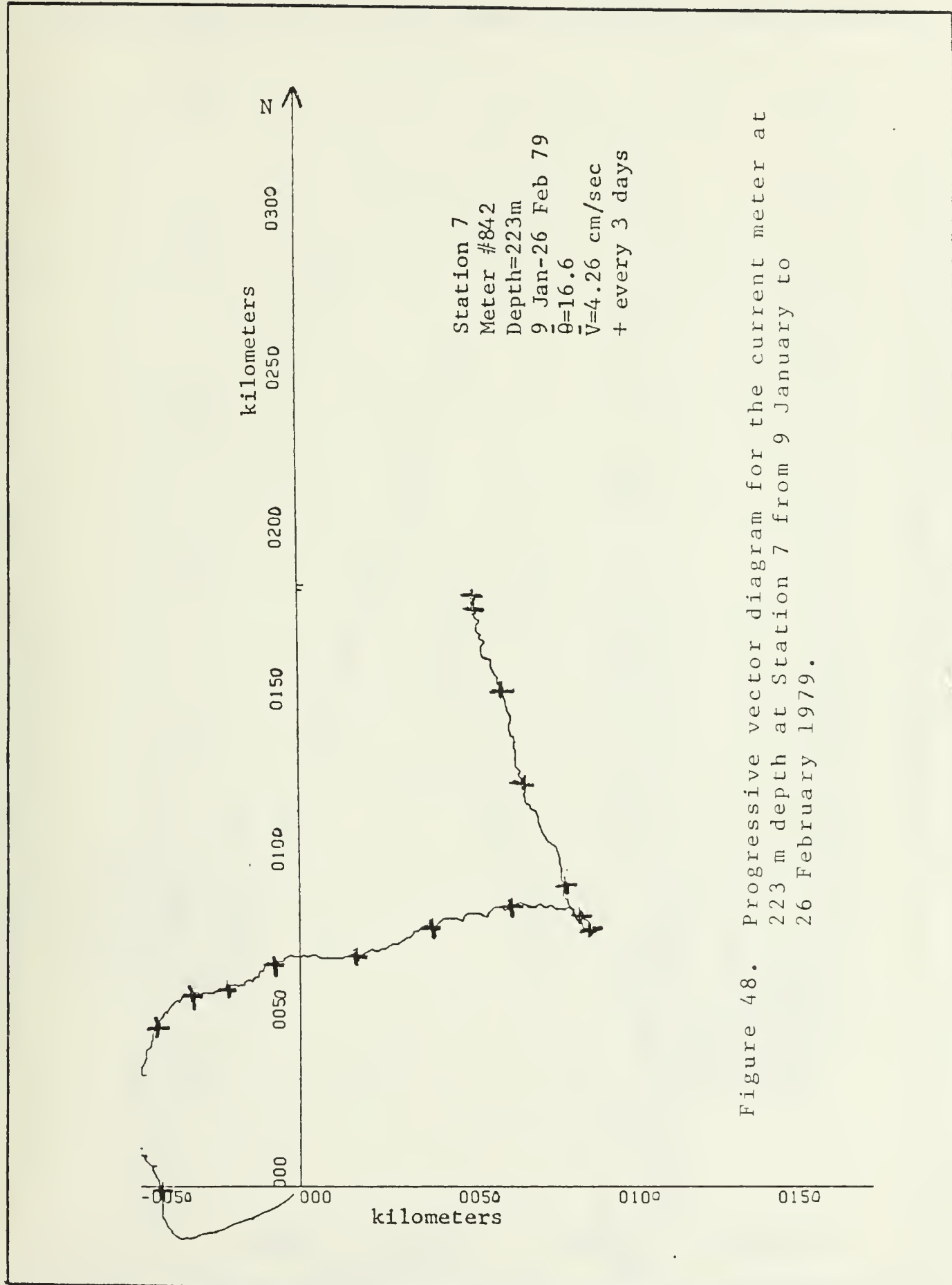


Figure 48. Progressive vector diagram for the current meter at 223 m depth at Station 7 from 9 January to 26 February 1979.

Station 2
Meter #1965
Depth=169m
24 Apr-13 June 79
 $\bar{\theta}=341.2$
 $\bar{V}=16.01$ cm/sec
+ every 3 days

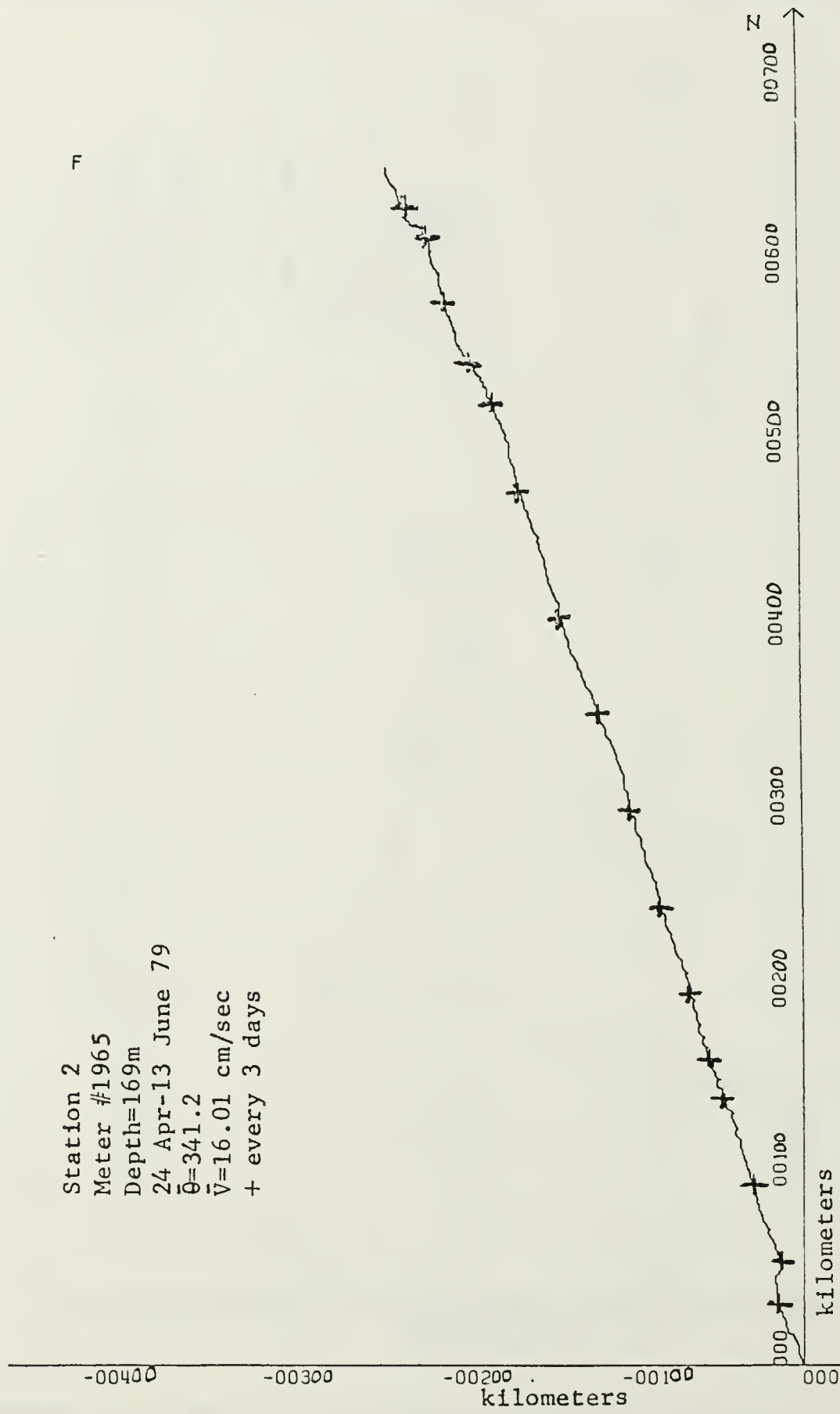


Figure 49. Progressive vector diagram for the current meter at 169 m depth at Station 2 from 24 April to 13 June 1979.

Station 2
Meter #1319
Depth=241m
24 Apr-12 June 79
 $\bar{\theta}=340.4$
 $\bar{v}=11.11$ cm/sec
+ every 3 days

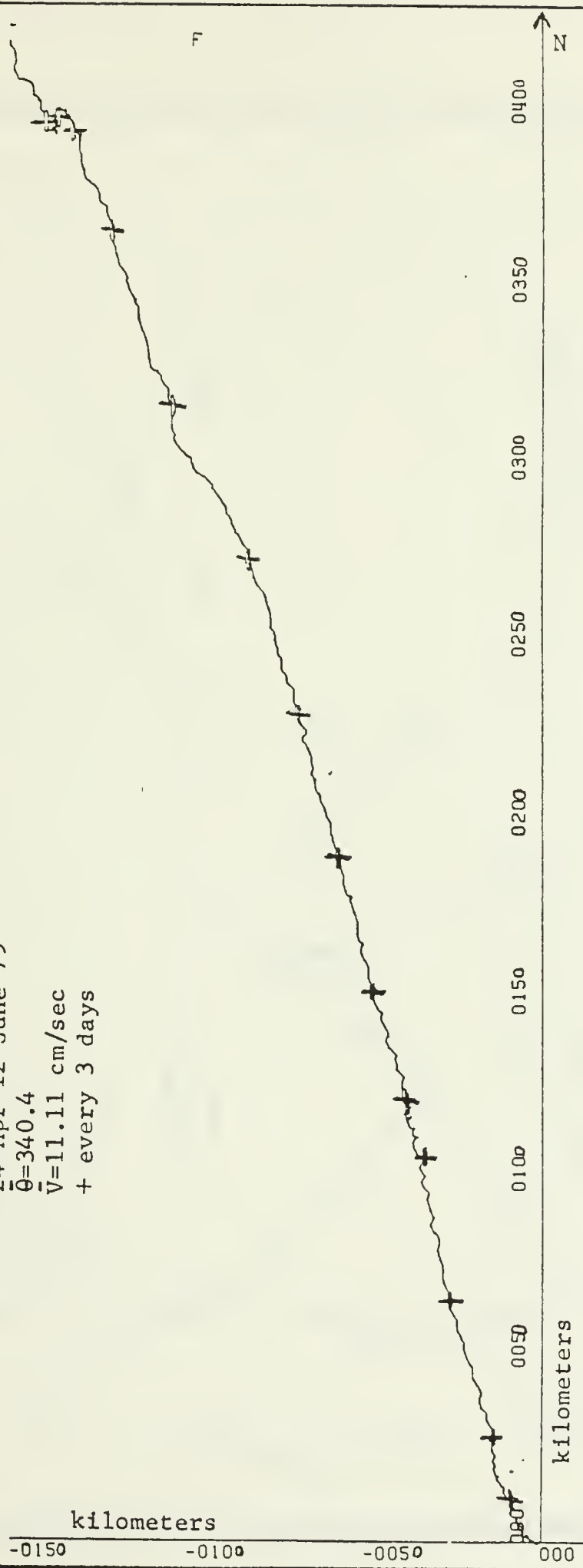


Figure 50. Progressive vector diagram for the current meter at 241 m depth at Station 2 from 24 April 12 June 1979.

Station 7
 Meter #2760
 Depth=158m
 9 Jul-30 Aug 79
 $\bar{\theta}=312.2$
 $\bar{v}=4.51 \text{ cm/sec}$
 + every 3 days

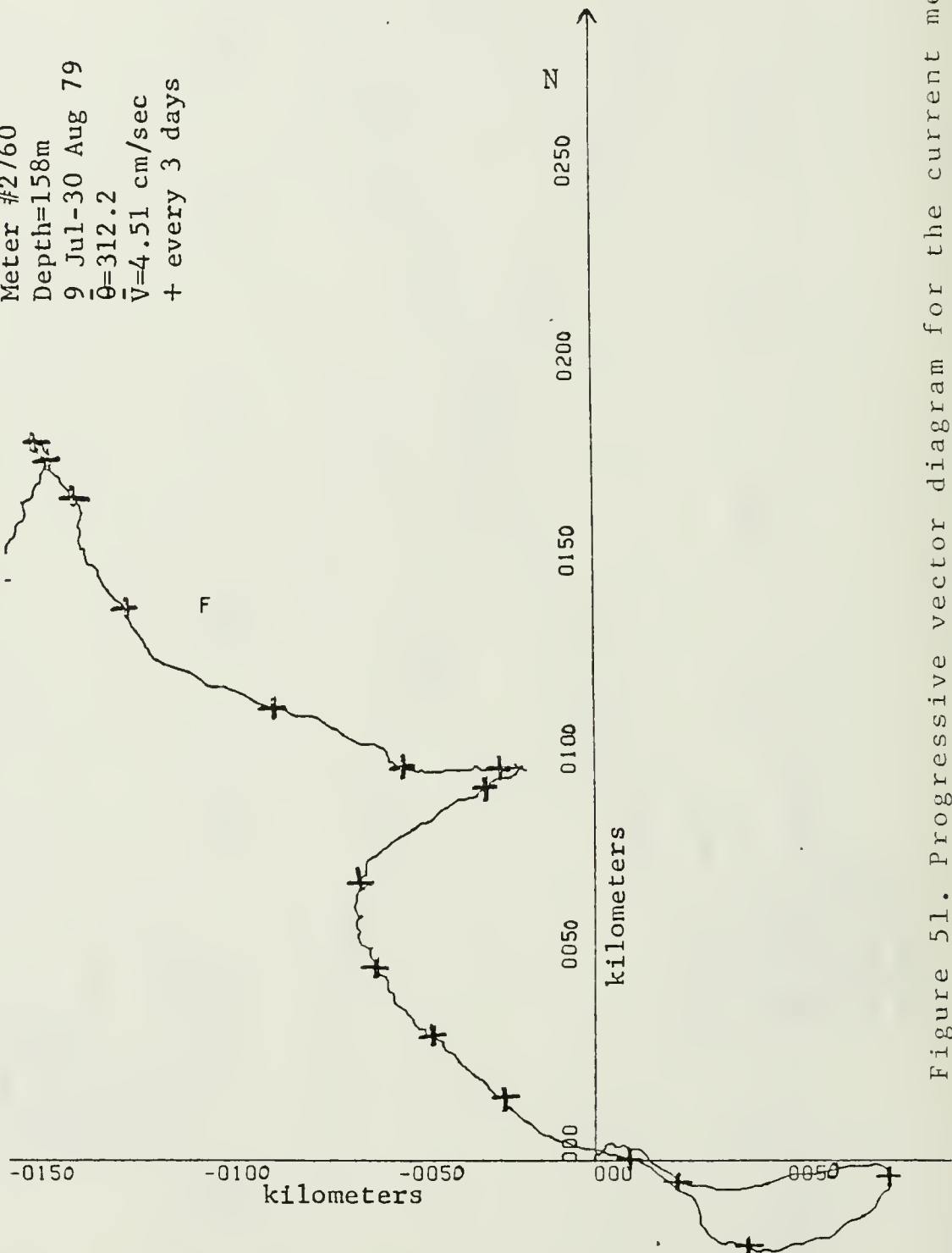


Figure 51. Progressive vector diagram for the current meter at
 158 m depth at Station 7 from 9 July to 30 August
 1979.

Station 7
Meter #842
Depth=231m
9 Jul-29 Aug 79
 $\bar{\theta}=330.6$
 $\bar{V}=5.84$ cm/sec
+ every 3 days

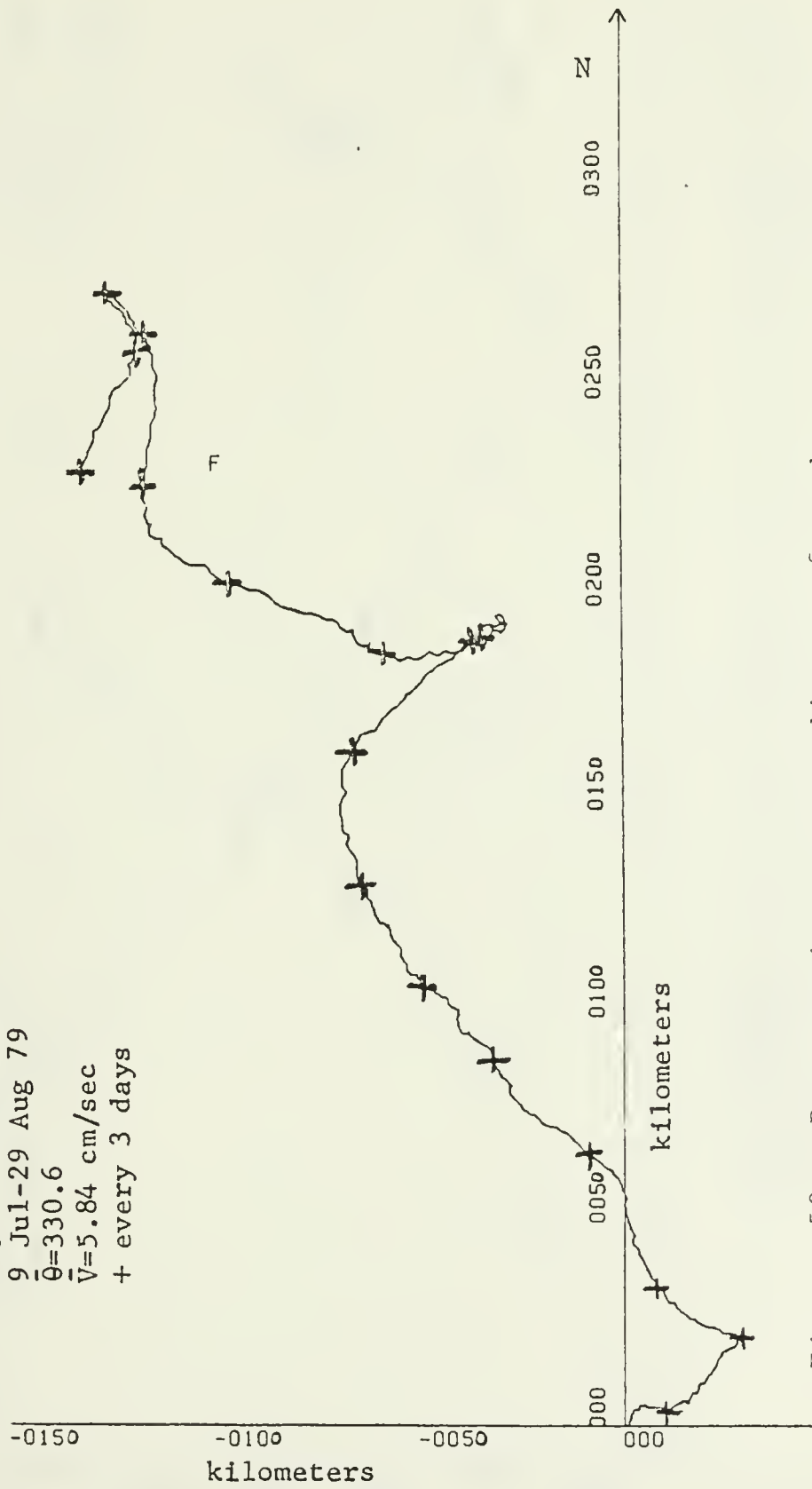


Figure 52. Progressive vector diagram for the current meter at 231 m depth at Station 7 from 9 July to 29 August 1979.

Station 7
Meter #362
Depth=356m
9 Jul-30 Aug 79
 $\bar{\theta}=338.6$
 $\bar{V}=2.77$ cm/sec
+ every 3 days

T

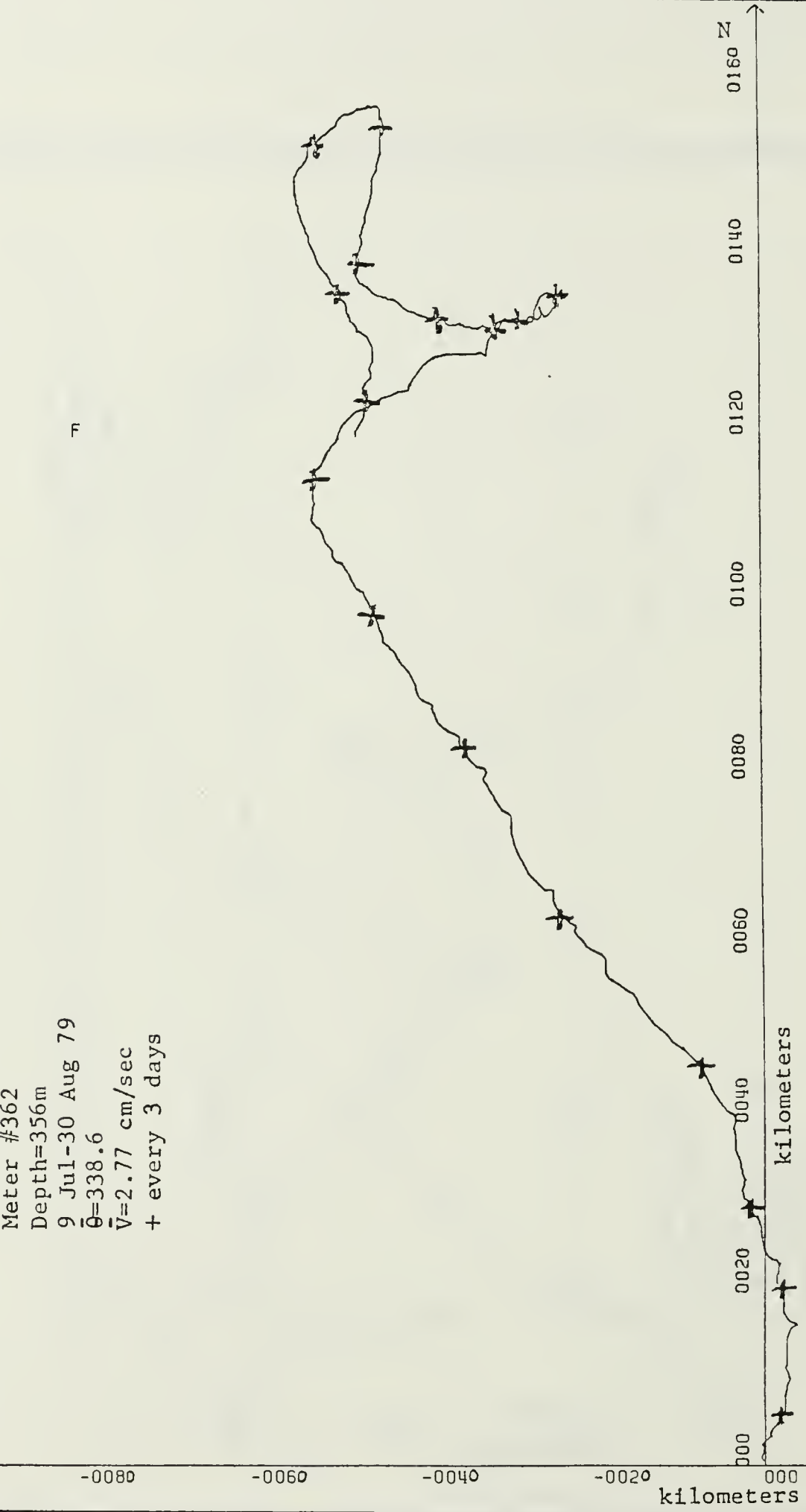


Figure 53. Progressive vector diagram for the current meter at 356 m depth at Station 7 from 9 July to 30 August 1979.

Station 2
Meter #1965
Depth=165m
23 Jul-11 Sep 79
 $\bar{\theta}=325.1$
 $\bar{V}=6.13 \text{ cm/sec}$
+ every 3 days

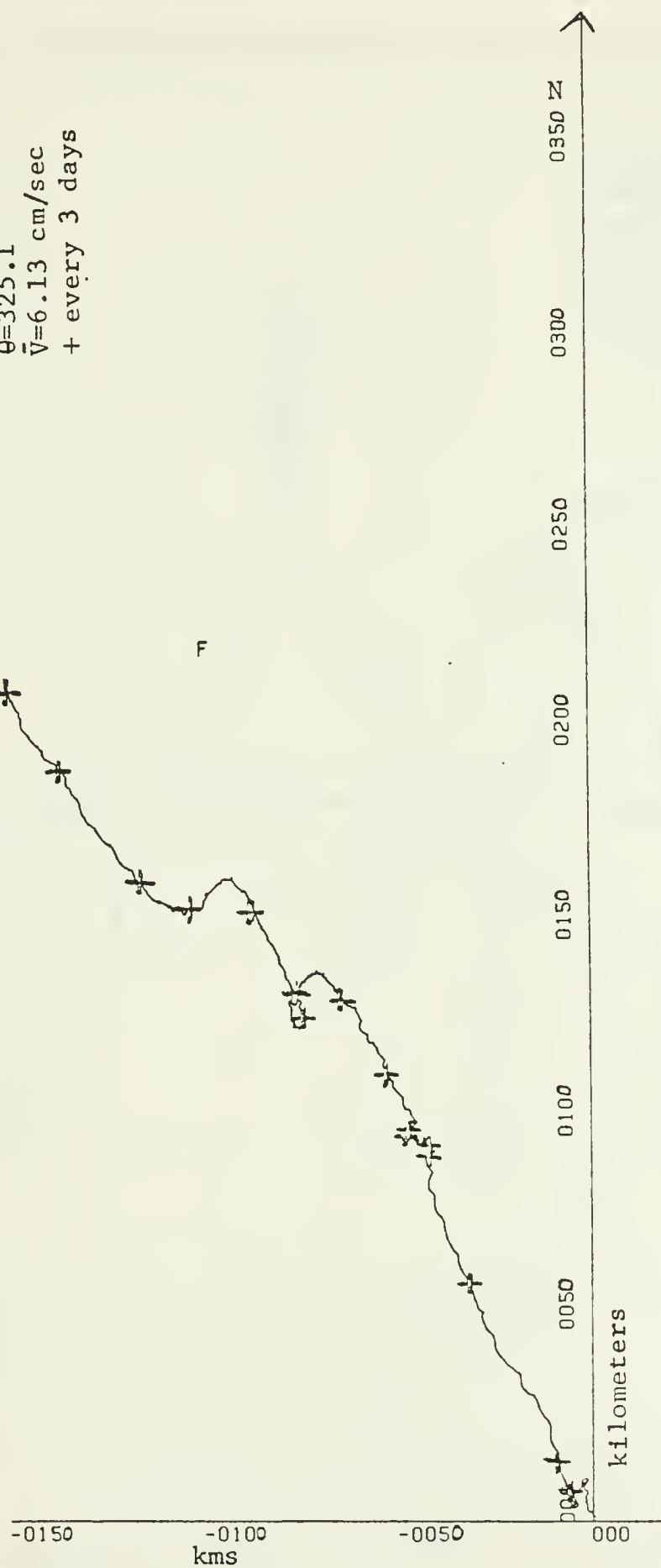


Figure 54. Progressive vector diagram for the current meter at 165 m depth at Station 2 from 23 July to 11 September 1979.

Station 2
Meter #1319
Depth=237m
23 Jul-13 Sep 79
 $\bar{\theta}=314.3$
 $\bar{v}=1.47$ cm/sec
+ every 3 days

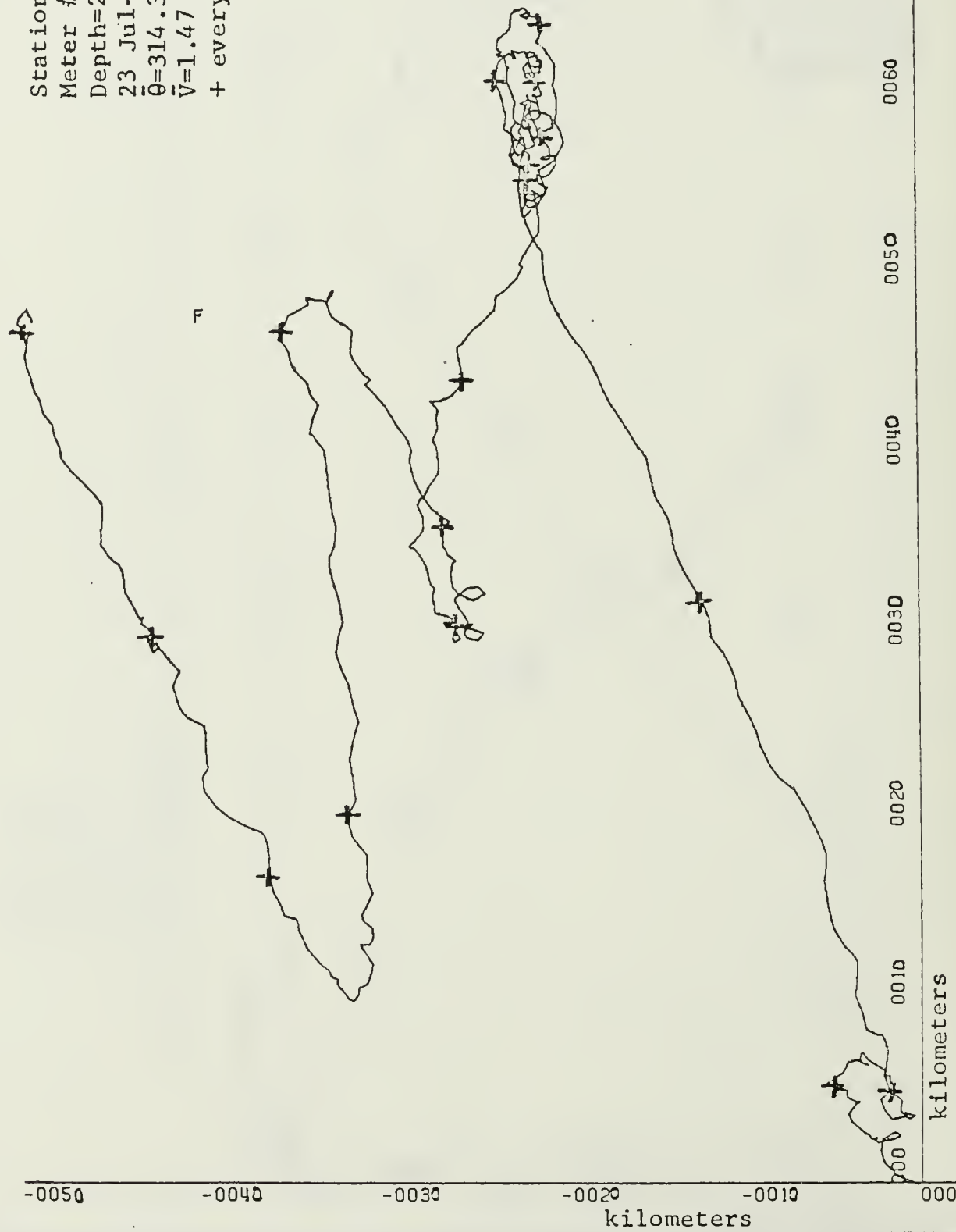


Figure 55. Progressive vector diagram for the current meter at 237 m depth at Station 2 from 23 July to 13 September 1979.

Station 7
Meter #2760
Depth=127m
9 Oct-29 Nov 79
 $\theta=68.1$
 $\bar{v}=5.05$ cm/sec
+ every 3 days

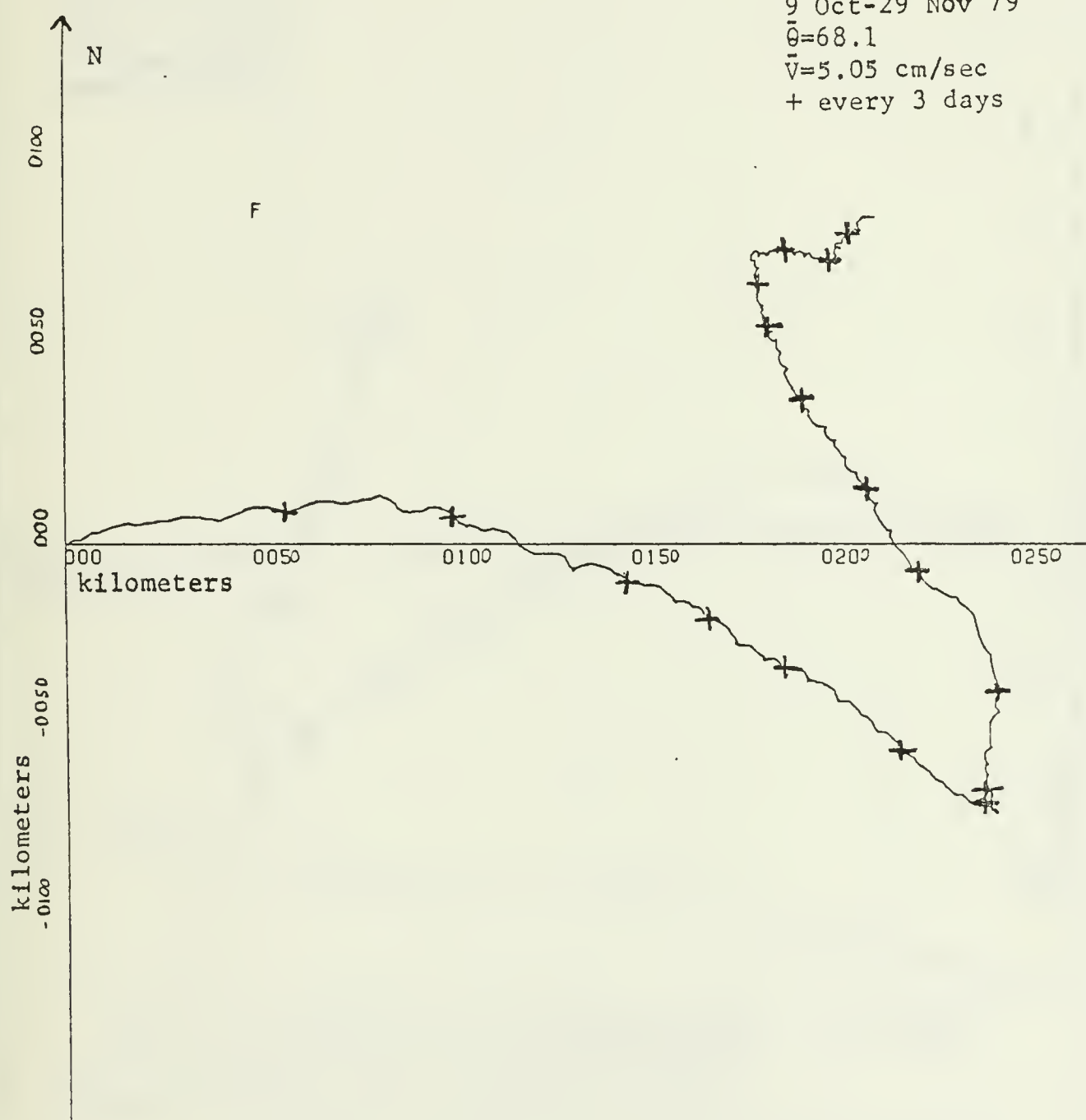


Figure 56. Progressive vector diagram for the current meter at 127 m depth at Station 7 from 9 October to 29 November 1979.

Station 7
Meter #842
Depth=200m
9 Oct-29 Nov 79
 $\theta=70.6$
 $V=4.07 \text{ cm/sec}$
+ every 3 days

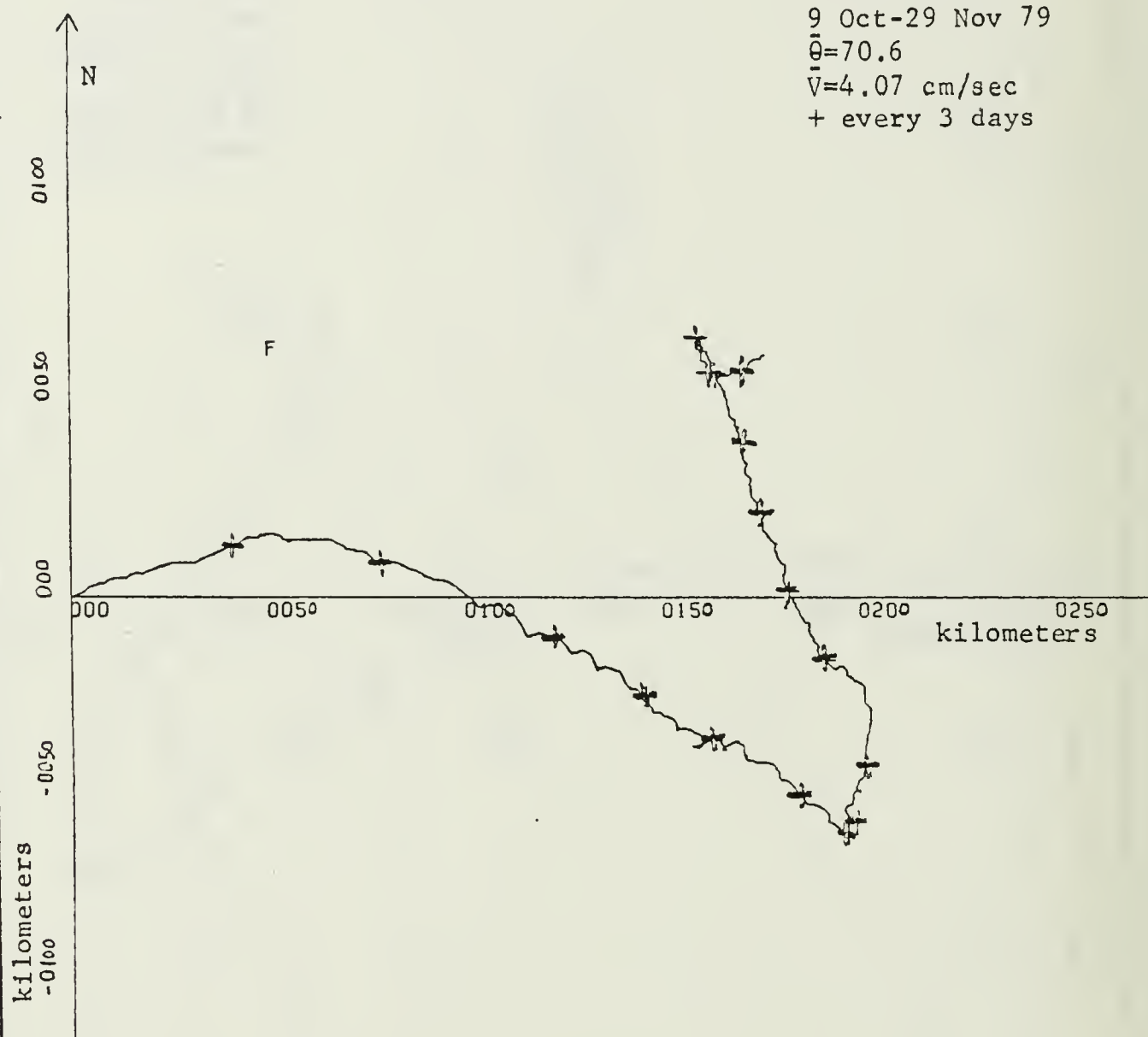


Figure 57. Progressive vector diagram for the current meter at 200 m depth at Station 7 from 9 October to 29 November 1979.

Station 2
Meter #1965
Depth=194m
27 Nov 79-16 Jan 80
 $\bar{\theta}=279.8$
 $\bar{V}=6.24$ cm/sec
+ every 3 days

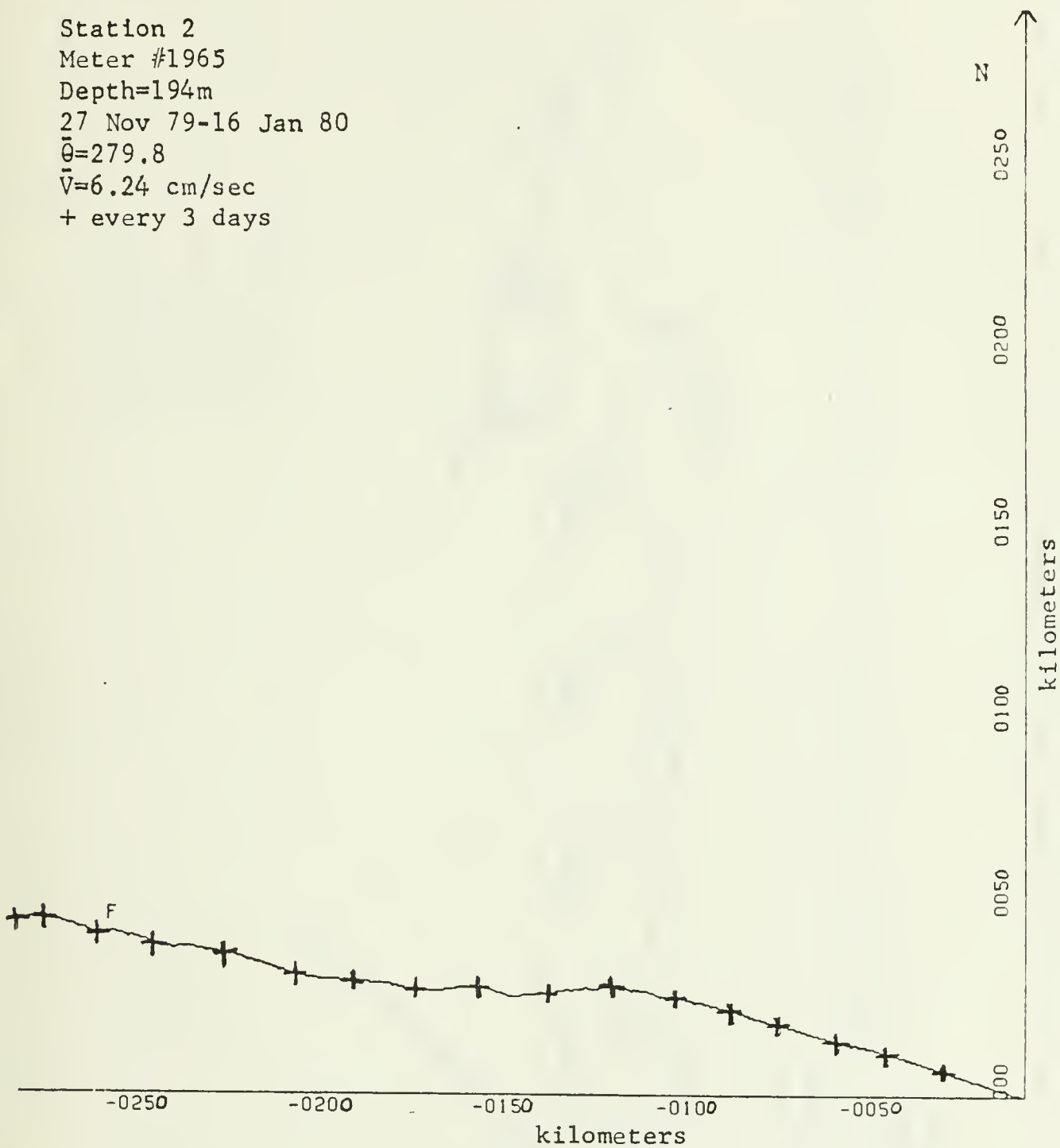


Figure 58. Progressive vector diagram for the current meter at 169 m depth at Station 2 from 27 November 1979 to 16 January 1980.

Station 2
Meter #1319
Depth=266m
27 Nov 79-18 Jan 80
 $\bar{\theta}=3.1$
 $\bar{v}=2.66$ cm/sec
+ every 3 days

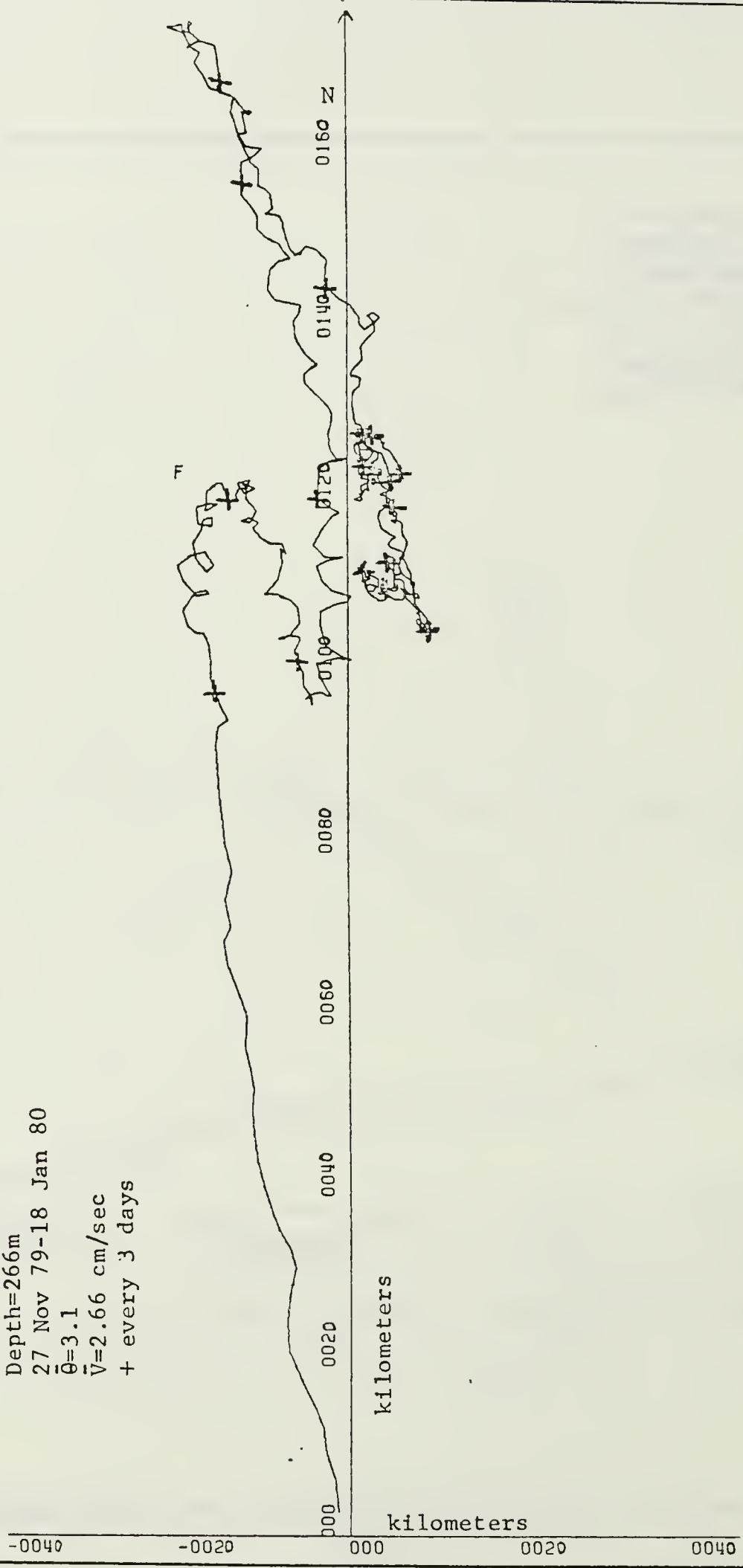


Figure 59. Progressive vector diagram for the current meter at 266 m depth at Station 2 from 27 November 1979 to 18 January 1980.

Station 7
Meter #2760
Depth=113m
4 Mar-15 Apr 80
 $\bar{\theta}=310.5$
 $\bar{V}=4.41$ cm/sec
+ every 3 days

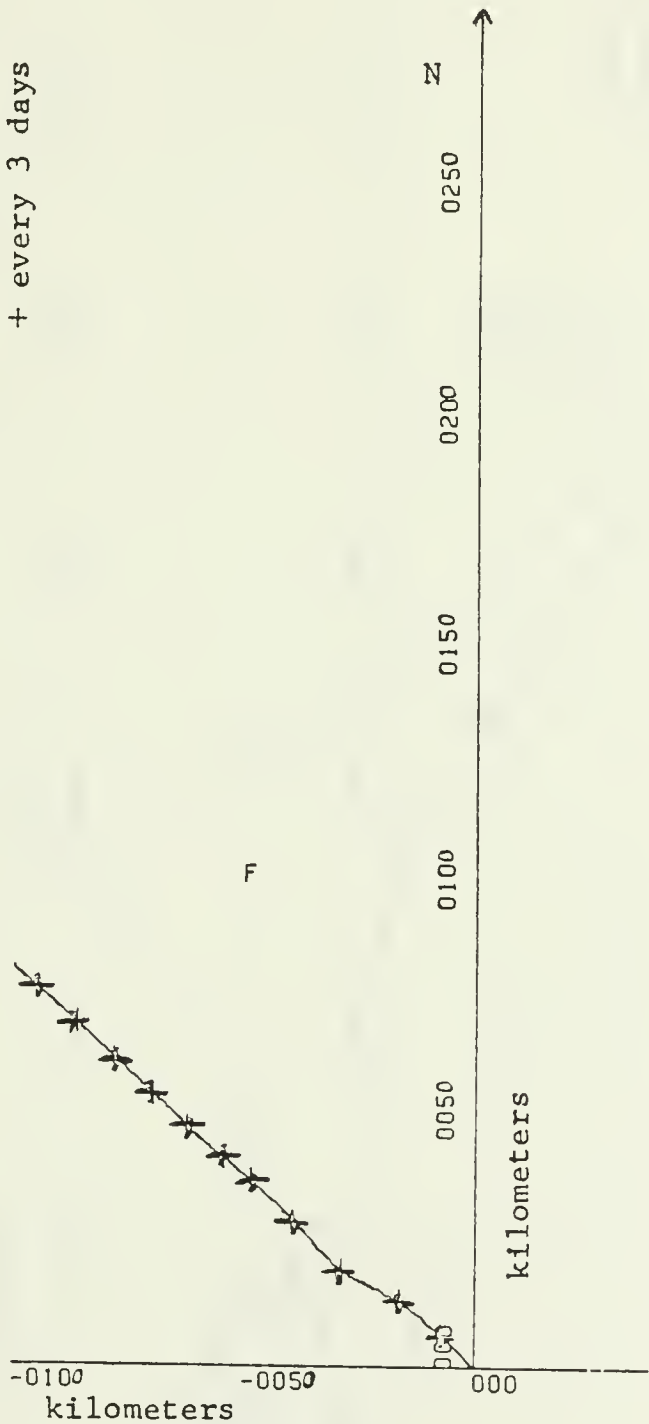


Figure 60. Progressive vector diagram for the current meter at 113 m depth at Station 7 from 4 March to 15 April 1980.

Station 7
Meter #848
Depth=186m
4 Mar-12 Apr 80
 $\bar{\theta}=328.7$
 $\bar{V}=3.43$ cm/sec
+ every 3 days

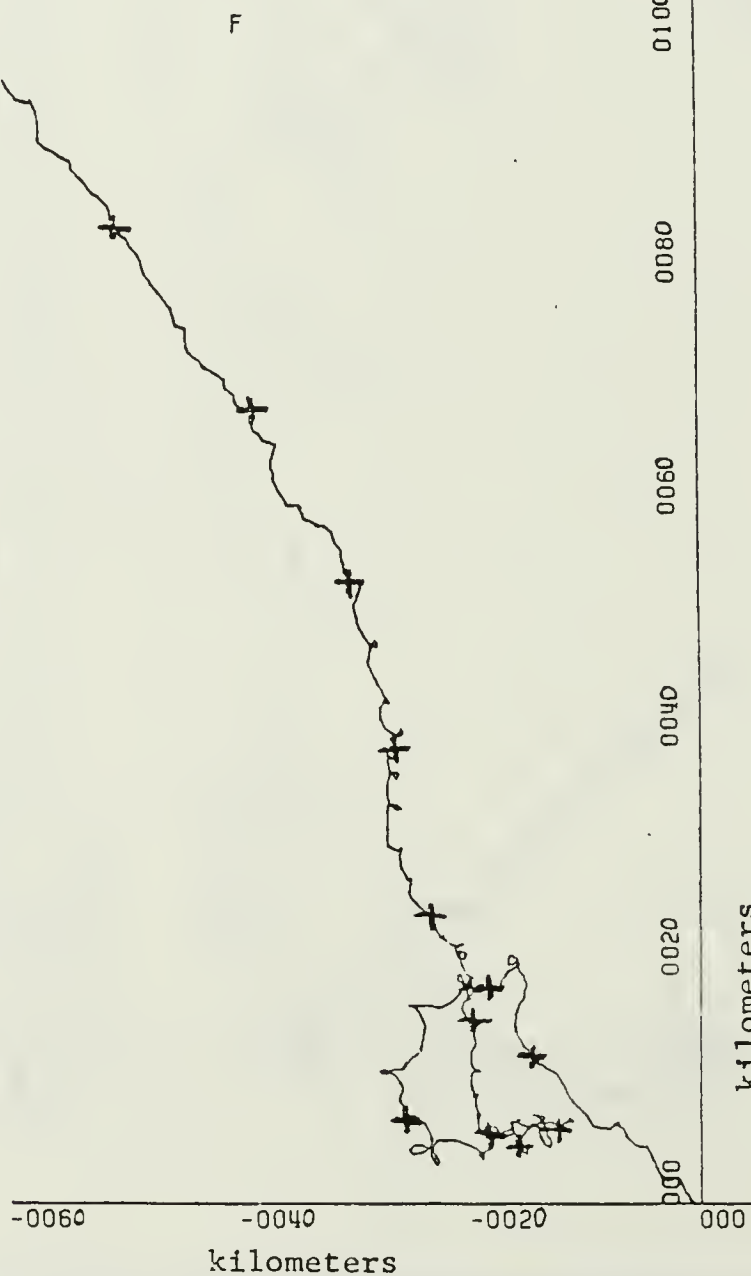


Figure 61. Progressive vector diagram for the current meter at 186 m depth at Station 7 from 4 March to 12 April 1980.

Station 7
Meter #762
Depth=311m
4 Mar-10 Apr 80
 $\bar{\theta}=8.2$
 $\bar{v}=2.67 \text{ cm/sec}$
+ every 3 days

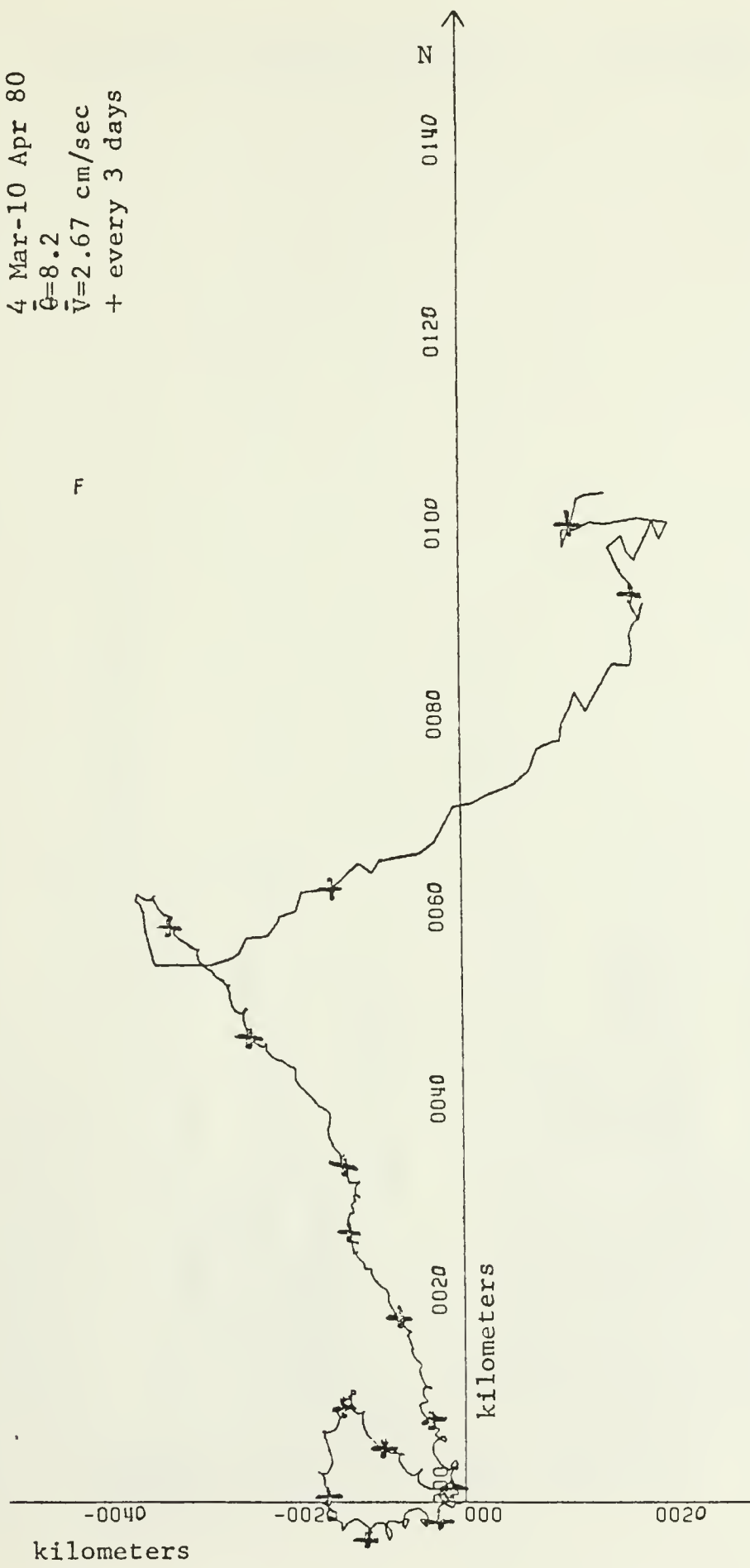


Figure 62. Progressive vector diagram for the current meter at 311 m depth at Station 7 from 4 March to 10 April 1980.

THIS PROGRAM FORMATS FREQUENTLY USED CURRENT METER DATA INPUT
 - SO THAT IT IS FOR TRAN READING. WRITTEN BY FANS DCELMAN NPS

```

C CXPURGE CPI CENTERMAIN; CONSECUTIVE;
C DCL INPUTFILE RECORD ENV( CONSECUTIVE );
C DCL OUTFILE CHAR(512) VAR YNAG STATIC;
C DCL FIELDY(512) CHAR(1) BASED(F);
C DCL 1SYRIC311(2) E1F(1),
C DCL 2SYRIC311(2) E1F(1),
C DCL (P,*) PFILE(SISNA) STATIC;
C NENDFILE(INPUTF) GCTCKCOUNT;
C ENDFILE(OUTTF) GCTCTEEEN;
C KKCOUNT;
OPEN FILE(INPUTF) INPUT;
OPEN FILE(OUTTF) OUTPUT;
P=WORD(FIELDX);
KOUT,KCOUNT=0;
KK=C;MAX=163;
I=0;
IF KK>MAX THEN GOTO THEEND;
KK=KK+1;
READ FILE(INPUTF) INTO(FIELDX);
K=LNGTH(FIELDX);
DO J=1 TO K;
IF I>1 THEN DO;
IF SYNCIT SYNC(J)= '1'E THEN DO;
I=J;
IF SYNCIT SYNC(J)= '1'E THEN DO;
END; /* IF SYNCIT SYNC(J+1)= '1'E THEN DO;
GOTO XX;
END;
I= I+1;
IF I<1 THEN GC;
IF I=1 THEN F1SKIP(1);
J=ACCR(FIELDY(J));
CALL STCREM(G,I); /*/
END; /* IF I<1 */
J=J+1;
XX:
EIC; /* DC .. = 1 TCK */ /
GOTC L0CP;
THEEND;

```

```

PUT EXIT (KK, *BLOCKS READ,
          *CUT, *RECCRS WRITTEN)
  (SKIP(1), F(6), A, F(6), A);
  (PCC(P,1));
  PCC(P,BIT(16) STATIC);
  DCL OUTFIELD(6) FIXED BIN(15) BASED(1);
  DCL OUTFIELD(6) FIXED BIN(15) BASED(1);
  DCL OUTFIELD(6) FIXED BIN(15) BASED(1);
  DCL P PICTURE(Z(16)) BASED(P);
  DCL INFILE(16) BASED(P);
  SUBSTR(DUTFIELD(I),1,6) = 'CCCCC' B;
  SUBSTR(DUTFIELD(I),1,6) = 'CCCCC' B;
  DO STR(DUTFIELD(I),II+1,1)=SUBSTR(INFILE,II+3,1);
  SUBSTR(DUTFIELD(I),II+6,1)=SUBSTR(INFILE,II+11,1);
  END;
  PUT EDIT(DUTFIELD(I))(X(4),F(6));
  IF I = 6 THEN DC;
  KOTI = KOTI + 1;
  YRITIE FILE(CUTFILE) FRGM(CUTFILE);
END; /* STUPID PROGRAM */
END;

```

THIS PROGRAM APPLIES CALIBRATION PARAMETERS TO A METER'S INDIVIDUAL CURRENT METERS
 XETER EQUATIONS ACCORDING TO EACH INDIVIDUAL CURRENT METER'S
 SPECIFICITIES.
 INITIALIZES AR(5000)
 REAL XX(X) /6(*)/.
 Y=7
 I1=1
 I2=2
 IR=1

C READ IN FILE DATA.

C 22 READ (2,2) EN.D=90)(AR(I), I=11, I2)

C 23 FCRMAT(6,2)

I1=I2+1

I2=I2+6

GO TO 22

C LOCATE REF NUMBER IN THE RECORD.
 C USE A WHICH APPROXIMATELY 20, IN CASE SYNCBIR SUPPS.

C 90 IF (AR(Y).LE.970 .AND. AR(Y).GE.540) GO TO 5

S=M+1

GO TO 55

IF (AR(Y).EQ.571 .AND. AR(Y).LE.539) GO TO 1C

C CALIBRATION PARAMETERS ARE FROM A ANDERAA
 C OPERATION MANUAL. SALINITY AND PRESSURE SENSORS ARE NOT USED.
 C T=-2.462*(0.02277*AR(Y+1)-(1.344*(-5)*(AR(Y+1)*(-8))+(AR(Y+1)*3)))
 1 S=0.1527*(10.0*(-8))+(AR(Y+1)*3))

P=1.0222*D=0.352*AR(M+4)
 IF (AR(Y+5).EQ.0.0) GO TO 5

V=1.5+168*AR(M+5)/600
 GO TO 55

Y=0.0
 REF=AR(Y)

WRITE(6,150) IR,REF,T,S,P,V

C 150 WRITE(CALIBRATED DATA VALUES (1) MINUTE) TO MASS STORAGE.
 WRITER(1) IR,REF,T,S,P,D,V
 IR=IR+1
 M=M+1
 IF (Y.GT.5000) GO TO 100

GO TO 55

```
10      WRITE (6,150) IR,XXX
      WRITE (1) IR,XXX
      IR=IR+1
      IF (N*CT*50000) GC TO 165
      N=N+6
      GO TO 1
      ENDFILE 1
      STCP
      END
100
```

8 E A] CALAEB [N MASS STEREE

BEAR (I : EN \cap 25) III : AB

REF(1) = AP(1)

K(2) = 10/3

$$PR \in S = PR(4) \cap S(5)$$

$$SPS(1) = AR(6)$$

卷之三

NP-1311

CREATE ARTIFICIAL VALUES FOR MISSING RECORDS. (THIS SUBROUTINE LEAVES THE REFERENCE NUMBER ZERO FOR READY IDENTIFICATION OF ARTIFICIAL VALUES.)

NPTS=NPTS-2
CJ7_{i=2},NPTS
WARNING: CURRENTS SEEDED GREATER THAN 100 CM/SEC ARE NOT
SUBSTITUTED WITH INTERPOLATED VALUES.

```
IF (SFULL) GOTO 100  
IF (REF(1)) NEQ 0 GOTO 105  
CALL FILLER(1,SPD,CTR,PFOUT,JROUT)
```

SURE (1) ENSURING THAT THE DATA IS SECURE, ACCURATE VALUES ARE WITHIN ACCEPTABLE LIMITS. AVOID SEARCHING EACH RECORD FOR AN

```

ACCESIBLE VALUE(1).GE.5.0:AND.TEN(1).LE.12.0)  GC TC 7
IF(I.EQ.(1))TEN(1)=5.0:AND.IEY(J+1)=IEY(J+2)
J=I+(TEN(1))-1:IEY(J)=IEY(J+1)+IEY(J+2):GO TO 3

```

```

J=J+1
CCSTO[2]=TEN^((I-1)+TEN^(J+1))/Z.
TEN=(TEN^((I-1)+TEN^(J+1))=LINE((I))

```

7 CONTINUE

C CREATE A REPRESENTATIVE FREQUENT CURRENT VALUE FROM THE 10 MINUTE
RECORDS.

NPTS6=(NPTS/6)
CALL RMEAN(NPTS,NPTS6,SPO,DIR,HRSPO,U,V,T,TRU,THETA,TER,
HOUR,HCURV,HOUR,T,RFOF)

1 CREATE DATA PLOTS.

NPTS=NPTS6

NPTS2=NPTS+2
CALL STKFLT(NPTS,NFTS2,IF,HRSPE,HOURU,FCURV,FCURT,RHUf)

STOP

END
SUBROUTINE FILLER (I,SPC,DIR,SPDOUT,CIFCUT)

C SUBROUTINE FILLER CREATES SPEED AND DIRECTION VALUES FOR THE CURRENT
METER READING. THIS IS DONE TO PROVIDE REASONABLE APPROXIMATIONS
FOR THE OCCASIONAL RECORD LOSS DUE TO INSTRUMENT (METER)
MALFUNCTION. THE AVERAGING ROUTINE AVOIDS INCORPORATING FAULTY
DATA.

C DIMENSION CIR(1),SPC(1)

3 IF(SPC(I+1).LE.130.)GC 1C 5

GC 1C 5

9 SPO=DIR(I-1)+SPC(J+1)/2.0
IF(DIR(I-1).GT.90..0)AND.EQ.(I+1).GT.270.) GC TO 10
IF(DIR(I-1).GT.270..0)AND.EQ.(I+1).LE.90.) GC TO 10
IF(DIR(I-1)-DIR(I+1).GT.180.)
IF(DIR(I+1)-DIR(I-1).GT.180.)
DIRULF=(DIR(I-1)+DIR(I+1))/2.
GC TO 2C

10 CIFCUT=(CIR(I-1)-CIR(I+1))/2.+DIR(I+1)+18C.

IF(CIFCUT.GE.360.) DIRCLT=DIRUT-360.
IF(CIFCUT.LE.-360.) DIRCLT=DIRUT+360.

15 CIFCUT=(CIR(I-1)+CIR(I+1))/2.+18C.

2C CONTINUE
RETURN
END

SUBROUTINE RMEAN(NPTS,NPTS6,SPC,DIR,FCURV,FCURT,THETA,
TER,HCURV,HOUR,T,RFOF)

1 TEN, FCURU, FCURV, FCURT, RHCUT

SUBROUTINE FMMEAN CREATES HCURU, VCURRENT VALUES AND TEMPERATURE
VALUES FROM A 9-POINT WEIGHTED BINOMIAL FILTER.

LIMENSIION SPC(NPTS), CIR(NPTS), HISPD(NPTS), FCURU(NPTS),
HCURV(NPTS), U(NPTS), V(NPTS), T(NPTS), TRU(NPTS),
TEM(NPTS),
1 NPTS=NFTS-8
DO 19 I=1,NPTS

APPLY VARIANCE CORRECTION TO MAGNETIC DIRECTIONS.

VAR=15.*CIR(I)+VAR
TRU(I)=CIR(I)*CE.360.*) TRU(I)=TRU(I)-360.

CNVTRK(1)=TRU(I)*(C17452)

THEETAK(I)=SPC(I)*SIN(THEET(I))

U(I)=SPC(I)*CCS(THEET(I))

V(I)=SPC(I)*COS(THEET(I))

WRITE(15,NINT(U(I),V(I))

NINT(250.)

FORMAT(2F12.5)

CONTINUE

K=0.
DO J=1, NPTS, 6

U1=1.*#L(I)

U2=8.*#L(I+1)

U3=26.*#L(I+2)

U4=56.*#L(I+3)

U5=76.*#L(I+4)

U6=56.*#L(I+5)

U7=28.*#L(I+6)

U8=8.*#L(I+7)

U9=1.*#L(I+8)

FCURU(I)=(U1+U2+U3+U4+U5+U6+U7+U8+U9)/

1 12.*28.+2.*56.+70.)

V1=1.*#V(I)

V2=8.*#V(I+1)

V3=26.*#V(I+2)

V4=56.*#V(I+3)

V5=76.*#V(I+4)

V6=56.*#V(I+5)

V7=28.*#V(I+6)

V8=8.*#V(I+7)

V9=1.*#V(I+8)

```

HOURV(1) = (V1+V2+V3+V4+V5+V6+V7+V8+V9)/
  (1+2+3+4+5+6+7+8+9)
1 T1=1
1 T2=3.*TEM(1+1)
1 T3=2.*TEM(1+2)
1 T4=5.*TEM(1+3)
1 T5=7.*TEM(1+4)
1 T6=5.*TEM(1+5)
1 T7=2.*TEM(1+6)
1 T8=3.*TEM(1+7)
1 T9=1.*TEM(1+8)
HOURT(1)=T1+T2+T3+T4+T5+T6+T7+T8+T9)/
  9
1 HRSPC(J)=SQR((HOURU(J)+2.*56.+73.)*
  IF (HOURT(J).LE.5.5) GC1C2
  IF (FCURT(J).GE.10.6) GO TO 20
  K=K+1
  HCURT(J)+HCT
  COUNTING MEAN TEMPERATURE FOR THE RECCE. (VALUE IS SCALED FOR
  COMPLETE PLOTTING)
  SUBSEQUENT PLOTTING.)
  RHCT=(PCT/K)*2.0)-14.
  WRITE(6,50) RHCT
  FORMAT(6,50,F6.2)
  RETURN
END
SUBROUTINE STKPLOT(NPTS,NPTS2,IR,HRSPD,HCURL,FCURV,HOURU,RHCT)
C
C SUBROUTINE STKPLOT CURRENT VECTORS AS A
C FUNCTION OF TIME, FOLLOWED BY PLOTS OF CURRENT VECTORS,
C AND TEMPERATURE VS TIME. IT IS USEFUL FOR REFERENCED
C POSTGRADUATE SCHOOL TECHNICAL NOTE AC. C141-24 IN REGARDING
C PLOTTING PARAMETERS.
C
C DIVIDE IR(NPTS),HRSPEC(NPTS2),HOURU(NPTS),FCURV(NPTS),
C HCURL(NPTS)
1 WRITE(6,42111/Z1111/Z1111/
  NPTS=NPTS/20.)*2.
  XLEN=NPTS/20.)*2.
  YLEN=8
  FORMAT(1,8X,1HJ,11X,2H1R,4X,5H,HRSPD,8X,
  1 1D11,2X1H,9X,1H,7X,2H1D,8X,24Y1)
200 1 FORMAT(1X,15,3X,1I6,6F16.2)
C
C SET UP THE STICKPLOT
C
C CALL FLUTIS(0,0,0)
C CALL FACTOR(0.35)

```



```

CALL PLCT(10.,-3) *SAMPLE NUMBER, -13, XLEN, C., 0., 20.)
CALL AXIS(0.,-5.,13) *SPEC(C1/SPEC), 13, YLEN, C., FVALS, OVS)
CALL AXIS(0.,-4.,13) *SPEC(C1/SPEC), 13, YLEN, C., FVALS, OVS)
CALL HLINE(0.,'XLEN',C.,Z1111)
CALL PLCT(0.,0.,-3)
B=0.*PLT TFE DATA
DO 12 I=1,NPTS
  X1=B*CURV(I)/CVS
  Y1=CALL PLCT(X1,Y1,2)
  CALL INFLT(0.,0.,99)
  SET UP TFE TEMPERATURE PLCT.
  CALL PLCT(0.,0.,0.)
  CALL FACTCR(0.,35)
  CALL PLCT(0.,10.,-3)
  CALL AXIS(0.,-5.,13) *SAMPLE NUMBER, -13, XLEN, C., 0., 20.)
  CALL AXIS(0.,-4.,13) *TEMPERATURE, 13, YLEN, RHT, Z1111)
  CALL PLCT(0.,'XLEN',RHT,Z1111)
  CALL PLCT(0.,RHT,+3)
  B=D+*.5
  PLCT TFE DATA
  DO 13 I=1,NPTS
    X1=B*(HUR((I)*2.0))-14.
    Y1=CALL PLCT(X1,Y1,2)
    CALL INFLT(0.,0.,99)
    RETURN
  END
  13

```

```

DIMENSION REF(1)000),DIR(10000),SPD(10000),AR(6),
1 ALONG(10000),CROSS(10000),YY(10000),PERI0C(10000),
2 FREQU(10000),U(10000),V(10000),TRT(10000),INT(10000),
C PROGRAM TO EVALUATE THE ENERGY DENSITY SPECTRUM OF OBSERVED CURRENTS
C THROUGH THEIR ALIGNMENT AND CROSS SHIELD COMPONENTS.
C
10 FORMAT (IX,110,2F16.2)
C
JDATA=5
C
C READ RAW DATA FROM MAGNETIC TAPE.
C
20 READ (1,END=25) II,AR
  AR(I)=AR(1)
  REF(I)=AR(2)
  TEMP=AR(3)
  SALES=AR(4)
  PRES=AR(5)
  DIR(I)=AR(5)
  SPE(I)=AR(6)
  GU(I)=20
  25 CONTINUE
C
C CREATE ARTIFICIAL VALUES FOR MISSING RECORDS. THIS SUBROUTINE
C LEAVES THE NUMBER ZERO FOR READY IDENTIFICATION
C ARTIFICIAL VALUES.
C
6   MPTS=NPTS-2
    CC(5)=3, NPTS=1
    IF (SPD(I)*GE.100) GC TO 6
    IF (REF(I)*NE.0) GC TO 5
    CALL FILLER(I,SPE,EIR,SPOCUT,CIRCUIT)
    SPE(I)=SPOCUT
    DIR(I)=CIRCUIT
    C CONTINUE
    L111=1,NPTS
    VAF=30.17
    TRT(I)=CIR(I)+VAK
    IF (TRT(I)*360.*TRT(I)=TRT(I)-360.
    TH(I)=17453
    U(I)=SPE(I)*SIN(TH(I))
    V(I)=SPE(I)*COS(TH(I))
    CROS(I)=U(I)

```

```

ALONG(I)=V(I)
CALL INLE
GO TO 1
1 IF (J.EG.1) GO TO 4
IF (J.EG.2) GO TO 50
IF (J.EG.3) GO TO 50
IF (J.EG.4) GO TO 60
CALL XCXCAR(ALONG,NPTS,24,1,NOJTI)
CALL XCXCAR(ALONG,NPTS,24,1,NOJTI)
CALL XCXCAR(ALONG,NPTS,25,1,NOJTI)
GOTO 40
CALL XCXCAR(CROSS,NPTS,24,1,NOJTI)
CALL XCXCAR(CROSS,NPTS,24,1,NOJTI)
CALL XCXCAR(CROSS,NPTS,25,1,NOJTI)

50   N=11
      DS=1
      DT=(1./6.*)
      DT=JST(J,4500)
      IF (J.GE.2) GO TO 41
      YYY(I)=ALONG(JSTART)
      GUY(I)=43
      YYY(I)=CROSS(JSTART)
      JSTART=JSTART+1
      COUNT=1
      IF (J.GE.2) GO TO 70
      CALL PREPFA(N,MS,CY,YY,F1,PERIOD,FREQUE,NF)
      CALL PREGT(0.0,C.C,SS)
      GUT=80
      CALL PREPFA(M,MS,DT,YY,F1,PERIOD,FREQUE,NF)
      70  COUNT=FLEI(C.0,C.0,499)
      STCP
      END
      SUBROUTINE FILLER (I,SFC,CIR,SCOUT,CIRCUIT)

SUBROUTINE FILLER CREATES SPEED AND DIRECTION VALUES FOR THE CURRENT
METER READING. THIS IS DONE TO PROVIDE REASSEMBLE APPROXIMATIONS
FOR THE SIGNAL RECORD ISSUED BY THE INSTRUMENT (METER).

```

```

DIMENSION CIR(I),SPC(I)
J=1
IF (SPC(I+1).LT.100.) GO TO 9
8   IF (SPC(I+1)) GO TO 9

```


510

DO 510 I=1, NF

F1(I)=C.

K=0 DO 21 IZ=0

IZ=1 ART(IZ)=YY(IZ)

CALL COUNT(NLE,ART,N,ANEEAN)

DO 22 IZ=1 NF=1 CALL(I28)=ART(I28)-ANEEAN

COUNT(NLE,N,I=1,MS)

DO 520 K=K+1 IZ=IZ+1

I2=IZ J=IZ+1 F1S(J)=C(I2)

WRITE(*,*) F1S,NM,ET,U1,U2,U41,URNS1)

CALL TREC(F1S,NM,V1,V2,U1,U2,U41,UFERF)

CALL SFEC(F1S,U1,U2,U3,U41,URMS1)

WRIFF(E,2E3)I=1,4

DO 540 F1(I)=F1S(I)+F1(I)

DO 550 CNT(NLE,I=1,NF)

F1(I)=F1(I)*I/(2.*MS)

IF(I.EQ.1)GC(TO/23)

PERIOD(I)=((FLCAT(NM)*(DT))/FLOAT(I-1))

FREQE(I)=1.0/PERIOD(I)

IF(F1(I).LE.10.0)GC(TC/55)

GOTO TO/24

PERIOD(I)=FLCAT(NM)

FREQE(I)=0.0

WRITE(*,*)F1(I),PERIOD(I),FREQE(I)

CALL COUNT(FREQUE,FL,NF,I=1,1,FREQUENCY(I,NM,HOUR),,36,C.0,C.2,0,0,0,0,12.C,6.0)

RETURN

END SUBROUTINE SPEC (FL,N,INV,S,IFERR)

C SUBROUTINE TO CALCULATE THE POWER SPECTRUM OF A SIGNAL USING RHEARM

DIMENSION INV(515),S(515),FL(515)

CALL RHEARM(FL,N,INV,S,IFERR)

NP=2*N-1

NF=2*N+1

NM=NM+1

```

F1(1) = F1(1)*F1(1)
DO 50 J=1,NP
J=2*I+1
L=I+1
XR=F1(J)*F1(J)
XI=F1(J+1)*F1(J+1)
F1(L)=XR+XI
CONTINUE
F1(NF)=F1(NL)**2
RETURN
END
SUBROUTINE TREND(FX,NTS,ET,MEAN,U2,U3,U4,URNS)
SUBROUTINE TREND(EDITS,CALIBRATES,FX(NTS))
CIVENSIGN FX(NTS)
EDIFING CATA

```

```

FNTS=NTS
CCMPUT I=1 . NTS THE LINEAR TREND
SUMF=0 . I=1 NTS
SUMF=SUMF+FX(I)
SUMF=I=C .
DO 102 I=1 , NTS
X1=I
SUMF=SUMF+X1*FX(I)
XAN=I-1
XNP=I+C-1
XN=(1.0/C)*SUMF/(FNTS-XNP*I/2.)
B=SUMF/FNTS
FMEAN=SUMF/FNTS

```

```

      WRITE(6,*) 'MEAN', XNB
      FOR IAT(2:X, MEAN=., FIG.5, 3X, 'SL)DE =., FIG.5, 2X, 'INTERCEPT =., F10.5
      1,1
      DO 103 I=1,NTS
      XI=1
      FX(I)=FX((I)-(B+XM*XI*DT)
      SUBROUTINE FOR CALCULATING VARIANCE, STD DEV, SKEWNESS, KURTOSIS
      U2=.3
      U3=.3
      U4=.3
      SUMU2=C.0
      SUMU4=C.0
      DO 151 I=1,NTS
      U2=FX(I)*FX(I)

```

```

U3=U2*F1*(1)
U4=U3*F1*(1)
SUMU2=SUMU2+U2
SUMU3=SUMU3+U3
SUMU4=SUMU4+U4
COUNTIN=1
FN1S=SUMU2/FN1S
U2=SUMU2/(FN1S*U2*URYS)
U3=SUMU4/(FN1S*U2*U2)
U4=SUMU2*U2
RETURN
END
SUBROUTINE PAGE
10
FORMAT(1,1)
WRITE(5,10)
RETURN
END
SUBROUTINE AVERA(A,NPTS,A'MEAN)
CIMENASICA A(NPTS)
SUM=C
DO 100 I=1,NPTS
SUM=SUM+A(I)
100 COUNTIN=SUM/NFLOAT(NPTS)
A'MEAN=SUM
RETURN
END
151

```

PROGRAM TRAJEC TO PLCT FRSJ; PROGRESSIVE VECTOR DIAGRAMS OF CURRENT
 METER DATA IF CCNFCN ARE GIVEN, WE SET COMP=T. WE SET SPEED INTO U AND
 DIRECTION INTO V. AND PUT A CANE PCINTS IS GIVEN AS N. WE PLCT
 PLOTTER POINTS CANC EXCEED SO. IF DRAW IS CALLED, THE TIME
 INTERVALS ARE SUBJECT TO USE OBJECT TIMES IRABLE. THAT NP*N
 INVECTOR SLENS ARE STCNCED IN CUAD CV. IT IS DAY. PLT IS TRUE,
 CORRECTION TO AN INTEGRAL FRACTION OF CNE DAY. THE VECTORS
 ARE KEENES SUBTRACTING READ FROM READING. CALLING A AND DISCARDING NSTRT PCINTS AT THE
 PROVIDED SIGN. PROVIDED FOR READING AND READ TWO OR MORE FILES IF NFILE
 BEG INISING. 2 OR MORE FILE CARDS MUST THEN BE
 SUPPLIED FOR EACH FILE. FOR READING EACH FILE SEQUENTIALLY.
 THIS IS PROVIDED FOR READING FILE NUMBER WITH WHICH GNE
 IF THEY ARE SEQUENTIAL LESS THAN THE FILE NUMBER WITH WHICH GNE
 MFILLES IS SET AS START SCN EINPNTL. FILE NUMBER ON WHICH YOU WANT TO STOP.
 NFILE MUST BE THE FILE NUMBER ON WHICH YOU WANT TO STOP.
 DIMENSION L(500), J(500), F(500), PU(200), PV(200), CU(900),
 1 CV() CO() I(9000) J(9000)
 REAL*8 TITLE1(12), TITLE2(12), PLT, RPT
 LOGICAL ICMP, PLT/COMP, N, NP, NX, DELT, RPT, PLT, NSTRT, NFILE/INPUT1/MFILE
 NAMELIST/INPUT/COMP/
 RAD=2.141552/180.
 NFILE=1
 RPT=.FALSE.
 PLT=.FALSE.
 ASTRI=C
 FILE=C
 READ(5, INFIL)
 4 IEND=0
 READ(5, INFIL)
 WRITE(6, INFIL)
 READ(PLCT, TITLE1)
 READ(5, TITLE1)
 WRITE(6, TITLE1)
 READ(5, TITLE1)
 WRITE(6, TITLE1)
 6 FORMAT(1A8)
 1C FORMAT(1A8)
 1C FORMAT(1A8)
 1C IREPT=0
 READ AND DISCARD NSTRT FCINTS

```

IF(NSTRF1.EQ.0) GC TC 12C
D(J1,1,J=1,NSTRT)
11 READ(2,12) JUNK
12 FCRMAT(2,14)
C      READ DATA
C      NJ=J
C      CO12=1.2*875;END=200,ERR=35; U(J),V(J)
875 FORJAT(2,12,5)
12 NJ=J

C      IF CCMF IS FALSE, FIND THE EAST AND NORTH COMPONENTS AND PUT
C      THEM IN U AND V.
14 IF(CCMF) GC TC 16
DO 15 J=1,N
UX=U(J)*RAC
VX=V(J)*RAC
U(J)=UX+SIN(VX)
15 V(J)=UX+CCS(VX)

C      PARAMETERS FOR COMPRESSING DATA
16 NPTS=NFX
NXI=NFX
NPT=NPTS*NXI
JEVN=N-JEVNP
KEVN=JEVN/NP
LEVN=JEVN-KEVN*N
WRITE(6,161) NP,NPIS,LEVNEVN,LEVNEVN,LEVNEVN,LEVNEVN
161 FORMAT(1X,NP,POTTING IS EVERY 13/5X, POINTS NOT PLOTTED AND
201 EVERSELY 13/5X, POINTS AFTER THE LAST CROSS. 1/)

C      SUM THE COMPONENT DISPLACEMENTS IN KILOCMETERS AND STORE NP POINTS
C      IN CU AND CV.
17 SUMU=0.
SUMV=0.
L=0
K=1
CU(1)=C.
CV(1)=C.
XD=L=2*1*3600.*1.E-5
CO27 LL=1,NX
20 CO26 LL=1,NX
L=L+1
CO25 KK=1,NP
K=K+1

```


UXN=SUM*(1.0E5/(TCIM*3600.))

VAN=SL*V*1.0E5/(TCIM*3600.)

CO 85 J=1, N

U(J)=U(J)-V(N)

E5 WRITE(6,86) UMN,VNN

EE FORMAT(5X,'SUBTRACT MEAN U AND MEAN V, * ,F6.2,2X,F6.2,* AND REPEA

11*/*
GU TC 17

C WE CHANGE N AND PROCESS AS USUAL

C 200 N=NJ
NFILE=NFILE+1
WRITE(6,205) NFILE,NJ
205 FORMAT(5X,'DETECTED EOF *,12,* BEFORE REACHING N; RESET IC *,
C 115,* AND PROCESS */)
115 SET IEND=1 TO PREVENT THE READ AND DISCARD OPERATION
IEND=1
GO TO 12

C 300 NFILE=NFILE+1
NWRITE(6,305) NFILE,NJ
305 FORMAT(5X,'END OF FILE *,12,* AFTER RECORD NC. *,15/)
IF(NFILE.GE.NFILE) GOTC 1000
GOTC 4
350 WRITE(6,355) NJ
355 FORMAT(5X,*READ ERROR AFTER RECORD *,15)
GO TC 1600

C READ AND DISCARD IC END CF FILE
999 IF(NFILE.EQ.1) GO TO 1000
IF(NFILE.EQ.1) GO TO 4
CO 900 J=1,10000
NJ=NJ+1
900 READ(2,fmt,END=300,ERR=355) XJUNK
1000 STCP
END

C THIS VERSION OF DRAWING SCALES WITH AXES SAME ON AUTOSCALE.
SEE CHANGES BEGINNING LABEL 2054. R.G.PAGETTE, FEB. 1974.
SUBROUTINE DRAW(NUMPS,XCUR,YCUR,TYPE,LABEL,
TITLE,ESCAL,YSCL,MCDAK,INVCYAX,INVCYX,
HIGH,123
1 DIMENSION X(900),Y(900),LTITLE(24),JXTIT(12),JYTIT(12),
2 LITTLE(14),LCURV(1840),JCRC(100),ICON(1)
3 DATA INTEGER IDATA(2)/1F*,1F/,IHY/,LABEL(2)

```

REAL*8 ICODE,BLANK/ER
REAL*8 ITIT,ICAT8(1E)/SHI WIDE,SHI LIGHT,SHI MODEXAX.,SHI IXUP
1 8H 4CD EYAX,I,8H YRIGHT,8H UNITS=,8H UNITS+,8H ACC-,8H ADC-
2,8H CNT IS 14,8H CHECK PREVIOUS OPERATIONAL ROUTINE, IF ANY. CODES ARE
C TEST = 0 IF PREVIOUS GRAPH, IF ANY, COMPLETED
C TEST = 1 IF PREVIOUS GRAPH NOT COMPLETED
C TEST = 2 IF ERROR FOUND WHILE PREVIOUS WAS ONE, CR IF
MGCURV WAS ILLEGAL.

C IPCINT = ITYPE - 1)1003,1CC1,1CC2,1CC3
1001 IF(MCC CURR)1003,1CC2,1CC3
1002 TEST = C
GO TO MCC CLR - 1)1004,1CC2,1CC4
1003 IF(MCC CLR = 2)
1004 LAST =
RETURN SET UP ERROR RETURN ROUTINE. ENTRY AT STATEMENT 1005.

C 1005 IF(LTEST)1CC5,1CC6,1CC7
1006 IF(MCC CURR)1007,1CC8,1CC9
1007 PRINT 1CC1
1008 FORMAT(59H NO FURTHER GRAPH OUTPUT UNTIL MCCURV NEXT IS ZERO CR
1 LTEST ,/)
1 LTEST = 2
LAST =
RETURN PRINT 1CC1
1101 FORMAT(59H THIS PLCT WILL NOT BE CLEARED. //)
LAST = 1
RETURN
1009 IF(MCC CURR = 2)1010,1CC8,1CC9
1010 IF(MCC CURR = 3)1007,1CC11,1CC7
1011 TEST = 3
GO TO MCC8
C 1000 IF(NUPTS - 2)1,2,2
1001 PRINT 1CC5
1002 FORMAT(59H NUMPTS MUST BE LESS THAN 2. )
1003 GO TO MCC5
C 1004 IF(IFC INT)9000,9004,9001
2 9005 PRINT 1CC5
1005 FORMAT(59H NUMPTS MUST BE LESS THAN 2. )
9100 GO TO MCC5
C 9001 IF(IPC INT = 5)9002,9002,9003
9002 IF(NUPTS = 30)3,9003
9003 PRINT 51
9101 FORMAT(59H NUMPTS MUST NOT EXCEED 30 FOR POINT PLACING. )

```

```

GO TO 105 - 9005
IF(NUMPITS - 9005 = 3,2,9005
PRINT 9102
28H NUMPITS MUST NOT EXCEED 900. )
GO TO 105
3 IX=ICDATA(1)
AIX=X(1)
AMAXX=Y(1)
AMINY=X=Y(1)
DC1C2C1=2(NUMPTS
AMAXX=AIX(1),AMAXX)
AMINY=AIN(1),AIN(X)
AINY=AIN(Y)
1020 IF(AIAXX-AMINX)1025,1024,1025
1022 IF(AIAXX-AMINY)1025,1024,1025
1023 PRINT 1103
1024 FFORMAT(1/,33+ ALL FCINTS HAVE THE SAME COORDINATES. )
GO TO 105
1025 IF(MODCUR-3)5,2240,5
5 IF(MODCUR-3)6,2240,6
6 PRINT 101
101 FFORMAT(1/,17H ILLEGAL OCCURR. )
7 GO TO 105
7 IF(MODCUR-1)6,9,8
8 IF(MODCUR-1)6,9,6
9 IF(MODCUR-1)11,12
10 PRINT 102,111,111
102 FORMAT(1/,9H ILLEGAL ,45,29H. GRAPH WILL BE PLOTTED WITH ,45,
11 JWHITE = 3
11 GC T C 14
12 IF(JWHITE - 9)13,13,1C
13 JWHITE = JWHITE
14 IF(JHIGH)15,16,17
15 ITIT=IDATE(2)
16 PRINT 102, ITIT, ITIT
16 JHIGH = 6.,/
11 JWHITE = 3
11 GC TOTAL 19
12 BACKSPACE 45
GO TO 24)
17 IF(IFIGF - 15)18,18,15
18 JHIGH = JHIGH

```

```

19 NOCXAX = NCCXAX
20 IF(MOD(XA,20)=27,21
21 IT=ICAT8(3)
22 IT=IT+1
23 PRINT(104,ITIT,ILEGAL,A8,22F GRAPH WILL BE PLOTTED WITH MODE,
1C4,FORMAT(/,9HITLEGAL,A8,/,/),THAX=0.,/),
1 NOCXAX = C
20 GOTO 27
21 IF(MOD(XA,-2)27,22,20
22 IF((IXUP-JHIGH)24,24,23
23 PRINT(104,ITIT,IX
24 GOF(IXUP)27,26,26
25 JXUP=IXUP
26 NOCYAX = NCCYAX
27 IF(MODYAX)28,25,25
28 ITIT=ICAT8(5)
29 PRINT(104,ITIT,IV
30 GOTC25
31 NODYAX = C
32 IF(MODYAX-2)25,30,28
33 ITIT=ICAT8(6)
34 PRINT(104,ITIT,IV
35 GOTC25
36 JYRIGHT=JYRIGHT,34
37 INITIALIZE PRICR IC SCALING AND AXIS LOCATING
38 IFLAG=0 FOR PASS WITH YDATA. IFLAG = 1 FOR PASS WITH XDATA.
C
39 BETA = C*EXSCAL
40 SCAL = C*EXSCAL
41 IXIS = JYRIGHT
42 MODE = NOCYAX
43 ISIZE = JYKIDE
44 IX = IX
45 YX = YX
46 AMAX = AYMAX
47 AMIN = AYMIN
48 GOTC = E2
49 IFLAG = 1
50 BETA = C*SCALE
51 SCALS = YSCALE
52 MODE = NOCXAX

```

```

ISIZE = JHIGH
AMAX = AMAX
AIN = AIN
IYX = IYX
      IF(SCALE)5159,58
      PRINT14,IYX,IY
      FORMAT(1,9H ILLEGAL ,A1,3SH SCALE. GRAPH WILL BE PLOTTED WITH AL
1141TO,1AL1,7H-SCALE.,/)

      GO TO155
      EXPRESS SCALING FIXED SCALE IN E FORMAT WITH ONE FIGURE SIGNIFICANCE.
      CALL SCAL FACTOR*(SCALE,1)*ISCL1FACTR,1)
      SCAL E=SCAL FACTOR*(SCALE,1)*ISCL1FACTR,1)
      CHECK AND COMPUTE AXES LOCAT ION IF NECESSARY. FIXED SCALE
      CASE.
      IF(1GAE=1
1030 ITAG=1
      GOTOC2
1031 PRINT11C4,IYX,IY,IYX,MODE,A1,24H MUST NOT BE 1 UNLESS A1,57H SCALE IS C
1104 FURIAI(/,5H AUTO-SCALE). GRAPH WILL 3E PLOTTED WITH A1C,A1,7H-SCALE.,/)

      GOTOC55
1032 IF((AMAX-AIN)1036,1C38,1C39
1039 IF(AMAX)1036,1034,1C37
1034 TAXIS=SIZE/2
      GOTOC1035
1036 TAXIS=SIZE
      GOTOC1030
1037 TAXIS=0
      GOTOC1030
1038 ASIZE=SIGN(1.*AMAX)-SIGN(1.,AIN)) 1040,1039,1040
1040 TAXIS=-AIN/(AMAX - AIN)*ASIZE +0.5
      GOTOC1030
      AUTOC SCALE ROUTINE.

C      55 IF(MCDE-1)60,64,69
60 AMAX=AIN*(0.*AMAX)
61 AMIN=AIN*(C.*AIN)
62 IF((AMAX-AIN)62,65,68
63 PRINT116,IYX,IY,IY
64 FORMAT(1,5H ALL A147H VALUES ARE IN-2E30. AND MCDE POSSIBLE ONLY
1161IFTHE A1,2SH VALUES ARE IN-2E30. AND MCDE POSSIBLE ONLY
65 GOTOC1035
66 ASIZE=SIZE
67 SCALE=(AMAX - AMIN)/ASIZE
68 GOTOC33
69 IF((AMAX-AIN)74,7C,74

```

```

7C IF (AM1X) 74,71,74
71 PRINT 112, IXY
72 5H ALL ,A1,2EH VALUES ZERO. AUTO SCALE NOT POSSIBLE. !
118 GOTC 105
73 IF (AM1X) 76,76,75
74 IF (SIZE - TAXIS) 77,76,77
75 SCALE1 = C.
76 GOTC 7E
77 AXIS = AXIS
78 SCALEx1 = AMAX/(AXIS - AXIS)
79 IF (AXI1) 81,79,80
80 SCALEx2 = C.
81 GOTC 82
82 AXIS = -AMIN/AXIS
83 IF (SCALE1 + SCALE2) 1984,1982,1984
84 PRINT 1152, IYX, IYX
1982 FORMAT (/,56H,NCNE CF THE PLOT LIES ON THE GRAPH WITH THIS SPECIF
1983 1IED,A1,47H-AXIS LOCATION. GRAPH WILL BE PLOTTED WITH MODE,A1,
     27HAX = C.,/)
85 GOTC 6C
86 SCALEx = AXI1(SCALE1,SCALE2)
87 CALL SCALIT(SCALE,1,SCL1),FACTOR,3)
88 IF (FACTOR - 5.C5) 85,85,84
89 FACTOR = 1SCL1+1
90 GOTC SC
91 IF (FACTOR = 2.02) 87,87,86
92 FACTOR = 2
93 GOTC SC
94 SCALEx = FACTOR*10.*TSCLL3
95 CCYPLATE AXIS LOCATION IF NECESSARY. AUTO SCALE CASE.
96 IF (1QUE - 1) 92,91,93
97 IF (SIGN(1.AMAX)-SIGN(1.E,AIN)) 92,94,92
98 IF (SIGN(1.AMIN/SCALE + 0.E) 92,94,96
99 GOTC 202
100 IF (ANAX) 95,95,200
101 TAXIS = -AMAX/SCALE
102 EETA = -AMAX/SCALE
103 IF (SE1A - 1.E+12) 99,99,99,96

```

```

56 PRINT 120, 15H THE ORIGIN CF ,AL, 43H CANNOT BE OFFSET MORE THAN 1
120 FURIA(12 INCHES, )
1.0E+12 IC5
      GO TO 100
99  BETA = -BETA + 0.5
      BETA = -BETA IS THE NUMBER OF INCHES OFF ORIGIN SUPPRESSION, POSITIVE IF
      TRUE CRIN IS BELCA CRTC LEFT CF THE GRAPH.
      IF(BETA + 1.07, 67, 97
97  ITAS = 1
      GO TO 203
200 ITAIS = AXIN/SCALE
      IF(BETA - 1.0E+12) 201, 56
201 ITET = BETA + 0.5
      BETA = BETA
      IF(BETA - 1.0) 53, 202, 202
202 ITAG = 1 RELEASE RESULTS TO REMAINING PART OF PROGRAM. START SECOND
      IF(IFLAG) 203, 204, 205
203 SCALEX = SCALE
      IXFACT = FACTOR
      IXSC12 = IXAIS
      ITAXIS = ITAG
      ITAXX = ITAG
      ITIZEX = ITIZE
      BETAX = BETA
      GOTC = BETA
      BEIAY = BETA
      SCALFY = SCALER
      IXFACT = FACTOR
      IXSC12 = IXAIS
      IYSC12 = IYTAG
      ITAYIS = ITAG
      ITAYY = ITSIZE
      MAKE THE SCALING THE SAME ON THE TWO AXES .
      IF(SCALEX * GT * SCALEY) GOTO 2055
      SCALEX = SCALEX
      IXFACT = IXFACT
      IXSC12 = IXSC12
      BETAX = BETAX * SCALEX / SCALEY
      SCALCY = SCALEX
      IYFACT = IYFACT
      IYSC12 = IYSC12
      BETAY = BETAY * SCALEX / SCALEY
      ENDF CHANGES
C

```

C THIS COMPLETES CALCULATION OF SCALE FACTORS ETC. NOW GENERATE RECORDS FIRST, THE SCALE FACTOR TITLES.

I 206 JXTTIT(1)=ICCDE(SCALEX)
 JXTTIT(2)=ICCDE(SCALEY)
 JXTTIT(3)=ICAT8(8)
 JXTTIT(4)=ICAT8(9)
 JYTIT(1)=ICCDE(SCALEY)
 JYTIT(2)=ICCDE(SCALEX)
 JYTIT(3)=ICAT8(8)
 JYTIT(4)=ICAT8(9)

DO 926 JXTTIT(1)=BLANK
 IF(JXTTIT(1) .EQ. BLANK) 207, 207, 207
 JXTTIT(1)=BLANK
 JXTTIT(2)=ICCDE(BETAX*SCALEX)
 JXTTIT(3)=ICCDE(BETAY*SCALEY)
 JXTTIT(4)=ICCDE(BETAZ*SCALEZ)
 JXTTIT(5)=ICAT8(14)
 JXTTIT(6)=ICAT8(11)
 JXTTIT(7)=ICAT8(12)
 JXTTIT(8)=ICAT8(15)
 JXTTIT(9)=ICAT8(13)
 JXTTIT(10)=ICAT8(16)
 JXTTIT(11)=ICAT8(13)
 JXTTIT(12)=ICAT8(14)
 JXTTIT(13)=ICAT8(13)
 JXTTIT(14)=ICAT8(13)
 JXTTIT(15)=ICAT8(11)
 JXTTIT(16)=ICAT8(16)

207 208 GO TO 212
 210 JYTIT(1)=BLANK
 IF(JYTIT(1) .EQ. BLANK) 211, 211, 211
 JYTIT(1)=BLANK
 JYTIT(2)=ICCDE(BETAY*SCALEY)
 JYTIT(3)=ICCDE(BETAX*SCALEX)
 JYTIT(4)=ICCDE(BETAZ*SCALEZ)
 JYTIT(5)=ICAT8(14)
 JYTIT(6)=ICAT8(11)
 JYTIT(7)=ICAT8(11)
 JYTIT(8)=ICAT8(15)

211 212 213 214 215 216
 CONTINUE TEST FOR ALL BLANK TITLE RECORDS.

C 9691 LFTMGN = C*100
 LH = LFTMGN
 LH = LFTMGN + IXAXIS*1CC
 LH = LFTMGN + ISIZEx*1CC - 107
 JL = JF - 13
 IH2 = -1CC
 IVH2 = -(ISIZEX - IXAXIS - 1)*IXFACT
 NH = ISIZEX
 ISH = ICAT8(17)
 IV = LFTMGN + IXAXIS*10J

```

JY = ISIZEY*100
IYL = IV-3
JYL = ISIGN + ISIZEY*1CC - 107
JYL2 = -1CC
JYY = (ISIZEY - IYAXIS - 1)*IFYACT
IYV2 = -IYFACT
ISV=ICAT8(18)
NOw GENERATE CURVES.
SCX = 100.*SCALEXY
SCY = 100./SCALEXY
EXAXIS = IYAXISS*100
YAXIS = LEFTMGN
ALFMGN = EXAXIS - LEFTMGN
SHIFIX = EXAXIS - BETAX*1CJ + ALFMGN
SHIFIY = YAXIS - BETAY*1CJ + BOTMGN
EXSIZE = ISIZEX*100 + LFTMGN + C
SIZEX = LEFTMGN - 6C
SIZEY = ISIZEY*100 + IBIGN + 70
SIF(POLY(NUMPTS,2),90C7,SC10
9007 IF(MGC(NUMPTS,2),9700,9700
9700 ISKICF=1
GO TO 242
9701 ISWTCH=((SUM PTS+1)/2)*4
242 C0 244 I=1,INUM,4
C1=X((I+1)/2)*SCX+SFIFTX
C2=Y((I+1)/2)*SCY+SFIFTY
240 C1F((I+3-INUM)/241,241,241
9242 C3=C1
C4=C2
GO TO 243
241 C3=X((I+1)/2+1)*SCX+SHIFIX
C4=Y((I+1)/2+1)*SCY+SFIFTY
9243 C1=ANIN(C1,EXSIZE)
C2=ANIN(C2,EXSIZE)
C1=ANIN(C1,YSIZE)
C2=ANIN(C2,YSIZE)
C1C2=ANIN(C3,EXSIZE)
C3=ANIN(C3,YSIZE)
C4=ANIN(C4,YSIZE)
ICURV((I+1)=IC1

```

C

```

ICURV(1+2)=IC3
ICURV(1+3)=IC4
244 GONT INLE
246 ACW WRITE RECORDS
C 9010 IF(MOD(LCT,1)26C,SC15
260 CALL FFCR
XAXIS=C.
YAXIS=C.
CALL SYMBCL(XAXIS,YAXIS,.14,JXTIT,0.,,72)
YAXIS=SYMBCL(XAXIS,YAXIS,.14,JYTIT,0.,,72)
261 CALL SYMBOL(XAXIS,YAXIS,.21,ITITLE,0.,,48)
9268 CALL YAXIS-.31
9270 CALL SYMBCL(XAXIS,YAXIS,.21,ITITLE(13),C.,,48)
9271 XAXIS=FLOAT(LH)/100.
YAXIS=FLCAT(JH)/100.
CALL FLCT(XAXIS,YAXIS,.3)
XAXIS=FLOAT(LH+LH)/100.
CALL SPECNO(LVH,1VH2,NH,YAXIS,1)
XAXIS=FLOAT(LV)/100.
YAXIS=FLCAT(JV)/100.
CALL PLCT(XAXIS,YAXIS,.3)
YAXIS=FLCAT(JV+LV)/100.
CALL FLCT(XAXIS,YAXIS,.2)
CALL SPECNG(LV,1V2,INV,YAXIS,2)
CALL SPECINT(9020,270,9020
9015 FF(FCLT(LCUR,V,272,9025
.270 CALL NFERE(XAXIS,YAXIS)
CALL SYBCL(XAXIS,YAXIS,.272,9025
.272 CALL NFERE(XAXIS,YAXIS,.272,9025
9020 IF(MOD(CUR-1)9025,272,9025
272 IF(IGRID-1)9025,272,9025
. . CALL GENERATE GRID IF CALLED FCR.
C 273 LY100=ISIZEY*100
NEXT1=LFTMGN+1x100
NEXT2=LFTMGN+1x100
GGRID(J)=LFTMGN
JGRID(J+1)=NEXT1
JGRID(J+2)=NEXT2
JGRID(NEXT1-LFTMGN)=NEXT1
JGRID(NEXT1-1)=NEXT1+100
JGRID(J+4)=NEXT2
JGRID(J+5)=NEXT1
1273 JGRID(J+6)=LFTMGN

```

```

JGRIC(J+7)=NEXT1
IF(NEXT1=IEXT1+100
NEXT1=EXT1+4)=NEXT2
JGRID(J+5)=NEXT1
JGRID(J+6)=NEXT2
JGRID(J+7)=NEXT1
1274 CALL COUNTLINE J+7 JGRID,NUMGRD)
1275 NEXT1=LEFTMGN + IY1C9
DO JGRID(J)=NEXT1
JGRID(J+1)=IBTMGN
JGRID(J+2)=NEXT1
IF(NEXT1=LEFT1+100
NEXT1=J+4)=NEXT1
JGRID(J+5)=NEXT2
JGRID(J+6)=NEXT1
JGRID(J+7)=IBTMGN - IY1C9
1276 IF(NEXT1=LEFT1+100
NEXT1=J+4)=NEXT1
JGRID(J+5)=NEXT2
JGRID(J+6)=NEXT1
JGRID(J+7)=NEXT2
1277 CALL COUNTLINE J+7 JGRID,NUMGRD)
1278 IF(IPCENTRATE PINT FLOT RECORDS IF CALLED FCC.
1279 NEXT1=LEFT1+100
JGRID(J+4)=NEXT1
JGRID(J+5)=NEXT2
JGRID(J+6)=NEXT1
JGRID(J+7)=NEXT2
1280 COUNTLINE J+7
CALL SUB1(JGRID,NUMRD)
9025 IF(IPCENTRATE PINT FLOT RECORDS IF CALLED FCC.
C 9020 IOUT=0 DO 1050 I=1,NUMPTS
C1 = X(I)*SCX + SHIFIX
C2 = Y(I)*SCY + SHIFY
1F(C1-EXSIZE)9031,5031,5034
1F(C2-ESIZE)9032,5032,5024
1F(C1-SIZE)9034,5034,5022
1F(C2-SIZEY)9035,5035,5025
9031 1050 = IOUT+1
9032 GO TO 50
9033 IC1=C1
9034 IC2=C2
9035 GO TO 36,9037,9038,9039,5340), IPCINT
C GENERATE CROSS.

```

9036 ICURV(1) = IC1-5
 ICURV(2) = IC2-5
 ICURV(3) = IC1+5
 ICURV(4) = IC2+5
 ICURV(5) = IC1-5
 ICURV(6) = IC2+5
 ICURV(7) = IC1+5
 ICURV(8) = IC2-5
 ICURV(9) = IC1+5
 ICURV(10) = IC2-5
 ICURV(11) = IC1-5
 ICURV(12) = IC2-5

C₉₀₃₆

GO TO C₉₀₃₇ GENERATE PLUS.

ICURV(1) = IC1-4
 ICURV(2) = IC2-4
 ICURV(3) = IC1+4
 ICURV(4) = IC2+4
 ICURV(5) = IC1-4
 ICURV(6) = IC2+4
 ICURV(7) = IC1-4
 ICURV(8) = IC2+4
 ICURV(9) = IC1+4
 ICURV(10) = IC2-4
 ICURV(11) = IC1+4
 ICURV(12) = IC2-4

GO TO C₉₀₃₈ GENERATE SQUARE.

ICURV(1) = IC1-4
 ICURV(2) = IC2-4
 ICURV(3) = IC1+4
 ICURV(4) = IC2+4
 ICURV(5) = IC1-4
 ICURV(6) = IC2+4
 ICURV(7) = IC1-4
 ICURV(8) = IC2+4
 ICURV(9) = IC1+4
 ICURV(10) = IC2-4
 ICURV(11) = IC1+4
 ICURV(12) = IC2-4

GO TO C₉₀₃₉ GENERATE DIAMOND.

ICURV(1) = IC2-5
 ICURV(2) = IC1+5
 ICURV(3) = IC2-5

C₉₀₃₉

```

ICURV(4)=IC2+5
ICURV(5)=IC1-5
ICURV(6)=IC2
ICURV(7)=IC1
ICURV(8)=IC2-5
ICURV(9)=IC1+5
ICURV(10)=IC2
ICURV(11)=IC1+5
ICURV(12)=IC2
INUM=12
GO TO SC41

```

C 904C ICURV(1)=IC1+5

ICURV(2)=IC2-2

ICURV(3)=IC1+6

ICURV(4)=IC2+6

ICURV(5)=IC1-5

ICURV(6)=IC2-3

ICURV(7)=IC1+5

ICURV(8)=IC2-3

INUM=3 CALL SUB1(ICURV,INUM)

IF(I-NUMFI\$)9043,SC42,9043

CALL WPERE(XAXIS,YAXIS,.C7,LABEL(2),0.,4)

GOTO SC46

IF(I-1)SC45,SC44,SC45

CALL SYNECL(XAXIS,YAXIS,.C7,LABEL(1),0.,4)

GOTO SC46

9045 CONTINUE

CALL SUB1(ICURV,INUM)

9050 CALL CNTRL(C45,276,SC46

IF(IOUT\$1C4,IOUT,29H FCINT(S) WERE OFF THE GRAPH. ,/)

9048 PRINT(/,1X,I2,29H RETURN.

I1)SE1 UP

276 IF(MCDCUR\$)278,277

277 IF(MCDCUR-3)275,278,275

278 ITES=0

YAXIS=FIG+4

CALL PLC1(0.0,YAXIS,-3)

CALL PLC1(0.0,YAXIS,-3)

WRITE(6,13)ITILE

13 FORMAT(13H GRAPH TITLE C/2(5X,12A4/),18H HAS BEEN PLOTTED.)

GOTO 2EC

275 ITESI = 1

LAST = C

THESE ARE THE NORMAL RETURNS.

```

2 CALL SCALIT(BNUMBER,ISCL10,FACTR,3)
ISGNSC=ISIGN(1,ISCL10)
ISCL1C=FACTS(1,ISCL10)
IFACT=YCC((ISCL10,10))
II(8)=YCC((ISCL10,10))
II(7)=ISCL10/10
IF((ISGNSC)4,3,3
3 GO TO 6=IYINS
4 II(5)=IE
II(4)=YCC(IFACT,10)
II(3)=(YCC(IFACT,100))/10
II(2)=IFER(IFACT/100
II(1)=IFACT/100
CALL ENCEE(3,YCCDE,II)
RETURN
END
FUNCTION IIP2 (ICU,YY)
RETURN TYPE KCRD GRAPH.
END
SUBROUTINE SUB1(IA,N)
DIMENS IA(2)
IPEN=2
DO 100 I=1,N,2
X=IA(I)
Y=IA(I+1)
CALL PLET(X,Y,IPEN)
IPEN=2
CONTINUE
100 RETURN
END
SUBROUTINE SPECNO (IVH,IYH2,NH,XAXIS,YAXIS,IA)
DATA MINUS /4HQJC-/,
CIMENSICN 11(4)
CINUS=-252645280
CJTO (100,200),IA
TH=0.*300
200 TH=SI A (TH*.0174533)
300 CT=CGS ((TH*.C174533)
X=XAXIS-1.*CTH-1.*STH
Y=YAXIS-1.*CTH-1.*STH
INLAM=IVH

```

C

```

DO 760  K=1,NH
I=0
INUM=INUMS
IF(INUM)400,500,500
400 I=I+1
INUM=-INUM
500 I=I+1
II(I)=INUM/100
INUM=INUM-II(I)*100
I=I+1
II(I)=INUM/10
INUM=INUM-II(I)*10
I=I+1
II(I)=INUM
CALL ENGCCDE(I,IS,IL)
CALL SYMBCL(X,Y,C7,IS,IR,I)
INUMS=INUMS+IVH2
X=X-.1.*CTH
Y=Y-.1.*STH
END
700 RETURN

```

LIST OF REFERENCES

Allen, J. S., "Models of wind-driven currents on the continental shelf", Annual Review of Fluid Mechanics, v. 12, pp. 389-433, 1980.

Bakun, A., "Coastal upwelling indices, west coast of North America, 1946-71, U.S. Department of Commerce", NOAA Technical Report NMFS SSRF-671, pp. 103.

Bakun, A., Personal communication, 1981.

Coddington, K., "Measurement of the California Countercurrent", M.S. Thesis, Naval Postgraduate School, Monterey, June 1979.

Dreves, D. A., "Sea levels and metered currents off central California", M.S. Thesis, Naval Postgraduate School, Monterey, September 1980.

Ekman, V. W., "On the influence of the earth's rotation on ocean currents", Arkiv for Matematik, Astronomi, och Fysik, 2(11), pp. 1-52, 1905.

Halpern, D., et al., "Oceanographic observations of the 1982 warming of the Tropical Eastern Pacific", Science, v. 221, pp. 1173-1175 16 September 1983.

Hamilton, P. and M. Rattray, "A numerical model of the depth dependent wind-driven upwelling circulation on a continental shelf", Journal of Physical Oceanography, v. 8, pp. 437-457, May 1978.

Hickey, B. M. and P. Hamilton, "A spin-up model as a diagnostic tool for interpretation of current and density measurements on the continental shelf of the Pacific Northwest", Journal of Physical Oceanography, v. 10, pp. 12-24, 1980.

Hickey, B. M., "The California Current System - Hypothesis and Facts", Contribution Number 1038 of the Department of Oceanography, University of Washington, 24 April 1978.

Hickey, B. M., A. Huyer and R. L. Smith, "The alongshore coherence and generation of fluctuations in currents and sea level on the Pacific Northwest continental shelf, winter and spring 1975", Journal of Physical Oceanography, v.11, pp. 822-835, June 1981.

Huyer, A., E. J. C. Sobey and R. L. Smith, "The spring transition in currents over the Oregon continental shelf", Journal of Geophysical Research, v. 84, pp. 6995-7011, 20 November 1979.

Janowitz, G. S., "A model and observations of time-dependent upwelling over the mid-shelf and slope", Journal of Physical Oceanography, v. 10, pp. 1574-1583, July 1980.

Munk, W. H., "On the wind driven ocean circulation", Journal of Meteorology, v. 7, pp. 79-93, 1950.

O'Brien, J. J. and H. E. Hurlburt, "A numerical model of coastal upwelling", Journal of Physical Oceanography, v. 2, pp. 14-26, January 1972.

O'Brien, J. J., "Upwelling in the ocean: Two and three dimensional models of upper ocean dynamics and variability", Modeling and Prediction of the Upper Layers of the Ocean, Pergamon Press, 1977.

Reid, J. L., G. I. Roden and J. G. Wyllie, "Studies of the California Current System", Progress Report of the California Cooperative Oceanic Fisheries Investigations, 1 July 1956 to 1 January 1958, pp. 28-56, Scripps Institution of Oceanography, La Jolla, California, 1958.

Reid, J. L., Jr. and R. A. Schwatzlose, "Direct measurements of the Davidson Current off central California", Journal of Geophysical Research, v. 67, pp. 559-565, June 1962.

Reid, J. L., Jr., "Measurements of the California Countercurrent at a depth of 250 meters", Journal of Marine Research, v. 20, pp. 134-137, 15 July 1962.

Ryther, J. H., "Photosynthesis and fish production in the sea", Science, v. 166, pp. 72-76, 30 October 1969.

Smith, R. L., "Peru coastal currents during El Nino: 1976 and 1982", Science, v. 221, pp. 1397-1399, 30 September 1983.

Stewart, R. W., "The influence of friction on inertial models of oceanic circulation", Studies on Oceanography, University of Washington Press, 1965.

Suginohara, N., "Coastal upwelling: onshore - offshore circulation, equatorward coastal jet and poleward undercurrent over a continental shelf slope", Journal of Physical Oceanography, v. 12, pp. 272-284, March 1982.

Sverdrup, H. U., M. W. Johnson and R. H. Fleming, The Ocean, their Physics, Chemistry, and general Biology, Prentice-Hall, Inc., Englewood Cliffs, N. J., 1942.

Sverdrup, H. U. and R. H. Fleming, "The waters off the coast of Southern California", Scripps Institute of Oceanography Bulletin, v. 4, pp. 261-375, 9 October 1941.

Wickham, J. B., "Observations of the California Undercurrent", Journal of Marine Research, v. 33, pp. 325-340, September 1975.

INITIAL DISTRIBUTION LIST

	No. Copies
1. Chairman Code 68 Department of Oceanography Naval Postgraduate School Monterey, CA 93943	2
2. Director Naval Oceanography Division (OP952) Navy Department Washington, DC 20350	1
3. Office of Naval Research Code 480 Naval Ocean Research and Development Activity NSTL Station, MSD 39529	1
4. Dr. Robert E. Stevenson Scientific Liaison Office, ONR Scripps Institution of Oceanography La Jolla, CA 92037	1
5. SIO Library University of California, San Diego P.O. Box 2367 La Jolla, CA 92037	1
6. Department of Oceanography Library University of Washington Seattle, WA 98105	1
7. Department of Oceanography Library Oregon State University Corvallis, OR 97331	1
8. Commanding Officer Fleet Numerical Weather Central Monterey, CA 93940	1
9. Commanding Officer Naval Environmental Prediction Research Facility Monterey, CA 93940	1
10. Commander Oceanographic Systems Pacific Box 1390 Pearl Harbor, Hawaii 96860	1

11.	Defense Technical Information Center Cameron Station Alexandria, VA 22314	2
12.	Library Code 0142 Naval Postgraduate School Monterey, CA 93943	2
13.	Commanding Officer Naval Ocean Research and Development Activity NSTL Station, MS 39529	1
14.	Commander Naval Oceanography Command NSTL Station, MS 39529	1
15.	Commanding Officer Naval Oceanographic Office NSTL Station, MS 39529	1
16.	Dr. S. P. Tucker, Code 68Tx Department of Oceanography Naval Postgraduate School Monterey, CA 93943	3
17.	Professor J. B. Wickham, Code 68Wk Department of Oceanography Naval Postgraduate School Monterey, CA 93943	3
18.	Lt. K. Coddington Department of Ocean Sciences U.S. Coast Guard Academy New London, Ct 06320	1
19.	LCDR R. L. Harrod IAGS, Blgd. 144 Ft. Sam Houston, TX 78234	3

/

1 3 3 7 5

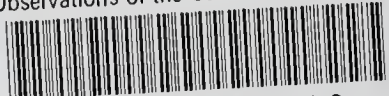
210236

Thesis
H29347 Harrod
c.1 Observations of the
California Counter-
current.

210236

Thesis
H29347 Harrod
c.1 Observations of the
California Counter-
current.

thesH29347
Observations of the California Countercur-



3 2768 002 08257 0

DUDLEY KNOX LIBRARY